

HIGH REYNOLDS NUMBER FLOW IN
COLLAPSIBLE PIPES AND CHANNELS

by

Owen Richard Tutty

A thesis submitted for the degree of
Doctor of Philosophy of the University of London

Physiological Flow Studies Unit
Imperial College of Science and Technology
London SW7 2AZ

Abstract

This study is concerned with steady, laminar, high Reynolds number flow of a Newtonian viscous fluid in a collapsible tube, where the position of the tube wall is a function only of the pressure exerted locally by the fluid on the wall. The nondimensionalized fluid-tube system is controlled by three main parameters: the Reynolds number of the incoming fully developed flow, the minimum radius (or half-width) of the tube, and the "pressure response", which characterizes the response of the wall to a change in fluid pressure. Restrictions are placed on these parameters so that the streamwise length scale is large and, to the order worked, the pressure is uniform across the tube.

For a model tube law - the relationship between the wall position and the local fluid pressure - the flow in a channel is investigated in detail. Solutions are presented for some of the possible parameter values. However, for no tube law are we able to find a complete solution for all possible values of the pressure response. The reason for this is not known definitely, but results from other studies suggest that perhaps steady solutions may not exist for at least some of these cases.

In general, the flow in an axisymmetric pipe is similar to that in the analogous channel. While the flow in a nonaxisymmetric pipe-fluid system retains a linear structure, it can be divided into axisymmetric and nonsymmetric parts, and it is the axisymmetric part which determines the pressure and hence the wall position. We find significant differences in the flow when the pipe collapse is a "bending collapse", with a constant wall perimeter, as opposed to a "stretching collapse", which involves a change in perimeter. In all cases considered the collapse is more gradual with a bending collapse.

Our results are compared qualitatively with some from experimental studies. In certain respects the results are consistent.

CONTENTS

1	INTRODUCTION	
1.1	General background and equations	1
1.2	The tube law	9
1.3	Previous work	17
2	CHANNELS WITH A FINE COLLAPSE	
2.1	Flows with a fast pressure response	25
2.2	Flows with a moderate pressure response	36
2.3	Flows with a slow pressure response	43
2.4	A collapse which starts far upstream	43
3	CHANNELS WITH A FINITE COLLAPSE	
3.1	Introduction	47
3.2	Channel flows with the collapse extending far downstream	48
3.3	Channels which collapse at a finite distance downstream	64
3.4	Channel flows with a fast pressure response	80
3.5	Channel flows with a slow pressure response	101
4	PIPE FLOW	
4.1	The governing equations	103
4.2	Axisymmetric pipe flow	105
4.3	A nonsymmetric collapse extending far upstream	107
4.4	Nonsymmetric pipe flows with a fast pressure response	111
4.5	Nonsymmetric pipe flows with a slow pressure response	126
5	COMPARISON WITH EXPERIMENTAL RESULTS	128
	APPENDIX 1.	132
	APPENDIX 2.	140

APPENDIX 3.	142
APPENDIX 4.	145
APPENDIX 5. Numerical methods	148
APPENDIX 6. The flow and phase velocity of an inviscid fluid in a collapsible tube	156
REFERENCES	160

FIGURES

1.1 The geometry and coordinate system of a collapsible channel 3

1.2 Pressure-area relationships for a dog vein and a latex tube 10

1.3 Pressure-area relationships and shape of tubes near zero transmural pressure 11

1.4 Change in perimeter versus change in area 10

1.5 The tube law $S(\mu p) = 1 - [1 + (\mu p)^2]^{-q/2}$ 16

1.6 Experimental apparatus 18

2.1 Pressure deviation \bar{P} against X 34

2.2 Skin friction perturbation τ_1 against X 35

2.3 Channel deviation S against X 35

3.1 Results for a channel with $\epsilon = q = 1/2$ 54

3.2 Results for a channel with $\epsilon = 1/2$ and $\mu = 1$ 56

3.3 Results for a channel with $q = 1/2$ and $\mu = 1$ 58

3.4 Results for a channel with $\epsilon = \mu = 1$ 60

3.5 Results for a channel with $\epsilon = 1$ and $q = 1/2$ 62

3.6 Half-width y_w against distance for a channel with $q = .4, \mu = 1$ and $\epsilon = .99$ 66

3.7 The energy function $V(g)$ 69

3.8 Coefficients of the asymptotic solution for $-\mu p \gg 1$ with $\epsilon = 1$ and $q = 1/2$ 73

3.9 Velocity profiles for $\epsilon = 1$ and $q = 1/2$ 74

3.10 The pressure in a channel with a fast pressure response 84

3.11 Results for a channel with $K = 1$ 95

4.1 Direction of the secondary velocity in an elliptical pipe 110

TABLES

2.1 The eigenvalues α_n 39

3.1 Critical values of μ 100

Acknowledgements

I would like to thank Dr. F.T. Smith of the Mathematics Department, Imperial College, for suggesting the topic and for supervising the work presented in this thesis. I acknowledge the receipt of a New Zealand University Grants Committee Postgraduate Scholarship throughout the course of this research.

Also, I wish to thank Susan for persevering during the drawn-out writing-up period.

Section 1. Introduction

1.1 General background and equations

It is thought that fluid dynamical properties, particularly the local behaviour of the shear stress, may have important physiological implications for flow in the blood vessels of animals (see Caro et al. (1969, 1971) and Lighthill (1972)), and attention has been given recently to flow in non-uniform tubes under a variety of conditions. Some idea of the range of problems attempted and approaches used, both theoretical and experimental, can be obtained for biomechanics in general, from the volume of Fung et al. (1972), and for blood flow in particular, from the volumes of Bergel (1972), Hwang and Norman (1972), and McDonald (1974). A comprehensive introduction to the mechanics of the circulation is provided by Caro et al. (1978), while a review of the clinical work and many relevant references are contained in Charm and Kurland's (1974) study.

It is convenient to divide the theoretical attempts at modelling physiological flow in non-uniform vessels into two categories: first, those that assume that the position of the vessel wall is known explicitly at any given time, and second, those that assume a relationship between the position or behaviour of the wall and the quantities characterising the behaviour of the fluid, such as the pressure and shear stress distributions. A major task in problems of the second type is to determine the position of the wall explicitly. Examples of the first category above are models of peristaltic pumping, which usually have a known pulsatile wall deformation travelling through an infinite tube (see Jaffrin and Shapiro 1971), and the axisymmetric model of a valved physiological pump developed by Uchida and Aoki (1977), which has a semi-infinite pipe contracting or expanding with the radius of the pipe a known function varying with time only. An example of the second category is the study by Schwerdt and Constantinesco (1976) of the flow in an initially stressed elastic tube, where the flow is given by a small perturbation to the Poiseuille flow and the elastic wall model is based on a small deformation shell theory. In applying work complementary to that of Uchida and Aoki (1977) to elastically constrained walls, Secomb (1978) includes both approaches.

The present study is concerned with a problem of the second type above, in which the wall position is not known explicitly. In particular, we are interested in the steady, high Reynolds number flow in an infinitely long collapsible tube, for which the position of the wall(s) is known only as a function of the pressure exerted by the fluid on the wall(s). As a point of notation, tube is used here in a general sense meaning both pipes and channels, a convention followed throughout this study. We assume that far upstream the tube has a constant cross-sectional area and shape, and that there is a known reference pressure above which the tube takes this rigid shape and below which the position of the wall(s) can vary. Also, we assume that the "tube law", the relationship between the position of the wall(s) or the cross-sectional area and the fluid pressure, is a continuous function. Hence, the change in position of the walls will be continuous everywhere the fluid pressure at the walls is continuous. The assumptions necessary for the use of such a tube law and the form of the tube law are discussed in Section 1.2 below.

We will now introduce the basic governing equations for flow in a collapsible channel. The equations for a pipe are given when required in Section 4.1 below. The fluid is assumed to be homogeneous, Newtonian, and incompressible and its motion to be laminar and steady. Let ρ be the density of the fluid, a be the half width of the channel when in its rigid upstream form, and \bar{U}_0 be a representative velocity far upstream. To nondimensionalise the two-dimensional channel problem, the pressure is written as $\rho \bar{U}_0^2 p$ and the velocity as $\bar{U}_0(u,v)$ in Cartesian coordinates (x,y) , where ax and ay are the distance downstream (parallel to the undisturbed channel wall far upstream) and across the channel respectively. The origin is taken as the centre of the channel at the point where the walls first deviate from the rigid upstream form (see Fig. 1.1). The reference pressure at which this deviation starts will be taken to be zero. If the Reynolds number is defined by

$$R = \bar{U}_0 a / \nu, \quad (1.1)$$

where ν is the kinematic viscosity of the fluid, then the governing steady Navier-Stokes equations are

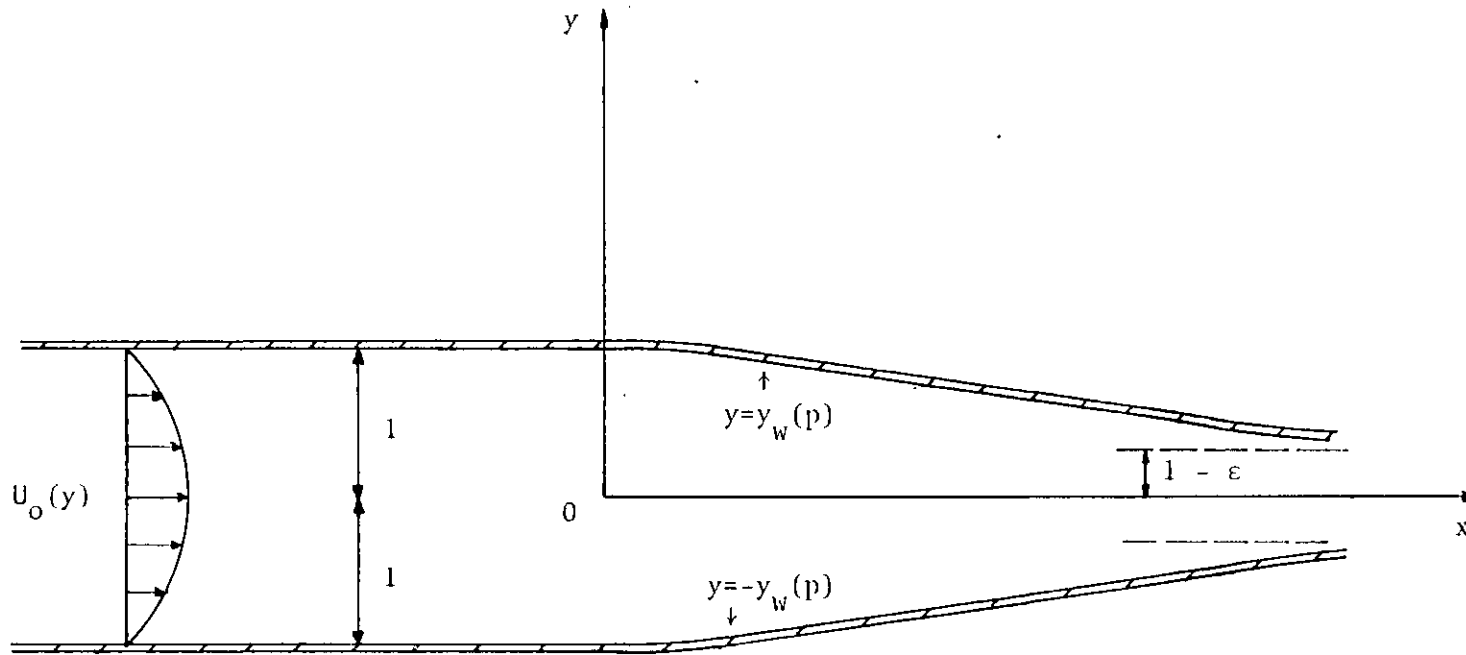


Figure 1.1. The geometry and coordinate system of a collapsible channel.

$$\left. \begin{aligned}
 u \frac{\partial u}{\partial x} + v \frac{\partial u}{\partial y} &= - \frac{\partial p}{\partial x} + R^{-1} \nabla^2 u, \\
 u \frac{\partial v}{\partial x} + v \frac{\partial v}{\partial y} &= - \frac{\partial p}{\partial y} + R^{-1} \nabla^2 v, \\
 \frac{\partial u}{\partial x} + \frac{\partial v}{\partial y} &= 0,
 \end{aligned} \right\} (1.2)$$

where $\nabla^2 = \partial^2/\partial x^2 + \partial^2/\partial y^2$. We assume that the properties of the upper and lower walls are identical. As a consequence, the flow is expected to be symmetric about the x-axis, although this will not be explicitly assumed in general. In the problems considered in this study, the restrictions placed on the parameters are such that the transverse momentum equation always implies that the pressure is independent of y , and thus that the positions of the walls can be expressed in the form $y = \pm y_w$, where $y_w = y_w(p)$ is the given tube law. The boundary conditions are that the components of velocity must vanish at the walls and must match to the incoming fully developed Poiseuille flow, that is,

$$\left. \begin{aligned}
 u = v = 0 \text{ at } y = \pm y_w, \\
 u \rightarrow U_0(y) \text{ and } v \rightarrow 0 \text{ as } x \rightarrow -\infty,
 \end{aligned} \right\} (1.3)$$

where $U_0(y) = \frac{1}{2} (1 - y^2)$. If it is assumed that the flow is symmetric then the no-slip condition at the lower (or upper) wall can be replaced by

$$v = 0 \text{ and } \frac{\partial u}{\partial y} = 0 \text{ at } y = 0. \quad (1.3a)$$

Throughout this study we use a tube law of the form

$$y_w(p) = 1 - \epsilon S(\mu p), \quad (1.4)$$

where $\mu > 0$ and $0 < \epsilon \leq 1$ are nondimensional constants and $S(t)$ is a continuous monotonic function such that $S(t) = 0$ when $t > 0$, $S(t) > 0$ when $t < 0$, $S(t)$ is $O(1)$ when $-t$ is $O(1)$, and $S(t) \rightarrow 1$ as $t \rightarrow -\infty$. Thus the rigidity of the wall whenever the pressure is above the reference value of zero is assured. The value of the parameter μ

depends on both the elastic response of the walls to changes in the fluid pressure and the velocity of the incoming flow, as will be seen in Section 1.2 below. For a given function $S(t)$, a larger value of μ will lead to a faster response of the channel walls to a given change in the fluid pressure. For this reason, a channel flow for which $\mu \gg 1$, $\mu = O(1)$, or $\mu \ll 1$ will be called a flow with a "fast", "moderate", or "slow" pressure response, respectively. The minimum possible half width of the channel is $1 - \epsilon$. Accordingly, a channel for which $\epsilon \ll 1$, $\epsilon = O(1 - \epsilon) = O(1)$, $0 < 1 - \epsilon \ll 1$ or $\epsilon = 1$ will be called a channel with a "fine", "moderate", "severe" or "complete" collapse, respectively.

Equations (1.2) - (1.4) form a general problem for steady flow in a collapsible channel. Our interest is in the structure of the fluid dynamics when the Reynolds number is large, and we assume that

$$R \gg 1 \tag{1.5}$$

throughout this study. In addition to (1.5), restrictions will be placed on the parameters μ , ϵ and R in such a way that, to the order of magnitude considered, the pressure will always be independent of y .

So far we have not specified the length scales to be used. For laminar high Reynolds number flow in a tube with a fixed constriction, the appropriate length scales are obtained from the known dimensions of the constriction, and the pressure distribution is determined largely by the size, shape and position of the constriction (see Smith 1976a,b; 1978a; 1979). In the present study we have, in a sense, the opposite situation; that is, it is the pressure distribution that determines the position of the wall(s), and it could be said that our major task is to follow downstream the development of the pressure from its incoming Poiseuille form. Accordingly, we will assume that sufficiently far upstream the pressure gradient is $O(R^{-1})$, and use this assumption to obtain initial length scales for any given situation.

The form of the tube law and previous work on flow in collapsible tubes are discussed below in Sections 1.2 and 1.3 respectively. In Section 2 we consider channels with a fine collapse ($\epsilon \ll 1$), while

Section 3 is concerned mainly with channels with a moderate, severe, or complete collapse ($\varepsilon = 0(1)$). In Sections 3.2 and 3.3 we study in detail a fluid-channel system with a moderate pressure response ($\mu = 0(1)$) and a tube law such that $S(\mu p) \sim (-\mu p)^{-q}$ as $p \rightarrow -\infty$, where q is a positive constant. For a complete collapse ($\varepsilon = 1$), we find that if $q < 1/2$ then the flow is essentially viscous in character when $-p \gg 1$, and that the collapse extends indefinitely far downstream if $0 < q \leq 1/3$ (Section 3.2), but not if $1/3 < q < 1/2$ (Section 3.3). The pressure has a singularity and $y_w \rightarrow 0$ at a finite value of $X = R^{-1}x$ if $1/3 < q < 1/2$. If $q > 1/2$ the inertial forces in the fluid necessarily dominate the pressure gradient as $p \rightarrow -\infty$, and we are not able to find a solution for the local problem with $-\mu p \gg 1$ (Section 3.3). If $q = 1/2$ then the inertial force and the pressure gradient in the fluid are of the same order as $p \rightarrow -\infty$, and μ is found to have a "critical" value of 18 such that an asymptotic solution for $-p \gg 1$ is obtained for $\mu < 18$, and in a limit sense as $\mu \rightarrow 18^-$, but not for $\mu \geq 18$. Comparison with numerical results, and with results from other studies, both theoretical and experimental, suggests that there may not be a complete steady solution for the problem with $q > 1/2$ and $\mu = 0(1)$, nor for that with $q = 1/2$ and $\mu \geq 18$ (Sections 3.3 and 5).

If the pressure response is slow ($\mu \ll 1$), then the flow is viscous dominated, and the streamwise velocity solution has a simple parabolic form (Sections 2.3 and 3.5). An exception to this can occur when $y_w \ll 1$ (Section 3.5).

If the pressure response is fast ($\mu \gg 1$; Sections 2.1 and 3.4), then immediately downstream of the origin, where the walls first vary from $y_w = 1$, thin viscous boundary layers form in the fluid adjacent to the walls. In this region the pressure is determined by the flow in the wall layers, while the core flow responds passively to changes in the wall layers (Sections 2.1 and 3.4). These boundary layers have a linear flow structure, and as long as they persist and the change in the channel width is small ($\varepsilon S \ll 1$) the core flow takes the form of a small inviscid rotational perturbation to the incoming Poiseuille flow. If the pressure response is fast and the collapse is fine such that ε is $0(\mu^{-2/3})$ or less (Section 2.1), then the wall layers expand downstream until eventually their thickness becomes finite and they merge

with the core flow. The flow can then be treated simply as a Poiseuille flow plus an $O(\epsilon)$ viscous perturbation.

If $\epsilon \gg \mu^{-2/3}$ then it is necessary to consider the behaviour of $S(\mu p)$ for $0 < -\mu p \ll 1$. A particular channel with $\epsilon \gg \mu^{-2/3}$ is studied in Section 3.4 below. The solution found for the linear viscous wall layers which form as the flow passes the origin has a singularity, with the pressure tending to infinity at a finite value of $\epsilon^{3/4} \mu^{3/2} R^{-1} x$. If $\mu^{-2/3} \ll \epsilon \leq O(\mu^{-1/2})$ then this singularity can be smoothed out by taking a shorter length scale locally, and we are able to complete the solution. However, if $\mu^{-1/2} \ll \epsilon \leq 1$ then this procedure is unsuccessful, and we do not find a complete solution for the problem, only the upstream solution of Poiseuille flow and the local solution for the flow immediately downstream of the origin.

The existence of viscous wall layers when the pressure response is moderate ($\mu = O(1)$) depends on the value of ϵ and the region of the channel under consideration; if the collapse is fine ($\epsilon \ll 1$) then no distinct boundary layers form, while if the collapse is moderate, severe or complete ($\epsilon = O(1)$), then in the region downstream of the origin where $0 < xR^{-1} \ll 1$, linear viscous wall layers form and the change in the core flow is passive. These wall layers grow in thickness downstream until they merge with the core flow when xR^{-1} is $O(1)$. When this occurs it is not appropriate to separate the flow into distinct regions across the channel. However, if $q = 1/2$, $0 \leq 1 - \epsilon \ll 1$, and $0 < 18 - \mu \ll 1$ then nonlinear viscous wall layers form and the core flow becomes essentially inviscid as $p \rightarrow -\infty$ (Section 3.3).

In Section 4 we study the flow in a model of a collapsible pipe. The results for axisymmetric pipes (Section 4.2) are broadly similar to those for the analogous channels, and Section 4 is mainly concerned with nonsymmetric pipes, i.e. genuinely three-dimensional flows. In general, because of the additional complexity introduced by the third velocity component and independent variable, the analysis is restricted to systems in which the change of the pipe wall from the upstream circular cross-section is small, although this does include the initial stage of a finite collapse with a fast pressure response. However, some significant features of the flow are revealed. For a fine collapse the flow can usually be divided into axisymmetric and nonsymmetric

parts, and it is the axisymmetric component of the flow, which is identical to the flow in an axisymmetric pipe with the same parameter values, which determines the pressure and thus the position of the pipe wall. Further, it is predicted that the type of collapse of the pipe wall will have a significant effect on the flow. For a "bending collapse", in which the internal perimeter of the wall remains constant as the pressure varies, we find that the pressure is undisturbed from its Poiseuille form, whereas for a "stretching collapse", in which the perimeter varies, the pressure deviates from the linear Poiseuille form. This is perhaps most important when the pressure response is fast and $\epsilon \gg \mu^{-2/3}$ (Section 4.4), when a singularity is found in the pressure for a stretching collapse but not for a bending collapse. This singularity is similar to that found in the analogous channel flow (Section 3.3). We stress that our study concerns a model of a collapsible pipe, and the extension of these results to more realistic pipe-fluid systems is by no means certain. Of course, the same is true for the channel-fluid systems we study.

A comparison of our results with some from other studies of flow in collapsible tubes can be found in Section 5 below. The numerical techniques used in this study are given in Appendix 5.

No evidence is found of any significant upstream influence in any of the fluid-tube systems investigated in this study. In contrast, an important prediction from the studies by Smith (1976a,b,e; 1977b; 1978a; 1979) of high Reynolds number flow in tubes with fixed constrictions and dilations is that, unless the dimensions of a constriction are sufficiently small, significant changes, including separation, can occur in the incoming flow ahead, even far ahead, of the constriction. There is no inconsistency between our results and those of Smith, as a necessary condition for a fixed constriction in a tube to have a significant influence upstream of the constriction is that the dimensions of the constriction are such that the pressure is dependent on y , whereas the restrictions placed on the parameters in the present study are such that, to the order worked, the pressure is always independent of y . Thus, although we do not assume it, we might expect from the results of Smith that there will be no significant changes to the flow ahead of the collapse in any of fluid-tube systems considered in the present study.

1.2 The tube law

A number of studies have been made of the relationship between the cross-sectional area and transmural pressure - the internal pressure minus the external pressure - for compliant tubes, some of which we will now review. Moreno et al. (1970) have determined experimentally the pressure-area relationship for certain dog veins and thin walled latex tubes (see Figure 1.2), which are in turn examples of naturally occurring and man-made collapsible tubes. The results from Moreno et al. can be summarised as follows:

(i) Both veins and latex tubes have a circular cross-section when the transmural pressure is sufficiently far above zero, and both lose their circular cross-section when the transmural pressure approaches zero. The walls of dog veins and latex tubes are not structurally self-supporting, and at zero transmural pressure the stresses in the wall result in an approximately oval shape. Near zero transmural pressure the change in area and shape with pressure is rapid (see Figure 1.3).

(ii) From flattened to circular cross-sections the perimeter of a latex tube remains constant and the change in area comes exclusively from bending of the wall, while an increase in area with a circular cross-section comes from stretching of the wall with a corresponding increase in the perimeter. Unlike latex tubes, veins do not show a distinct two-region behaviour but a combination of bending and stretching when changing from a circular cross-section. Figure 1.4 shows plots of change in area versus change in perimeter for a vein and a latex tube.

(iii) Bending of the walls is either the exclusive or the dominant mechanism responsible for changes in cross-sectional area of veins and thin-walled latex tubes in the neighbourhood of zero transmural pressure. Further, no single modulus of elasticity can relate the pressure and the cross-sectional area when bending is predominant, and it is the product of the Young's modulus and the moment of inertia of the wall that is the significant parameter in this regime.

We judge from the above that non-axisymmetric collapses are of great practical importance, particularly those of a pipe which has a

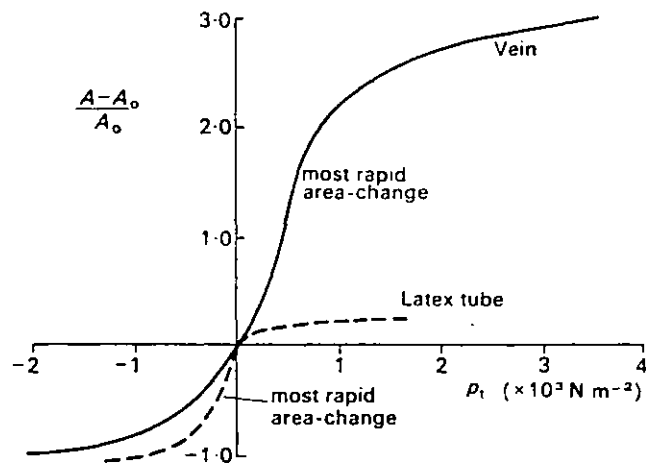


Figure 1.2. Pressure-area relationships for a segment of dog vein and a thin-walled Latex tube. A is the cross-sectional area, p_t the transmural pressure, and $A = A_0$ at $p_t = 0$. (From Caro et al. 1978, after Moreno et al. 1970).

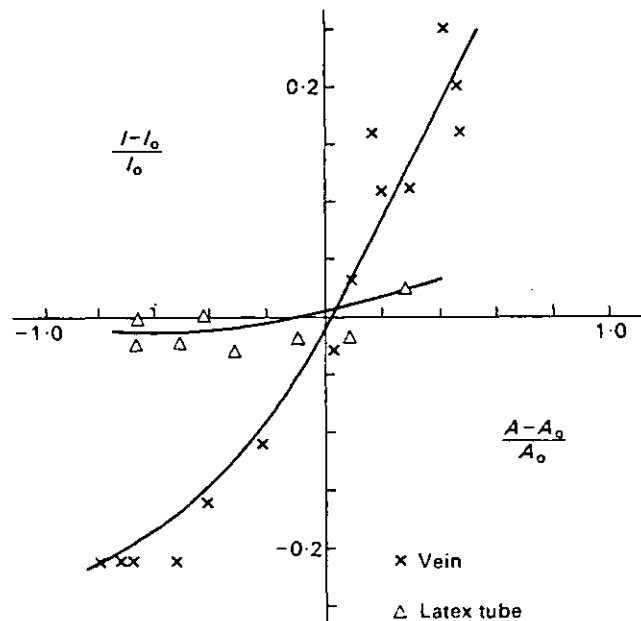


Figure 1.4. Fractional change in perimeter versus fractional change in area for a segment of dog vein and a thin-walled Latex tube. A is the cross-sectional area, l the perimeter, and $A = A_0$ and $l = l_0$ at zero transmural pressure. (From Caro et al. 1978, after Moreno et al. 1970).

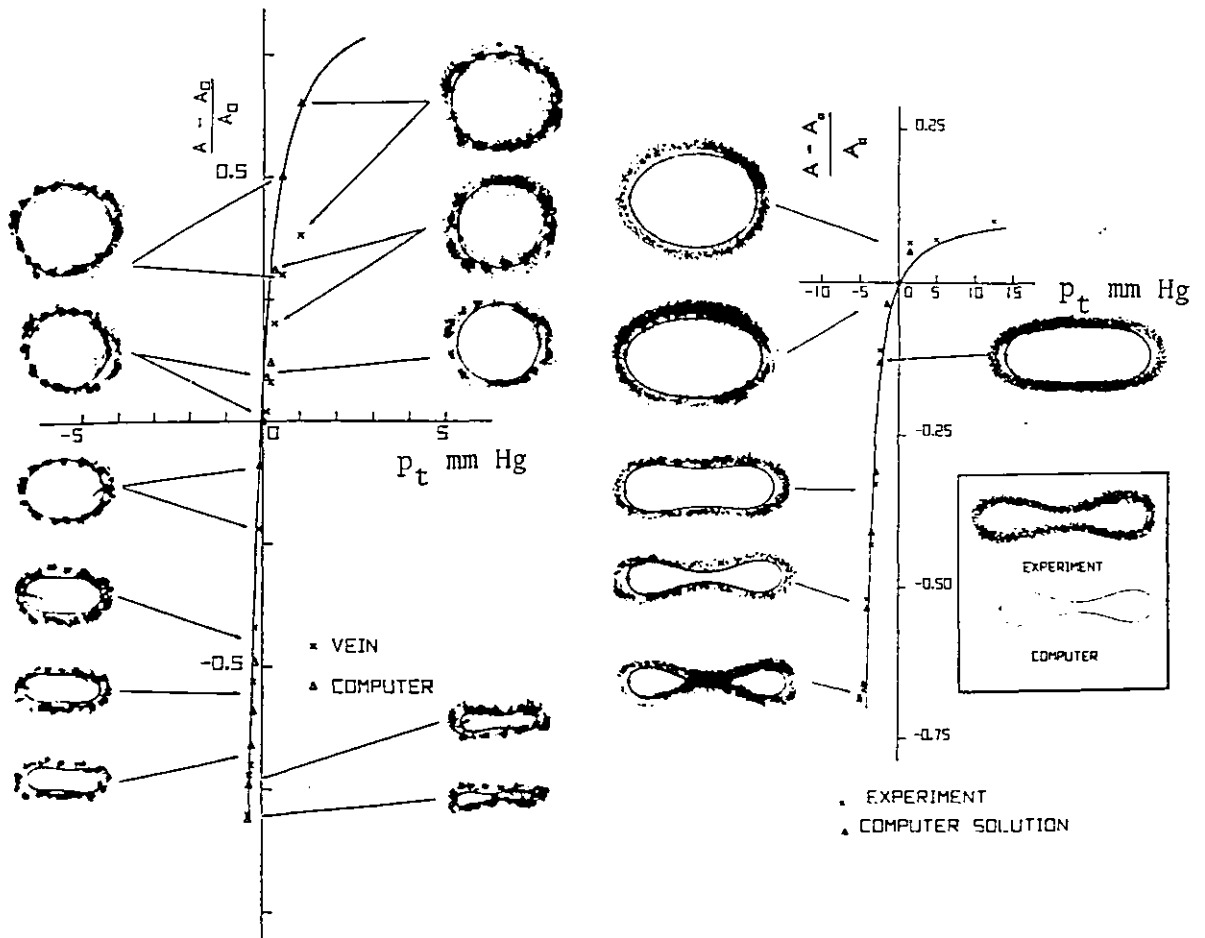


Figure 1.3. Pressure-area relationships and shape of tubes near zero transmural pressure. A is the cross-sectional area, p_t the transmural pressure, and $A = A_0$ at $p_t = 0$. (i) For a segment of dog vein. The solid line is $(A - A_0)/A_0 = 0.019 \tan^{-1}[3(p_t + .35)] - 0.81$. (ii) For a thin-walled Latex tube. The solid line is $(A - A_0)/A_0 = 0.0091 \tan^{-1}(p_t + 4.1) - 0.70$. (From Moreno et al. 1970).

constant perimeter. A model of this problem is studied in Section 4. The results suggest that the type of collapse, i.e. bending or stretching, can have a significant effect on the flow and the behaviour of the tube.

We turn now to the form of the tube law. Taylor and Gerrard (1977) have formulated various theoretical pressure-radius relationships for a distended elastic vessel with a circular cross-section, i.e. a pure stretching regime. They conclude that theories which take account of the thickness of the wall produce a significantly better representation than those which treat the wall as a membrane, but also that there is little difference between the results of more exact theories and those for a thin membrane corrected by a simple thickness factor. Their "best simple relationship" shows reasonable agreement with experimental results from a rubber pipe.

Taylor and Gerrard's (1977) work applies only to elastic pipes with a circular cross-section and a positive transmural pressure. When the transmural pressure is negative the pipe wall buckles and opposing walls will eventually come into contact. The analysis of Flaherty et al. (1972) suggests that when this happens the tube law for an elastic pipe has the similarity form $A = k(-p_t)^{-n}$, where p_t is the transmural pressure and $n > 0$ and k are constants. The simplest case has $n = 2/3$ and a "dumb-bell" shaped pipe. Latex tubes display this "dumb-bell" shape (see Figure 1.3), and it has been verified experimentally that they closely obey this law with $n = 2/3$ (Shapiro 1977). Note that this relationship does not give the shape of the pipe, merely the area in terms of the pressure. We know of no simple theoretical relationship between the cross-sectional area or shape of an elastic pipe and the transmural pressure for the intermediate regime in which the pipe is nonsymmetric but the walls are not in contact. Flaherty et al. (1977) obtained numerical solutions for the similarity problem for this intermediate regime, but did not find an explicit relationship between the pressure and area. Earlier, Moreno et al. (1970) developed a nonlinear differential equation for the pipe shape and hence for the area, but unfortunately could not find an analytical solution for it. However, its numerical solution shows good agreement with experimental results (see Figure 1.4). Also, Moreno et al. found that $(A_0 - A)/A_0 = b \tan^{-1}(p_t + c) - d$, where

p_t is the transmural pressure, b , c and d are constants and $A_0 = A(p_t = 0)$, shows close agreement with experimental results (Figure 1.4). However, they were unable to find any physical basis for the form of this relationship and it must be regarded merely as an exercise in curve fitting.

Using least squares, Rubinow and Keller (1972) produced a pressure-radius relationship for a piece of human external iliac artery distended by positive transmural pressures, and assumed it to be valid for negative transmural pressure as well. Wild et al. (1977) used this expression with an adaptation to make it mathematically consistent.

Strictly, the discussion above is concerned with compliant tubes that are filled with a stationary fluid and are distended by a transmural pressure that is uniform along the tube. If the fluid is viscous and in motion, the pressure is unlikely to be uniform and there will be a shearing force from the fluid on the inner wall of the tube. Further, in any rigorous analysis it would be necessary to consider the effects of the bending stiffness of the wall and the conditions at the outer surface at the wall. In studies of flow in collapsible tubes it is commonly assumed that the use of a tube law relating the local pressure and the cross-sectional area or shape is valid (e.g. Ling and Alabek 1972, Shapiro 1977, Wild et al. 1977, Secomb 1978). It may be necessary to place severe restrictions on the fluid-tube system to justify this assumption. For example, consider an axisymmetric fluid-pipe system with internal pipe radius r_w , $|dr_w/dx| \ll 1$, and the pipe wall so thin that a shell theory of elasticity can be used. Let T_θ and T_ℓ be the circumferential and longitudinal tensions respectively, p_t be the transmural pressure, and R_ℓ the radius of curvature in the longitudinal plane. If $|T_\ell/R_\ell| \ll p_t$ then

$$T_\theta = p_t r_w.$$

Note that this does not yet imply that r_w is a function of p_t only. Further assumptions are necessary for $r_w = r_w(p_t)$ to hold. For example, that $T_\theta \gg T_\ell$ or that the longitudinal Poissons ratio is so small that the effect of T_ℓ on r_w is negligible.

In general, it is unlikely that the cross-sectional area and shape of a pipe will depend on p_t only unless p_t is $O(1)$ or greater, $|T_\ell/R_\ell| \ll |p_t|$ and $|dr_w/dx| \ll 1$. If we make the further assumptions that $p_t > 0$, the fluid-pipe system is axisymmetric, there is no longitudinal displacement of the pipe, and the pipe material is isotropic, homogeneous, and incompressible, then theoretical pressure-radius relationships can be derived. Taylor and Gerrard (1977) present such formulae for both thick- and thin-walled pipes, obtained using a linear stress-strain relationship for small deformations and a strain-energy-density function for finite deformations. This system is of some practical interest since experimental evidence suggests that, although not homogeneous or isotropic, an artery can be regarded as an incompressible thick-walled pipe with negligible longitudinal displacement. McDonald (1974) states that the longitudinal motion caused by the shear drag on the inner surface of an artery is so small that it had not been measured experimentally. Patel and Fry (1966) found that the perivascular tethering to the outer surface of an artery acts much more to prevent axial motion than radial motion. Patel and Vaishnav (1972) report that arteries are essentially incompressible. Although a full treatment of the elasticity of an arterial wall requires an approach considerably more complex than assuming the material to be isotropic and homogeneous, it is felt by Taylor and Gerrard (1977) that, because of the difficulties in obtaining necessary information, no improvement will result from the use of more refined theories.

For a thin-walled pipe with a negative transmural pressure, Shapiro (1977) and Kamm and Shapiro (1979) assert that the effect of the longitudinal tension T_ℓ is roughly equivalent to a change in the transmural pressure by an amount of order $-T_\ell/R_\ell$, and that if $|T_\ell/R_\ell| \ll |p_t|$ then the use of a local tube law provides a good approximation. This tube law must relate p_t , the cross-sectional area, and the local properties of the pipe, including presumably the effects of T_ℓ on the pipe circumference and wall thickness. Note that, as with $p_t > 0$, assuming $|T_\ell/R_\ell| \ll |p_t|$ does not necessarily imply that the cross-sectional area and shape of the pipe are independent of T_ℓ .

It would be desirable to include a detailed analysis of the elastic behaviour of the tube rather than assume that a tube law can

be used. However, this approach has several disadvantages:

(i) The necessity of specifying the exact nature of the tube, which restricts the generality of the analysis.

(ii) Tubes of interest may be complex in form, e.g. biological tubes, and the necessary information may not be available and may be difficult to obtain with sufficient accuracy.

(iii) The resultant fluid-tube problem is likely to be so complex that major simplifications in the assumptions and governing equations would be necessary to produce a tractable problem. For example, Womersley (1955) and Schwerdt and Constantinesco (1976) use a shell theory of elasticity, assuming that the deformations to the wall are small, the wall thickness is constant, the flow is axisymmetric, and the Navier-Stokes equations can be linearised.

We are primarily interested in the fluid mechanics of the problem, and throughout this study we assume that the cross-sectional area and shape of the tube are known explicitly as a function of the local pressure. We stress that caution is necessary both in using this assumption and in interpretation of the results.

Where the tube law is required explicitly, we will use

$$S = \begin{cases} 0 & p \geq 0 \\ 1 - \{1 + (\mu p)^2\}^{-q/2} & p < 0 \end{cases} \quad (1.6)$$

where μ and q are positive non-dimensional constants. This relationship has a similar general form to those derived for certain elastic tubes (Taylor and Gerrard, 1977; Flaherty, 1972), and those used in other studies of flow in collapsible tubes (e.g. Oates, 1975; Shapiro, 1977). Writing $\mu = \bar{\mu} \rho \bar{U}_0^2$, we see that there are three parameters, $\bar{\mu}$, q and ϵ , which characterise the elastic response of the tube to changes in the pressure $\rho \bar{U}_0^2 p$, and that, unlike q and ϵ , μ is a composite parameter and its value depends on both the elastic properties of the wall and the characteristic values of the incoming flow. An important feature of (1.6) is that $dS/dp = 0$ at $p = 0$. This choice was made to ensure a smooth transition between the "rigid" and "collapsible" sections of the tube ($p \geq 0$ and $p < 0$ respectively), and thus eliminate any "entrance effects" that might arise from a discontinuous change in the slope of the walls where $p = 0$. Also, such a discontinuous change could invalidate the assumption that S is a function of p only. Note

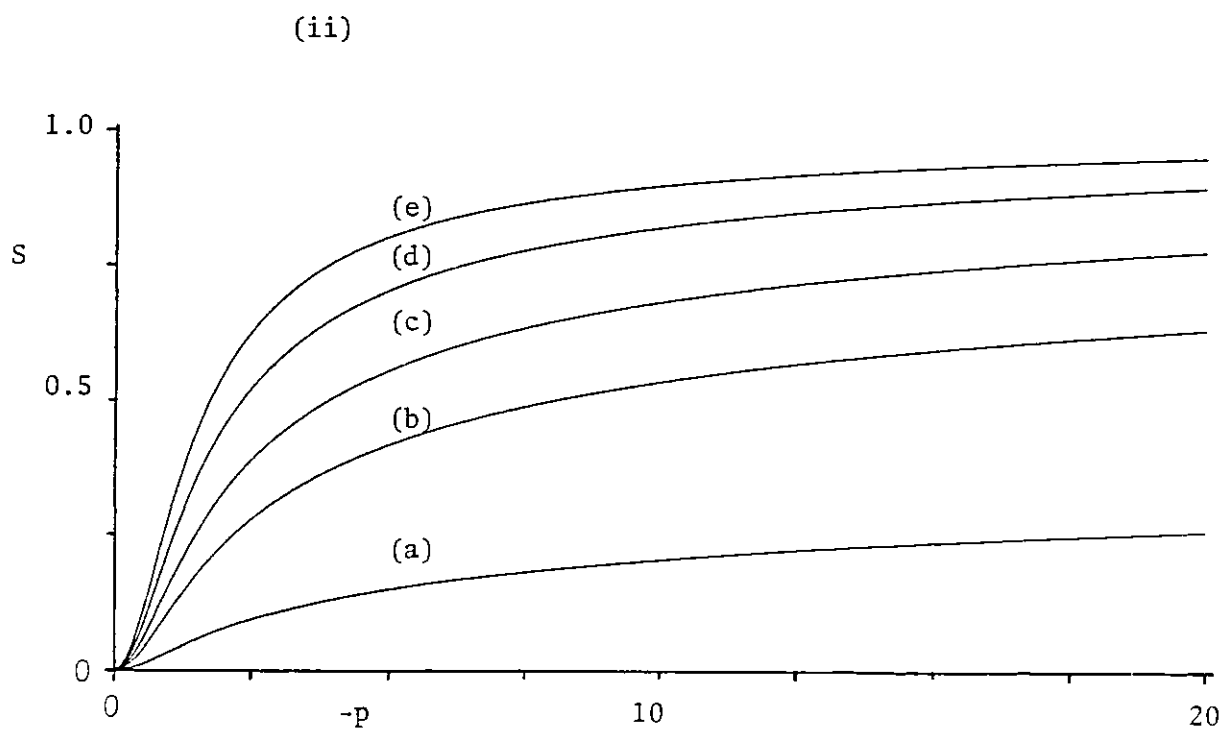
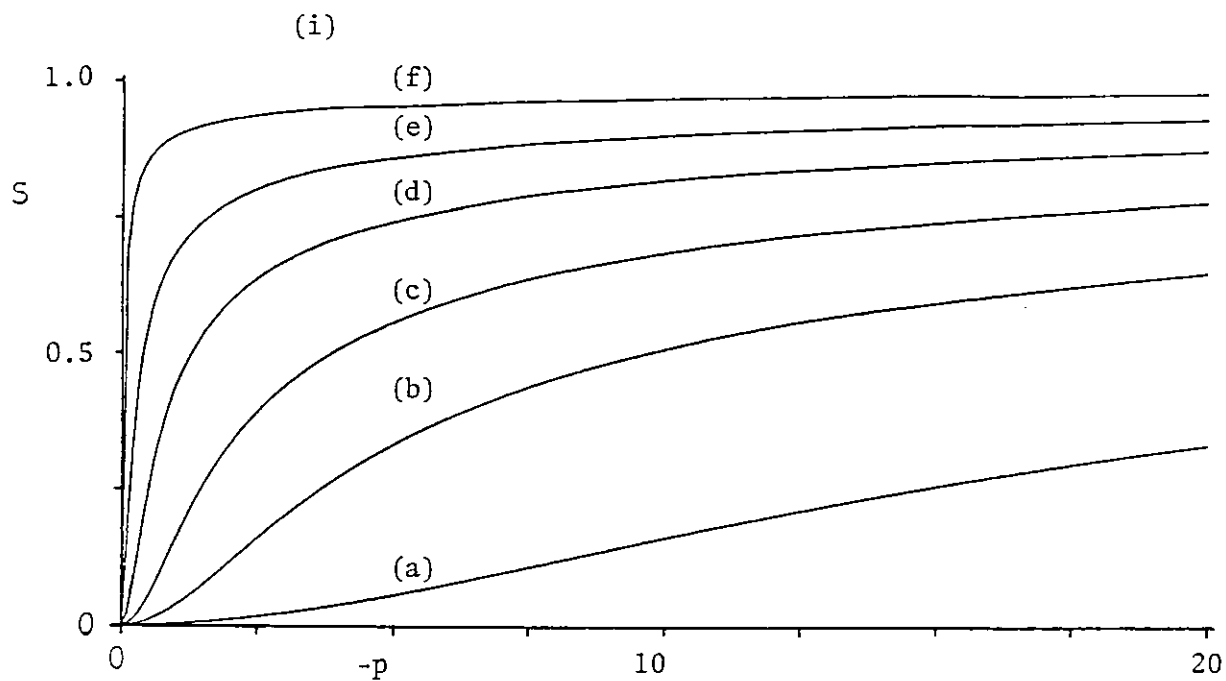


Figure 1.5. The tube law $S(\mu p) = 1 - [1 + (\mu p)^2]^{-q/2}$.
 (i) various μ with $q = 1/2$: (a) $\mu = 0.1$, (b) $\mu = 0.4$,
 (c) $\mu = 1.0$, (d) $\mu = 7.5$, (e) $\mu = 10.0$, (f) $\mu = 100.0$.
 (ii) various q with $\mu = 1$: (a) $q = 0.1$, (b) $q = .325$,
 (c) $q = 0.5$, (d) $q = 0.75$, (e) $q = 1.0$.

that if $(\mu p)^2$ in (1.6) is replaced by $(\mu p)^m$, where $m > 1$, then the slope is continuous at $p = 0$, and an analysis similar to that presented below could be carried out, with essentially the same results. Figure 1.5 shows $S(\mu p)$ for various values of q and μ .

1.3 Previous work

Experimental work on flow in collapsible tubes has been conducted on apparatus similar to that shown in Figure 1.6 by a number of workers, e.g. Holt (1944, 1953 and 1959), Conrad (1969), Katz et al. (1969) and Brower and Scholten (1975). This apparatus is sometimes known as a "Starling resistor" and consists of a thin-walled compliant pipe (usually Penrose surgical tubing) mounted at its ends on rigid piping and contained in a closed chamber. The chamber pressure p_e can be given any chosen value and the inlet and outlet pressures, p_1 and p_2 in turn, can be controlled independently. A misconception common in the experimental literature is that there are three independent pressures in this system. In fact, the relevant parameters are two independent pressure differences, i.e. two of $p_1 - p_e$, $p_2 - p_e$ and $p_1 - p_2$. The theoretical problem given in Section 4.1 for flow in a nonsymmetric collapsible pipe (which is similar to the problem for a channel given in Section 1.1) could be compared to an experimental system in which the inlet transmural pressure difference ($p_1 - p_e$) is such that the slope of the wall is continuous at the junction between the rigid and compliant tubes, the reference pressure is chosen so that $p_1 - p_e$ is zero, and the outlet is so far downstream that the end effects from the outlet do not significantly affect the major part of the collapse.

For a variety of reasons (see Shapiro 1977), precise interpretation of the results from the experimental studies mentioned above is difficult. There is, however, a commonly observed phenomenon of interest to the present study. This is the occurrence of "self-excited oscillations" in the tube. If the tube is substantially collapsed at the outlet, i.e. $p_2 - p_e$ is large and negative, and the mass flow rate Q is sufficiently large, then the fluid-tube system can become unstable spontaneously and cannot be regarded as quasi-steady (see e.g. Katz et al. 1969). Brower and Scholten (1975) report that

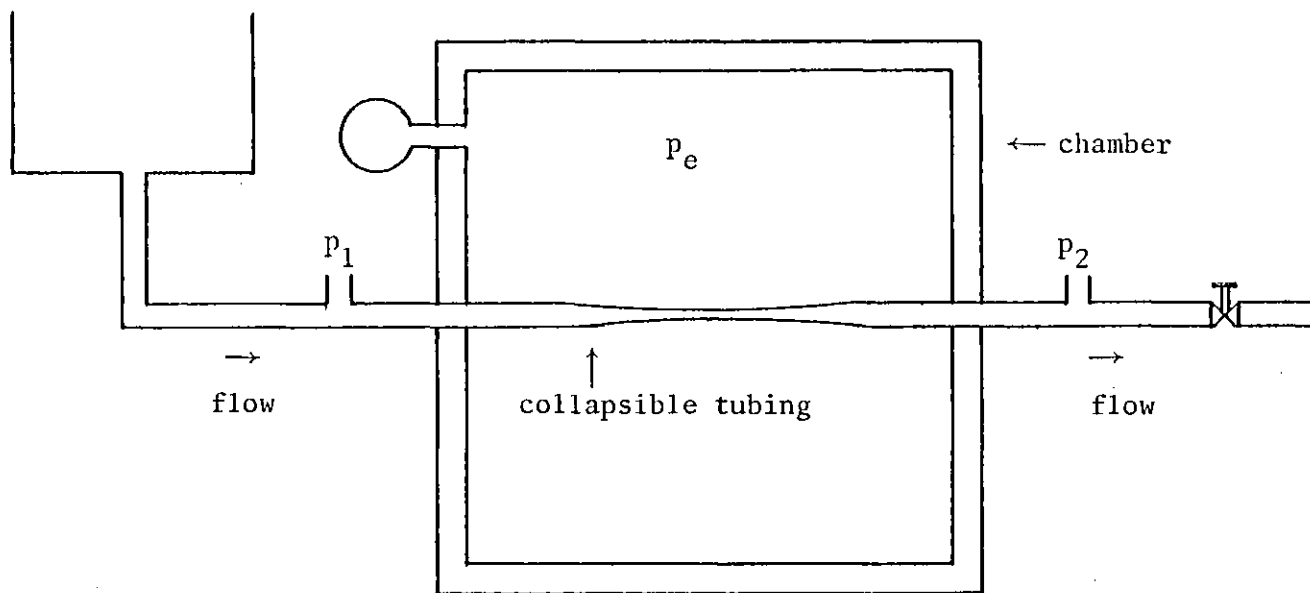


Figure 1.6. Experimental apparatus.

"for a given tube, there seems to be a critical flow, characteristic only of the collapsible tube, which determines when oscillations are initiated". Further, Brower and Scholten propose that this instability occurs when the mean fluid velocity in the tube exceeds the "phase velocity" (the speed of propagation of a small pressure disturbance along the elastic tube), or more precisely, the low frequency limit of the phase velocity. This proposed connection between the phase and fluid velocities and the stability of the fluid-tube system has appeared also in recent theoretical studies (see below).

For any given tube law a larger mass flow rate implies a faster pressure response, i.e. a larger value of μ , as well as an increased Reynolds number. When the appropriate scalings have been adopted, it is μ , not the Reynolds number, which appears explicitly in the problems considered in this study. Accordingly, Brower and Scholten's proposals can be restated in the form: for any given tube there is a critical value of μ , μ_c say, such that the fluid-tube system will become unstable spontaneously when μ exceeds μ_c , and that μ_c is the minimum value of μ for which the mean fluid velocity can match the phase velocity at any stage of the collapse.

Although the evidence cannot be regarded as conclusive, Brower and Scholten feel that their experimental results are consistent with the above hypothesis. The results of the present study are also consistent with this hypothesis, in the sense that for all tubes considered satisfying (1.4) there exists a value of μ , $\bar{\mu}_c$ say, such that both the analytical and numerical methods applied to the problem fail to produce a solution for $\mu > \bar{\mu}_c$. In particular, for a tube obeying (1.6) with $q = 1/2$ and $\epsilon = 1$, we find that the mean fluid velocity can match the inviscid phase velocity (see below) when $\mu = 18$, and we find a solution of the steady problem for $\mu < 18$, but not for $\mu \geq 18$ (see Section 3.3). A discussion of our results in connection with Brower and Scholten's hypothesis can be found in Section 5 below.

It appears that these oscillations occur only when the Reynolds number is large. Brower and Scholten (1975) report that the oscillations are initiated when the Reynolds number (calculated on the tube radius as in Section 4.1) is in the range 1600 to 4800 approximately, while oscillations are not observed when the Reynolds number is small (Fung and Sobin 1972).

We turn now to theoretical studies of flow in collapsible tubes. Rubinow and Keller (1972) assumed that Poiseuille flow is valid locally and produced a simple model of steady flow of a viscous fluid in a collapsible tube. Under certain conditions this model predicts an upper limit for the mass flow Q . This limit was found without considering the phase velocity. We note that for a collapsible tube a high Reynolds number incoming flow is not necessarily incompatible with locally valid Poiseuille flow. For example, for a collapsible channel we find that if the Reynolds number is large and the pressure response slow then the flow is viscous dominated and has a Poiseuille form throughout most, if not all, of the collapse (Section 3.5). For low Reynolds number flows, Wild et al. (1977) extended the work of Rubinow and Keller (1972) to include the minor effects of inertia to first order, a non-uniform external pressure distribution, and tubes of elliptical cross-section. In a series of papers, Griffiths (1969; 1971a; 1971b) considers an inviscid one-dimensional model, and finds that the ratio of fluid velocity to phase velocity is an important parameter concerning the stability of such a system. Later, Griffiths (1975a,b) extended this model, studying a steady two-dimensional flow near an elastic constriction. Oates (1975) includes a frictional term in the governing equation of a steady one-dimensional flow model, and gives a simple stability argument which indicates that an inviscid steady one-dimensional flow in a collapsible pipe will become unstable if the fluid velocity exceeds the inviscid phase velocity.

The most interesting papers presenting one-dimensional models of flow in collapsible tubes are probably those by Shapiro (1977), which is concerned with steady flow and draws analogies with flows in gas dynamics and open channels with free surfaces, and Kamm and Shapiro (1979), which is concerned with unsteady flow, including the effects of friction, inflow from tributaries, and various non-uniformities. We do not intend to comment on these papers in detail, but note that an important conclusion is that if, in the absence of special conditions (which are not found in our problems), the fluid velocity exceeds the phase velocity then steady flow is impossible and flow limitation usually occurs, a phenomenon said to be analogous to choking in a nozzle in gas dynamics.

We stress that caution is necessary when interpreting results from the studies discussed above, as their relationship to real fluid flows or the Navier-Stokes equation is by no means certain. However, it is clear that the ratio of fluid to phase velocity is an important parameter for one-dimensional flows, and that this ratio should not be ignored when considering more realistic flows.

We will now briefly outline some of the attempts that have been made to find an expression for the phase velocity. By "phase velocity" we refer to the speed of propagation of a small disturbance relative to the average cross-sectional velocity of the fluid. The velocity of the pressure disturbance will be known as the "pulse velocity". The phase velocity referred to above is that for a system basically at rest, where the only motion is that of the disturbance and the pulse and phase velocities are the same. We now consider attempts to find the phase velocity of such a system. The original equation is the so-called Moens-Korteweg equation

$$c_0 = \left(\frac{Eh}{2a\rho} \right)^{1/2} \quad (1.7a)$$

where c_0 is the dimensional phase velocity, E , h and a are the Young's modulus, thickness and internal radius of the tube respectively, and ρ is the density of the fluid. This expression was obtained by, amongst others, Lamb (1898), who found a second solution also, viz.

$$c_1 = \left[\frac{E}{\rho_1(1 - \sigma^2)} \right]^{1/2}, \quad (1.7b)$$

where ρ_1 and σ are respectively the density and Poisson's ratio of the tube material. Note that these formulae apply to thin-walled cylindrical elastic tubes which have a uniform stress distribution in the tube wall and are filled with a compressible inviscid fluid. They do not apply to collapsible tubes which may change shape. If the fluid in a tube can be regarded as inviscid and incompressible, the velocity of the pulse wave is uniform across the tube, and the non-dimensional cross-sectional area of the tube is given by $A = A(p)$, then the dimensionless phase velocity c is given by

$$c = \left(A \frac{dp}{dA} \right)^{1/2}, \quad (1.8)$$

a formula presented by Bramwell and Hill (1922).

A number of studies have been published concerning the phase velocity in fluid-tube systems that are more realistic physically than those discussed above. In a linearized analysis of the propagation of infinitesimally small waves in a thin-walled tube, Morgan and Kiely (1954) studied the effects on the wave motion of fluid viscosity and internal damping in the tube wall. For a similar system, Womersley (1955, 1957) studied the effects of a number of factors, including wall viscosity and internal viscous damping and elastic constraint of the tube wall. Atabek and Lew (1966) examined, again in linearized fashion, the problem of an elastic tube with initial stressing. Atabek (1968) studied the effect on phase velocity of tethering the tube. Cox (1968) considered a thick-walled visco-elastic tube, and later extended his study to include the effects of wall compressibility (Cox 1970). Kresch and Noordergraaf (1969) made a simple attempt to include the effects on the phase velocity of a change in shape of the tube. However, their results, if correct, are difficult to apply as they include a shape factor which was not determined exactly.

The most detailed studies of wave propagation in a compliant tube are those of Rubinow and Keller (1971, 1978). They investigated small amplitude, axially symmetric waves in thin-walled elastic or visco-elastic tubes containing a viscous (Rubinow and Keller 1971) or inviscid fluid (Rubinow and Keller 1978). They consider both compressible and incompressible fluids at all frequencies of propagation. Commonly (see e.g. Morgan and Kiely 1954, Womersley 1957), it is assumed that the fluid is incompressible and that the waves are long wavelength, low frequency waves, assumptions that are usually valid for the flow and pressure pulse of blood in mammalian arteries. Each wave solution of the equations of motion is called a mode of propagation, and Rubinow and Keller found that for each frequency of propagation there are infinitely many modes of propagation. However, all except two "tube modes" are acoustic in nature, and are absent when the fluid is incompressible. The two tube modes are related to the two solutions (c_0 and c_1 above) found by Lamb (1898). Most investigators consider

only one of the tube modes, that relating to c_0 . Rubinow and Keller (1971) discuss some reasons for this. We merely observe that for a thin-walled tube c_0/c_1 is small and that under appropriate conditions c_0 and c from (1.8) are the same. An important result from Rubinow and Keller (1978) is that under certain conditions, e.g. those found in the human aorta, the phase velocities from the tube modes are close to the inviscid phase velocities c_0 and c_1 . Brower and Scholten (1975) found that for a collapsible latex tube this result applies to the "low frequency limit" of the experimentally determined phase velocity, where the inviscid phase velocity is found from (1.8). Thus there is some justification for the use of the inviscid phase velocity c when considering tubes of practical interest in which the fluid is basically at rest.

We will now consider the phase velocity of a system with a steady stream in a compliant tube. Unfortunately, comparatively little work has been done on this problem. Morgan and Ferrante (1955) studied a thin-walled cylindrical tube using a linear theory of elasticity. They found that if the fluid is inviscid and incompressible and the steady stream has constant uniform velocity u_i , then the phase velocity is given by c_0 (equation 1.7a) and the pulse velocities by $u_i \pm c_0$. Also, they found that the form of the steady stream, the viscosity of the fluid, and the inertia of the wall can all affect the phase and pulse velocities. We have extended some of Morgan and Ferrante's results to a collapsible tube with cross-sectional area $A = A(p)$ (Appendix 6). In particular, for an incompressible, inviscid fluid with the steady stream given by $u_i = \text{constant}$ and the pressure by $p_i = \text{constant}$, we have found that the phase velocity is given by (1.8) and the pulse velocities by $u_i \pm c$. Note that the only assumption additional to those of Morgan and Ferrante required here is that the disturbance is small compared to u_i , and that under appropriate conditions this result applies also to inviscid flows in collapsing tubes (see Appendix 6). Womersley (1957) considers a tube filled with a streaming viscous fluid. His results suggest that under certain conditions the presence of a steady stream can increase the phase velocity.

We found little in the literature on the phase velocity in the

presence of a steady stream, and none on the problem of most interest to us, that of a viscous flow with the fluid and phase velocities of the same order. When the phase velocity is required explicitly we will use c from (1.8), as this expression can be regarded as approximately correct under certain conditions, and has the advantage of simplicity.

Section 2. Channels with a fine collapse

2.1. Flows with a fast pressure response

In this section we consider a channel-fluid system in which the walls can be displaced by a small distance only and are highly responsive to changes in pressure. In particular, we assume that $0 < \epsilon \ll 1$ and $1 \ll \mu \ll R$. The tube law suggests the pressure scaling $p = \mu^{-1}P$, where $P = O(1)$, which, since we require the pressure gradient to match with the incoming Poiseuille gradient, introduces the long streamwise length scaling $x = \mu^{-1}RX$.

Smith (1976 a,b) has studied the problem of high Reynolds number flow through constricted tubes in which the constriction is small, is known explicitly in terms of x , and has slope α where $R^{-1} \ll \alpha \ll R^{-1/3}$. This restriction ensures that the streamwise length scale remains large. For asymmetric flows Smith reports large nonlinear effects close to the walls, including a free interaction upstream which can eventually lead to separation. For symmetric flows, although the flow is affected nonlinearly close to the wall, there is no such significant upstream influence until the slope of the constriction is increased to $O(R^{-1/3})$ and the length scale shortened to $O(1)$. Even then the upstream influence is restricted to the core flow, and the wall layer is not affected until the constriction is reached. The constriction height must be increased to $O(R^{-1/6})$ with x of $O(1)$ for there to be any significant nonlinear upstream response in the wall layer (Smith 1978a). In view of Smith's results, it is not surprising that, since the scaling on x is large and the collapsible nature of the channel ensures that the adjustment of the flow close to the wall remains linear, no significant upstream effects are found in the channel-fluid systems considered in this section.

Let us now further restrict μ such that $1 \ll \mu \ll \epsilon^{-3/2}$. We propose that the major viscous effects occur in thin wall layers of thickness order $\delta = \mu^{-1/3}$, and that in the channel core the motion takes the form of a small inviscid rotational perturbation to the Poiseuille flow; viz.

$$\left. \begin{aligned}
 u &= U_0(y) + \varepsilon \delta u_1(X, y) + o(\varepsilon \delta), \\
 v &= \varepsilon \delta^{-2} R^{-1} v_1(X, y) + o(\varepsilon \delta^{-2} R^{-1}), \\
 P &= -X + \varepsilon \delta P_1(X, y) + o(\varepsilon \delta^{-2}).
 \end{aligned} \right\} \quad (2.1)$$

The transverse momentum equation implies that $P_1 = P_1(X)$ is independent of y , and after some manipulation the conservation equations for mass and streamwise momentum produce the perturbation solutions

$$\left. \begin{aligned}
 u_1 &= -\frac{P_1(X)}{U_0(y)} \left[1 + U_0(y) U_0'(y) \int_0^y U_0^{-2}(\eta) d\eta \right], \\
 v_1 &= P_1'(X) U_0(y) \int_0^y U_0^{-2}(\eta) d\eta.
 \end{aligned} \right\} \quad (2.2)$$

Here and below a prime will denote differentiation with respect to the relevant variable. It is the wall layer solution (see below) which determines the pressure perturbation P_1 . We see from (2.2) that there can be no upstream influence in the core unless it is forced by the wall layer, and that (2.1) will match with the incoming Poiseuille flow if $P_1 \rightarrow 0$ as $X \rightarrow -\infty$.

For a fixed symmetric constriction the core flow is undisturbed if the length scaling remains large (Smith 1976a). This would be true here only if P_1 were zero, which, as will soon be demonstrated, does not hold. We find that P_1 is negative, and hence the effect of the core perturbation is to concentrate the flow towards the centre of the channel. If $-P_1$ increases downstream then (2.1) will become invalid when $-P_1$ is $O(\delta^{-1} \varepsilon^{-1})$.

As $y \rightarrow 1$ both u_1 and v_1 remain finite and non-zero. If $y = 1 - \delta Y$ then from (2.2)

$$\left. \begin{aligned}
 u_1 &\sim P_1 [\ln Y + O(\delta)], \\
 v_1 &\sim P_1' [1 + O(\delta)],
 \end{aligned} \right\} \quad (2.3)$$

as $y \rightarrow 1^-$. The solution in the viscous wall layer must match to these

slip velocities. In fact we do not obtain a matching for u_1 . However, we note that (2.3) suggests that there will be a minor term of $O(\epsilon\delta)$ in the boundary layer expansion for u .

The core solution suggests that in the upper viscous wall layer

$$\left. \begin{aligned} u &= \delta Y - \delta^2 Y^2/2 + \epsilon \hat{u}_1(X, Y) + o(\epsilon), \\ v &= -\epsilon \delta^{-2} R^{-1} \hat{v}_1(X, Y) + o(\epsilon \delta^{-2} R^{-1}), \end{aligned} \right\} (2.4)$$

with the pressure p as in (2.1). Substitution of (2.4) in the Navier-Stokes equations shows that the secondary motion in the wall layer is governed by the linearized boundary layer equations. That is, u_1 , v_1 and P_1 must satisfy

$$\left. \begin{aligned} Y \frac{\partial \hat{u}_1}{\partial X} + \hat{v}_1 &= -P_1' + \frac{\partial^2 \hat{u}_1}{\partial Y^2}, \\ \frac{\partial \hat{u}_1}{\partial X} + \frac{\partial \hat{v}_1}{\partial Y} &= 0. \end{aligned} \right\} (2.5)$$

In turn the boundary conditions of no slip at the wall, merging of (2.4) with (2.1) at the edge of the layer, and matching to the incoming Poiseuille flow, are given by

$$\left. \begin{aligned} \hat{v}_1 &= 0 \text{ and } \hat{u}_1 = -S(-X) \text{ at } Y = 0, \\ \hat{u}_1 &\rightarrow 0 \text{ and } \hat{v}_1 \rightarrow -P_1' \text{ as } Y \rightarrow \infty, \\ \hat{u}_1 &\rightarrow 0 \text{ and } \hat{v}_1 \rightarrow 0 \text{ as } X \rightarrow -\infty, \end{aligned} \right\} (2.6)$$

where $S(-X)$ is from the tube law (1.4).

The linear boundary layer problem defined by (2.5) and (2.6) is that of a shear flow along a wall which has a small fixed disturbance. The method of solution is basically that used by Smith (1976b) for an unsteady tube constriction. As several similar

problems will be encountered in the present study we will present the method in some detail. Applying the Generalised transform with respect to X , $f^*(\phi, Y) = \int_{-\infty}^{\infty} f(X, Y) e^{-i\phi X} dX$, the equations of motion (2.5) become

$$\left. \begin{aligned} i\phi Y \hat{u}_1^* + \hat{v}_1^* &= -i\phi P_1^* + \frac{\partial^2 \hat{u}_1^*}{\partial Y^2}, \\ i\phi Y \hat{u}_1^* + \frac{\partial \hat{v}_1^*}{\partial Y} &= 0. \end{aligned} \right\} (2.7)$$

Upon differentiating the momentum equation in (2.7) with respect to Y , we find the solution

$$\frac{\partial \hat{u}_1^*}{\partial Y} = B(\phi) \text{Ai}(\alpha Y),$$

where $\alpha = (i\phi)^{1/3}$, Ai is the Airy function, and $B(\phi)$ is a function to be determined. By setting $Y = 0$ in the momentum equation we now obtain

$$B(\phi) = \alpha^2 P_1^* / \text{Ai}'(0). \quad (2.8a)$$

It follows that the solution of (2.7) which satisfies the outer matching condition in (2.6) is

$$\left. \begin{aligned} \hat{u}_1^* &= -B(\phi) \int_Y^{\infty} \text{Ai}(\alpha \eta) d\eta, \\ \hat{v}_1^* &= i\phi B(\phi) \int_0^Y dt \int_{\eta}^{\infty} \text{Ai}(\alpha \eta) d\eta. \end{aligned} \right\} (2.8b)$$

The no slip condition at the wall implies that

$$P_1^* = 3\text{Ai}'(0) S^* / \alpha,$$

where S^* is the Generalised transform of $S(-X)$.

Since P_1^* is regular in $\text{Im}\phi < 0$, we see immediately that $P_1 = 0$ for $X < 0$. Hence (2.8) satisfies the upstream matching condition in (2.6). Further, there is no significant upstream influence in the present problem, and there is a definite point (the origin) at which the flow first deviates from the incoming Poiseuille flow, and from which numerical techniques can be applied if necessary.

Inverting the transforms in (2.9) produces

$$P_1 = \frac{3\text{Ai}'(0)}{\Gamma(1/3)} \int_0^X (X-t)^{-2/3} S(-t) dt. \quad (2.10)$$

If the skin friction is given by $\tau = -1 + \epsilon\delta^{-1}\tau_1 + o(\epsilon\delta^{-1})$, where $\tau = \partial u/\partial y$ at $y = y_w$, then we find

$$\tau_1 = -\frac{3\text{Ai}(0)}{\text{Ai}'(0)\Gamma(2/3)} \int_0^X (X-t)^{-1/3} \frac{dS(-t)}{dt} dt. \quad (2.11)$$

If $S(-t) \sim kt^n$ for $0 < t \ll 1$, where $n > 0$, then (2.10) and (2.11) yield

$$\left. \begin{aligned} P_1 &\sim 3\text{Ai}'(0) \frac{\Gamma(n+1)}{\Gamma(n+4/3)} k X^{n+1/3}, \\ \tau_1 &\sim -\frac{3\text{Ai}(0)}{\text{Ai}'(0)} \frac{\Gamma(n)}{\Gamma(n+2/3)} nkX^{n-1/3}, \end{aligned} \right\} (2.12)$$

for $0 < X \ll 1$. We see from (2.12) that P_1 will always be continuous at the origin, but if $0 < n < 2/3$ then P_1 will have infinite slope as $X \rightarrow 0+$, and finite but discontinuous slope at $X = 0$ if $n = 2/3$. The situation is more complicated for the skin friction perturbation τ_1 . If $1/3 < n < 4/3$ then τ_1 is continuous with infinite slope at the origin, while if $0 < n < 1/3$ then (2.12) predicts τ_1 will be infinite as $X \rightarrow 0+$. We will not investigate these irregularities in the solution further, but will assume that they can be smoothed out

locally by expanding close to the origin on a shorter length scale, as is usually the case in boundary layer flows.

We turn our attention now to the flow far downstream where $X \gg 1$. Suppose that for $-\mu p \gg 1$

$$S(\mu p) \sim 1 - K(-\mu p)^{-N},$$

where K is a positive $O(1)$ constant and $N > 0$. Then for $X \gg 1$

$$S \sim 1 - KX^{-N}, \quad (2.13)$$

and from (2.10)

$$P_1 \sim 9 \frac{Ai'(0)}{\Gamma(1/3)} X^{1/3} + O(X^{-N+1/3}). \quad (2.14)$$

We could now develop a formal asymptotic flow structure valid for large X (c.f. equation 3.53 in Section 3.4). However, for our purposes the important feature of this asymptotic behaviour is that since $P_1 \propto X^{1/3}$ then the wall layer thickness is also proportional to $X^{1/3}$. Thus, as $X \rightarrow \infty$ the boundary layer thickens until it merges with the core flow when X is $O(\delta^{-3}) (= O(\mu))$. Inspection of (2.1) reveals that when this occurs both the pressure and core velocity perturbations are $O(\varepsilon)$. Hence, we will now investigate the viscous perturbation to the Poiseuille flow given by

$$\left. \begin{aligned} u &= U_0(y) + \varepsilon \tilde{u}_1(\tilde{X}, y) + o(\varepsilon), \\ v &= \varepsilon R^{-1} \tilde{v}_1(\tilde{X}, y) + o(\varepsilon R^{-1}), \\ p &= -\tilde{X} + \varepsilon \tilde{p}_1(\tilde{X}, y) + o(\varepsilon), \end{aligned} \right\} (2.15a)$$

where $\tilde{X} = R^{-1}x$. The no slip condition at the walls and mass conservation require

$$\left. \begin{aligned} \tilde{v}_1 = 0 \text{ and } \tilde{u}_1 = -1 \text{ at } y = \pm 1, \\ \int_{-1}^1 u_1 dy = 0, \end{aligned} \right\} (2.15b)$$

respectively.

As before, the transverse momentum equation implies that the pressure perturbation is independent of y , i.e. that $\tilde{P}_1 = \tilde{P}_1(\tilde{X})$. One solution of (2.15) is

$$\left. \begin{aligned} \tilde{u}_1 &= \frac{1}{2} (1 - 3y^2), \\ \tilde{v}_1 &= 0, \\ \tilde{P}_1 &= -3\tilde{X} + \tilde{P}_0, \end{aligned} \right\} (2.16)$$

where \tilde{P}_0 is an arbitrary constant.

This solution was obtained without considering any initial conditions and, clearly, it does not match with the incoming core flow given by (2.1) and (2.2). However, (2.16) is the $O(\epsilon)$ term in the expansion of the Poiseuille flow which can exist in a channel of half-width $1 - \epsilon$ and mass flow equal to that of the present problem. Thus (2.16) can be regarded as a solution for (2.15) which is valid far downstream in the limit as $\tilde{X} \rightarrow \infty$ (and $p \rightarrow -\infty$). It may be that the most practical way to obtain a solution of (2.15) consistent with (2.1) is to proceed numerically. Alternatively, it may be possible to use eigenvalue solutions to effect a matching upstream. In Section 2.2 below we study eigenvalue solutions which are $O(\epsilon)$ in magnitude and develop on an $O(R)$ streamwise length scale. The eigenvalues found are such that the downstream decay of the eigenvalue solutions is extremely fast, which suggests that any solution of (2.15) will quickly take the form of (2.16).

This concludes our study of the problem with $\mu \ll \epsilon^{-3/2}$. It is felt that a broadly satisfactory description of the fluid-channel system has been provided.

Suppose now that $\lambda = \mu\epsilon^{3/2}$ is of $O(1)$. As above, we assume

that the pressure gradient must match with the incoming Poiseuille gradient, and that the pressure is initially of $O(\mu^{-1})$. We propose that the core flow is given by an inviscid rotational perturbation to the Poiseuille flow, that is

$$\left. \begin{aligned} u &= U_0(y) + \varepsilon^{3/2} U_1(X, y) + o(\varepsilon^{3/2}), \\ v &= R^{-1} V_1(X, y) + o(R^{-1}), \\ p &= \varepsilon^{3/2} P(X, y) + o(\varepsilon^{3/2}), \end{aligned} \right\} (2.17)$$

where $x = \varepsilon^{3/2} R X$. Note that here we have used ε to scale the variables instead of μ . Again, the pressure $P = P(X)$ is independent of y . The solution for (U_1, V_1) is obtained directly from (u_1, v_1) in (2.2) by replacing P_1 by $P + X$. Slip velocities, similar to those of (2.3), can be obtained by expanding (U_1, V_1) for $1 - y \ll 1$.

Redefining $Y = (1 - y)/\varepsilon^{1/2}$, the flow structure in the upper viscous wall layer is given by

$$\left. \begin{aligned} u &= \varepsilon^{1/2} Y + \varepsilon \hat{U}_1(X, Y) + o(\varepsilon), \\ v &= -R^{-1} \hat{V}_1(X, Y) + o(R^{-1}). \end{aligned} \right\} (2.18)$$

The governing equations in upper wall layer are, with appropriate changes of variable, the linear boundary layer equations (2.5). The boundary conditions of no slip at the wall, merging of (2.17) and (2.18) at the outer edge of the layer, and matching to the incoming Poiseuille flow, are in turn

$$\left. \begin{aligned} \hat{V}_1 &= 0 \text{ and } \hat{U}_1 = -S(\lambda P) \text{ at } Y = 0, \\ \hat{U}_1 &\rightarrow -\frac{1}{2} Y^2 \text{ and } \hat{V}_1 \rightarrow -(P' + 1) \text{ as } Y \rightarrow \infty, \\ \hat{U}_1 &\rightarrow -\frac{1}{2} Y^2 \text{ and } \hat{V}_1 \rightarrow 0 \text{ as } X \rightarrow -\infty. \end{aligned} \right\} (2.19)$$

Let $\hat{U}_1 = \bar{U} - \frac{1}{2} Y^2$ and $P = \bar{P} - X$. Proceeding as above, we find that the transform solution for \bar{U} , \hat{V}_1 and \bar{P} is given, with appropriate changes of variable, by (2.8). Inverting the transform of \bar{U} at $Y = 0$

and applying the no slip condition from (2.19) produces

$$S[\lambda\bar{P}(X) - \lambda X] = \frac{1}{3\text{Ai}'(0)\Gamma(2/3)} \int_0^X (X-t)^{-1/3} \frac{d\bar{P}(t)}{dt} dt, \quad (2.20)$$

the solution of which determines P , and hence y_w , in terms of X .

Again no significant upstream influence has been found, and $u = U_0(y)$ in $X < 0$. We note that it is the Poiseuille pressure, $-X$, that forces (2.20) to have a nontrivial solution for $\bar{P} = P + X$ in $X > 0$. More generally, it is the pressure from the Poiseuille flow that forces the change in the position of the walls, and thus the change in the flow and the pressure itself.

Writing the skin friction at the upper wall as

$$\tau = -1 + \epsilon^{1/2}\tau_1 + o(\epsilon^{1/2}),$$

where $\tau = \partial u / \partial y$ at $y = y_w$, we find that

$$\tau_1 = -\frac{\text{Ai}(0)}{\text{Ai}'(0)\Gamma(1/3)} \int_0^X (X-t)^{-2/3} \frac{d\bar{P}(t)}{dt} dt. \quad (2.21)$$

Close to the origin the pressure deviation \bar{P} and skin friction perturbation τ_1 have behaviours similar to those in (2.12), i.e. $\bar{P} \propto X^{n+1/3}$ and $\tau_1 \propto X^{n-1/3}$ as $X \rightarrow 0+$. Again it will be assumed that an expansion on a shorter length scale can smooth out any local irregularity. As before, far downstream where $1 - S \ll 1$ the boundary layer thickness grows as $X^{1/3}$, and hence the solution above becomes invalid when X is $O(\epsilon^{-3/2})$ ($= O(\mu)$). The flow then takes the form of (2.15), with (2.16) as the limit solution far downstream.

Figures 2.1 - 2.3 present graphically the solutions for the pressure deviation \bar{P} , the skin friction perturbation τ_1 , and the channel wall deviation S for a channel with $S(\lambda P) = 1 - [1 + (\lambda P)^2]^{-1/4}$. Also shown in Figure 2.1 is the predicted downstream behaviour for \bar{P} when $S \rightarrow 1$ as $X \rightarrow \infty$ (see equation (2.14)). It is noticeable that, except for λ large and X small, the magnitude of \bar{P} is small compared with that of the Poiseuille pressure $-X$. For λ small, the change

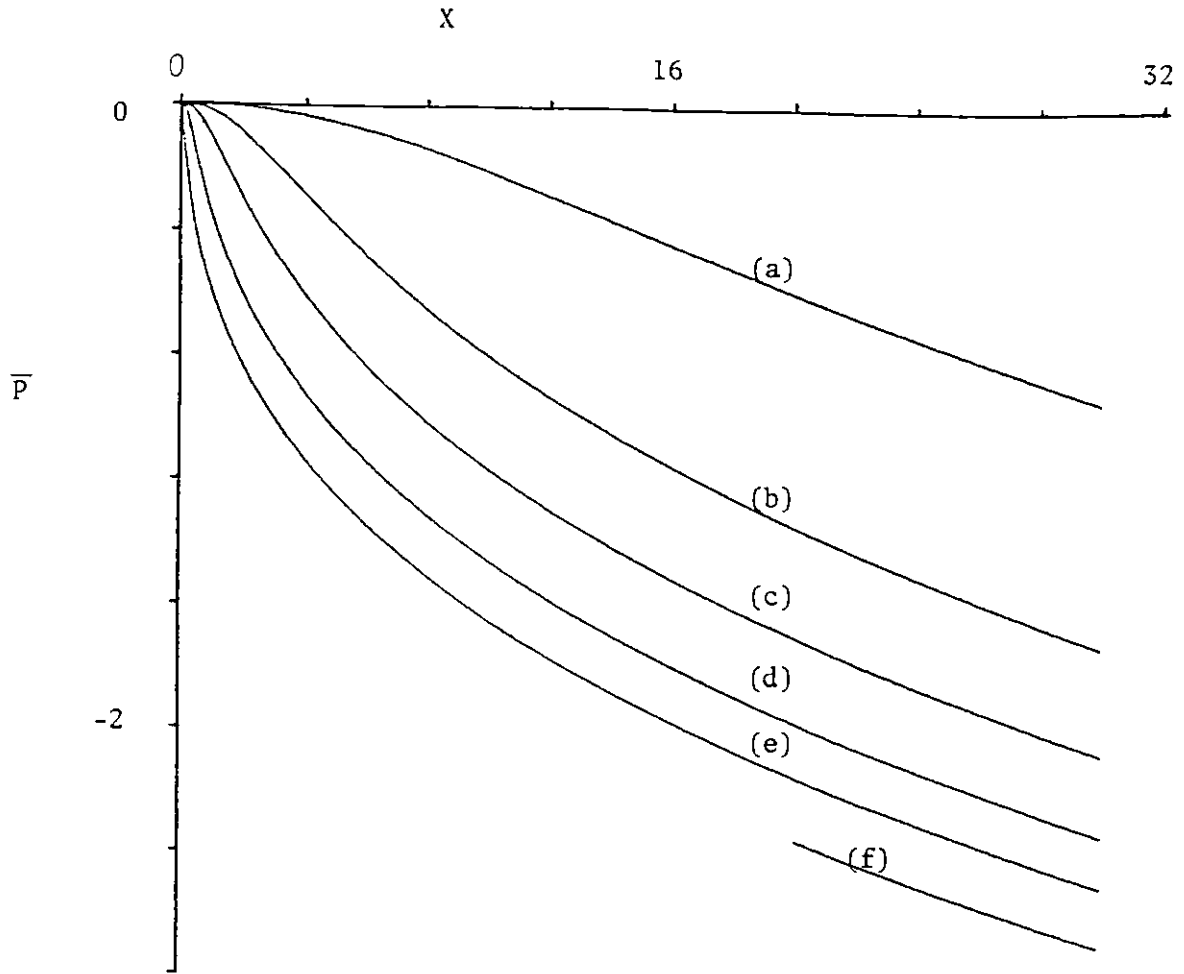


Figure 2.1. The pressure deviation $\bar{P} = P + X$ against X for a channel with $S(\lambda P) = 1 - [1 + (\lambda P)^2]^{-1/4}$ and λ of $O(1)$:
 (a) $\lambda = .1$, (b) $\lambda = .4$, (c) $\lambda = 1.0$, (d) $\lambda = 3.0$, (e) $\lambda = 10.0$,
 (f) $\bar{P} = 9 \frac{Ai'(0)}{\Gamma(1/3)} X^{1/3}$, from the far downstream analysis (see equation 2.14).

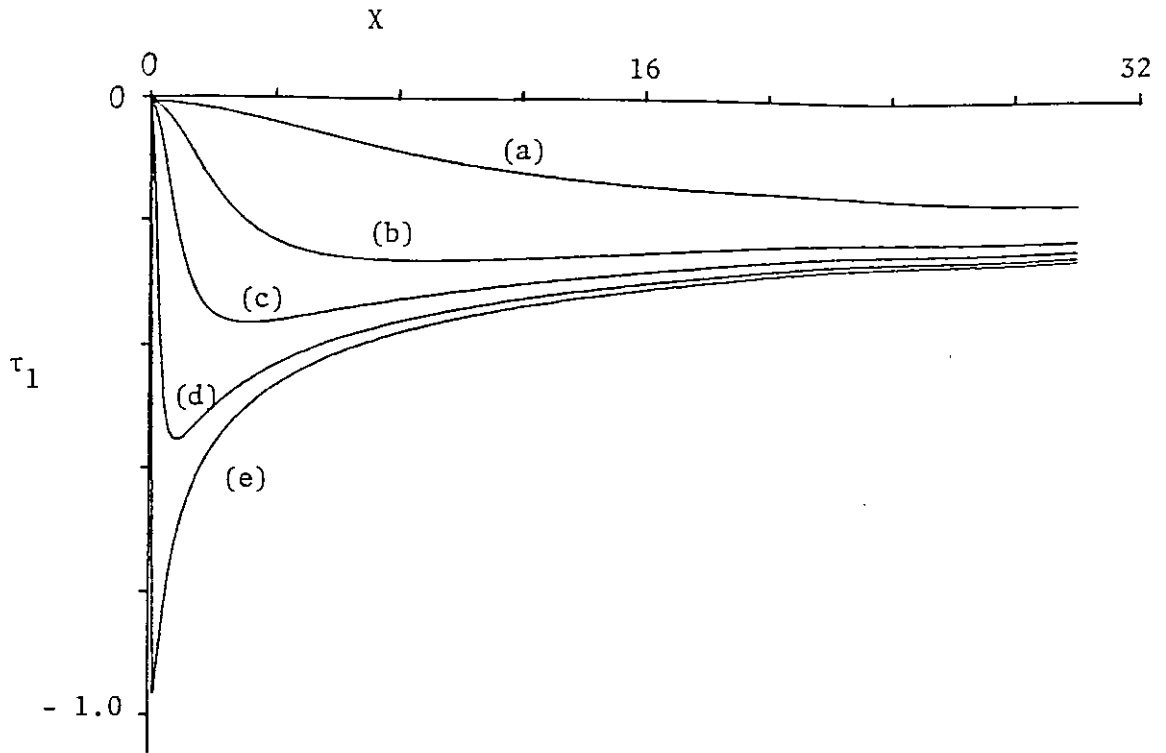


Figure 2.2. Skin friction perturbation τ_1 against X for various λ . See Figure 2.1 for details.

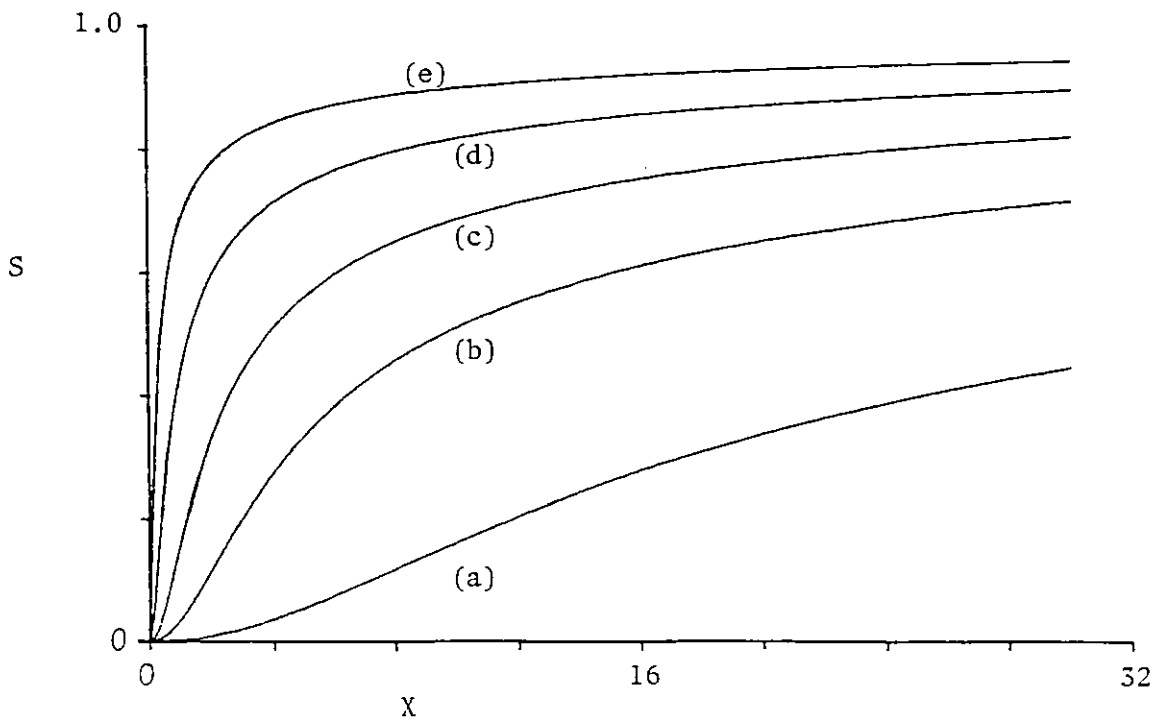


Figure 2.3. Channel deviation S against X for various λ . See Figure 2.1 for details.

in \bar{P} , τ_1 and S from zero at the origin is gradual and proceeds slowly downstream, and the values obtained were found to be consistent with those from the analysis for $\mu \ll \epsilon^{-3/2}$, as would be expected. Also as expected, larger values of λ lead to a faster change in all dependent variables. For very large values of λ , e.g. $\lambda = 10$, the major part of change in the channel width occurs close to the origin (Figure 3.3). With the present choice of S , it follows from (2.12) that $\tau_1 \propto \lambda^2 X^{5/3}$ as $X \rightarrow 0+$. Hence, although τ_1 and $d\tau_1/dX$ will be continuous at the origin, $|\tau_1|$ should increase rapidly with X if $\lambda \gg 1$ and $0 < \lambda X \ll 1$. As can be seen from Figure 2.2, this expected behaviour is realised, and $|\tau_1|$ reaches a maximum very close to the origin. The pressure deviation \bar{P} shows a similar concentration of effect close to the origin when $\lambda \gg 1$ (this can be seen more clearly by considering $d\bar{P}/dX$, whose behaviour is very similar to that of τ_1). Detailed examination of the solutions confirmed that they take the predicted form as $X \rightarrow \infty$ (see equations 2.13 and 2.14).

The solution obtained earlier for $\mu \ll \epsilon^{-3/2}$ can be derived from the solution found for λ of $O(1)$ by expanding for $\lambda \ll 1$. Also, the flow structure derived for λ of $O(1)$ is suggested by letting ϵ tend to δ^2 in (2.1) and (2.4). Thus, there is a natural development between the flow structures for $\mu \ll \epsilon^{-3/2}$ and $\lambda = \mu\epsilon^{3/2}$ of $O(1)$.

Clearly, for a fluid-channel system with $\lambda \gg 1$ it will be necessary to adopt a shorter streamwise length scaling, and to take into account the behaviour of $S(\mu p)$ for $0 < \mu p \ll 1$. This local problem arises also in the analysis found in Section 3.4 below for a system with ϵ of $O(1)$ and $\mu \gg 1$, and it is convenient to leave any discussion until then.

2.2 Flows with a moderate pressure response

We will now study channel-fluid systems which have a small wall variation ($\epsilon \ll 1$) and a moderate pressure response ($\mu = O(1)$). Requiring the pressure gradient to match with the incoming Poiseuille gradient introduces the scaling $x = RX$. The flow is given by a vis-

cous perturbation to the Poiseuille flow, viz.

$$\left. \begin{aligned} \psi &= \psi_0(y) + \epsilon \psi_1(X, y) + O(\epsilon^2), \\ p &= -X + \epsilon P_1(X, y) + O(\epsilon^2), \end{aligned} \right\} (2.22)$$

where $\psi(X, y)$ is the stream function and $\psi_0(y) = \frac{1}{2} (y - \frac{1}{3} y^3)$ is the Poiseuille term. The velocity perturbation is given by

$$(u_1, v_1) = (\partial \psi_1 / \partial y, -\partial \psi_1 / \partial X).$$

The transverse momentum equation implies that $P_1 = P_1(X)$ is independent of y , and substituting (2.22) in the streamwise momentum equation produces

$$U_0(y) \frac{\partial^2 \psi_1}{\partial X \partial y} - U_0'(y) \frac{\partial \psi_1}{\partial X} = -P_1'(X) + \frac{\partial^3 \psi_1}{\partial y^3}. \quad (2.23)$$

From mass conservation, no slip at the walls, and matching with the incoming Poiseuille flow in turn, the boundary conditions are

$$\left. \begin{aligned} \psi_1(X, \pm 1) &= 0, \\ \frac{\partial \psi_1}{\partial y}(X, \pm 1) &= -S(-\mu X), \\ \psi_1 &\rightarrow 0 \text{ as } X \rightarrow -\infty. \end{aligned} \right\} (2.24a)$$

These boundary conditions admit nonsymmetric solutions. If we require the flow to be symmetric then the conditions at $y = -1$ in (2.24) should be replaced by

$$\psi_1 = \frac{\partial^2 \psi_1}{\partial y^2} = 0 \text{ at } y = 0. \quad (2.24b)$$

We note that our problem here is similar to that defined by (2.15a,b) in the previous section. However, since the boundary conditions (2.24a) are X -dependent, (2.16) does not provide a solution

for the present problem, although it is the far downstream solution, valid in the limit as $X \rightarrow \infty$ and $S \rightarrow 1$.

For $X < 0$ the boundary conditions (2.24b) are homogeneous, and one possible solution is $\psi_1 = P_1 = 0$. However, there are also nontrivial eigenvalue solutions, which we will now investigate. Suppose that

$$\psi_1(X,y) = \sum_{n=1}^{\infty} f_n(y) e^{-\alpha_n X}, \quad (2.25)$$

where the α_n are a sequence of eigenvalues of increasing magnitude, the $f_n(y)$ are such that $|\epsilon f_n(y)| \ll 1$, and X includes an implicit change of origin. If we substitute (2.25) into (2.23) and differentiate with respect to y , we find that the $f_n(y)$ must satisfy

$$\frac{d^4 f_n}{dy^4} + \alpha_n \left\{ U_0(y) \frac{d^2 f_n}{dy^2} + f_n \right\} = 0. \quad (2.26a)$$

We will consider both symmetric and asymmetric modes, and take as boundary conditions

$$f_n(\pm 1) = \frac{df_n}{dy}(\pm 1) = 0. \quad (2.26b)$$

Essentially the same problem was studied by Wilson (1969) with reference to the entry flow in a channel. The results from Wilson of interest here are that the first eigenfunction is even (corresponding to an asymmetric flow), that all eigenvalues found are real and positive, and that all even eigenvalues are real. The eigenvalues found by Wilson were verified using numerical methods, and the first five are given in Table 2.1. Numerical experimentation indicated that there are no real negative eigenvalues. Certainly none exist between zero and -1000 . Thus it seems reasonable to assume that all the eigenvalues are real and positive, and hence that the smallest eigenvalue is 43.35. This suggests that any upstream disturbance will decay extremely quickly, and that there will be no significant upstream influence. It follows that any numerical integration of

n	α_n
1	43.35
2	56.43
3	146.61
4	172.56
5	313.29

Table 2.1. The eigenvalues α_n (from Wilson 1969).

the governing equations can be started at the origin.

Returning to the basic problem formed by (2.23) and (2.24), it appears that, in general, the solution must be found numerically. One exception is when $S(\mu p)$ can be expressed as a linear sum of exponentials. In this case a partial solution, which is closely related to the eigenvalue solutions, can be obtained using separation of variables. Suppose that S is given by, or can be approximated by

$$S(p) = \begin{cases} 0 & p > 0, \\ 1 + \sum_{n=1}^N A_n e^{\beta_n p} & p < 0, \end{cases} \quad (2.27)$$

where μ has been absorbed into the β_n , $\sum_{n=1}^N A_n = -1$, to ensure that

S is continuous, and the $\beta_n > 0$ do not equal any of the odd eigenvalues. Since μ is $O(1)$, the smallest β_n must be of $O(1)$. Consider

$$\psi_1 = g_0(y) + \sum_{n=1}^N g_n(y) e^{-\beta_n X}. \quad (2.28)$$

For $n \geq 1$, the $g_n(y)$ must satisfy the eigenvalue equation (2.26a) with α_n replaced by β_n . If we require the flow to be symmetric, then from (2.24a,b) the boundary conditions are

$$\left. \begin{aligned} g_n(0) &= g_n(1) = 0, \\ \frac{d^2 g_n}{dy^2}(0) &= 0, \\ \frac{dg_n}{dy}(1) &= -A_n, \end{aligned} \right\} \quad (2.29)$$

for $n \geq 0$, where $A_0 = 1$. Note that no upstream matching condition has been specified at this point. The solution for $g_0(y)$ is found to be

$$g_0(y) = \frac{1}{2} (y - y^3).$$

There are two basic power series solutions for each $g_n(y)$ that are relevant here, viz.

$$g_n^I(y) = y \sum_{m=0}^{\infty} a_{2m}^n y^{2m},$$

$$g_n^{II}(y) = y^3 \sum_{m=0}^{\infty} b_{2m}^n y^{2m},$$

where the coefficients are related by

$$2(m+2)(m+3)(m+4) a_{m+3}^n + \beta_n \{ (m+2) a_{m+1}^n - (m-2) a_{m-1}^n \} = 0 \quad m \text{ odd},$$

and

$$2(m+2)(m+3)(m+4) b_{m+1}^n + \beta_n \{ (m+2) b_{m-1}^n - (m-2) b_{m-3}^n \} = 0 \quad m \geq 3 \text{ odd},$$

with $a_0^n = a_2^n = b_0^n = 1$ and $b_2^n = -\beta_n/40$.

The mass conservation and symmetry conditions are satisfied by

$$g_n(y) = c_n \{ g_n^{II}(1) g_n^I(y) - g_n^I(1) g_n^{II}(y) \},$$

as is the no slip condition if

$$c_n = -A_n \left\{ g_n^{II}(1) \frac{dg_n^I}{dy}(1) - g_n^I(1) \frac{dg_n^{II}}{dy}(1) \right\}^{-1},$$

where $n \geq 1$. This completes the solution of ψ_1 as given by (2.28).

Expressing the pressure perturbation in the form

$$P_1(X) = P_0(X) + \sum_{n=1}^N p_n e^{-\beta_n X}, \quad (2.30)$$

where the p_n are constants, equation (2.23) can now be used to obtain

$$P_0(X) = -3X - \sum_{n=1}^N p_n,$$

$$p_n = -\frac{1}{2} - 6 \frac{c_n}{\beta_n} (g_n^{II}(1) - g_n^I(1)).$$

As in Section 2.1, a solution has been found without considering any initial conditions. This is possible because the partial differential equation (2.23) does not impart its parabolic nature to the ordinary differential equation (2.26a), and an arbitrary condition cannot be imposed on its solution at an initial value of X . In general, ψ_1 as given by (2.28) will not be zero at the origin, and the solution obtained above is incomplete and will not match with the incoming Poiseuille flow. However, any further components of the solution must have homogeneous boundary conditions, and the extremely rapid decay of the eigenvalue solutions found above suggests that the solution given for ψ_1 will not show any significant inaccuracy except in the immediate vicinity of the origin where $X\alpha_1$ is $O(1)$ or less. We compared the analytical solutions for ψ_1 and P_1 ((2.28) and (2.30)) with the numerical solution of (2.23) and (2.24) (obtained using a standard implicit difference scheme) for various $S(\mu p)$ of the form (2.27). The results supported this last conjecture, i.e. that (2.28) and (2.30) provide a generally accurate solution. We note that it may be possible to use the eigenvalue solutions to effect a matching at the origin. However, numerical integration established that the eigenfunctions $f_n(y)$ are not orthogonal, and there is no direct way of doing this. We note also that in the limit as $X \rightarrow \infty$ downstream, (2.28) and (2.30) take the expected form (2.16).

The solution of (2.23) and (2.24) was found numerically for various tube laws of the algebraic form (1.6), as well as for those of the form (2.27). As would be expected from the results of Section 2.1 for a channel with $\mu \ll \epsilon^{-3/2}$, the pressure, pressure gradient and skin friction perturbations all show a gradual monotonic

change from zero at the origin, with the flow perturbation tending towards the far downstream form (2.16). This change from zero was of course faster with a faster pressure response, i.e. with a larger value of μ .

2.3 Flows with a slow pressure response

Here we consider the channel-fluid system with a small wall deviation and a slow pressure response, i.e. $\epsilon \ll 1$ and $\mu \ll 1$. The flow develops very slowly, and the appropriate pressure and stream-wise length scalings are $p = \mu^{-1}P$ and $x = \mu^{-1}RX$ respectively. The motion takes the form of a viscous perturbation to the Poiseuille flow, and is given by

$$u = U_0(y) + \epsilon U_1(X, y) + O(\epsilon^2),$$

$$P = -X + \epsilon P_1(X) + O(\epsilon^2),$$

where the pressure perturbation P_1 is again independent of y . The stream-wise momentum equation is found to be of the lubrication type, with only the pressure gradient and a viscous force dominant. A solution, which matches with the incoming flow and satisfies no slip at the walls and mass conservation, is

$$u_1 = \frac{1}{2} (1 - 3y^2) S(-X),$$

$$P_1 = - \int_0^X S(-t) dt.$$

Clearly, this solution takes the expected form (2.16) in the limit as $X \rightarrow \infty$ and $S \rightarrow 1$.

2.4 A collapse which starts far upstream

In this section we consider a channel in which the wall deviation extends far upstream. In particular, we assume that when the pressure is large and positive ($p \gg 1$) the wall relationship takes the form

$$y_w = 1 - cp^{-N} + o(p^{-N}), \quad (2.31)$$

where c and N are positive constants such that $cp^{-N} \ll 1$. Since far upstream the pressure will be given to leading order by the linear Poiseuille pressure, (2.31) implies that for $-X \gg 1$

$$y_w = 1 - c(-X)^{-N} \quad (2.32)$$

to first order, where $X = R^{-1}x$.

The asymptotic analysis for X large and negative is straightforward, and we will omit the details and present the results only. If $N > 1$, then, using the stream function ψ , the flow is given by

$$\left. \begin{aligned} \psi(X,y) &= \psi_0(y) + (-X)^{-N} \psi_1(y) + \\ &\quad + (-X)^{-N-1} \psi_2(y) + o((-X)^{-N-1}), \\ p &= -X + (-X)^{1-N} p_1 + (-X)^{-N} p_2 + o((-X)^{-N}), \end{aligned} \right\} \quad (2.33)$$

where

$$\psi_0(y) = \frac{1}{2} (y - \frac{1}{3} y^3)$$

is the Poiseuille term,

$$\psi_1(y) = \frac{c}{2} (y - y^3),$$

$$\begin{aligned} \psi_2(y) &= Nc \left\{ \frac{6}{35} \psi_0(y) - \frac{1}{24} \left(\frac{11}{5} y - y^3 + \right. \right. \\ &\quad \left. \left. + \frac{1}{5} y^5 + \frac{1}{35} y^7 \right) \right\}, \end{aligned}$$

$$p_1 = -\frac{3c}{N-1} \text{ and } p_2 = -\frac{6}{35} c.$$

If $N < 1$ and $N \neq 1/2$ then

$$\begin{aligned}
 \psi(X,y) &= \psi_0(y) + (-X)^{-N} \psi_1(y) + \\
 &\quad (-X)^{-2N} \hat{\psi}_2(y) + o((-X)^{-2N}), \\
 p &= -X + (-X)^{1-N} p_1 + (-X)^{1-2N} \hat{p}_2 + o((-X)^{1-2N}),
 \end{aligned}
 \tag{2.34}$$

where $\hat{\psi}_2(y) = \frac{c^2}{2} (y - 2y^3)$

and $\hat{p}_2 = -\frac{6c^2}{N-1}$.

If $N = 1/2$ then the term of $o((-X)^{1-2N})$ in the pressure expansion in (2.34) must be replaced by $\hat{p}_2 \ln(-X)$, where $\hat{p}_2 = 6c^2$.

In both (2.33) and (2.34) the first perturbation in the expansion of ψ is viscous in nature and is forced by the no slip condition at the walls, as is the second perturbation for $N < 1$. For $N > 1$, the second perturbation satisfies homogeneous wall conditions and is forced by the inertial effects from the first perturbation, i.e. it represents the viscous response of the flow to the inertial force from $\psi_1(y)$. Obviously both expansions will include similar terms eventually, but their relative importance will depend on the value of N .

If $N = 1$ then

$$\begin{aligned}
 \psi(X,y) &= \psi_0(y) + (-X)^{-1} \psi_1(y) + \\
 &\quad (-X)^{-2} \tilde{\psi}_2(y) + o((-X)^{-2}), \\
 p &= -X + \tilde{p}_1 \ln(-X) + (-X)^{-1} \tilde{p}_2 + o((-X)^{-1}),
 \end{aligned}
 \tag{2.35}$$

where

$$\begin{aligned}
 \tilde{\psi}_2(y) &= -\tilde{p}_2 \psi_0(y) - \frac{5}{2} c^2 y - \frac{c}{24} \left(\frac{11}{5} y - y^3 + \frac{1}{5} y^5 - \frac{1}{35} y^7 \right), \\
 \tilde{p}_1 &= 3c \text{ and } \tilde{p}_2 = -\frac{6}{35} c - 6c^2.
 \end{aligned}$$

The second perturbation in (2.35) comes from a balance between viscous and inertial forces in the fluid as well as satisfying

nontrivial conditions at the walls. As might be expected, the solution for $N = 1$ is effectively a combination of the solutions for $N < 1$ and $N > 1$.

In the above we have made no assumption about the eventual size of the wall displacement, but have assumed simply that far upstream the wall deviation is small and is given by (2.31), and that the incoming flow is fully developed. It is clear that the analysis presented here is valid for both small and finite ϵ .

Finally, we note that a similar asymptotic analysis can be done for a channel with a small wall deviation extending far downstream, i.e. for a channel obeying

$$y_w = 1 - \epsilon + D(-p)^{-M} + o((-p)^{-M}),$$

where $-p \gg 1$ and D and M are positive constants.

Section 3. Channels with a finite collapse

3.1 Introduction

In Section 3 our main concern is with channel-fluid systems with moderate, severe, or complete collapses, i.e. those with $\epsilon = O(1 - \epsilon)$, $0 < 1 - \epsilon \ll 1$, and $\epsilon = 1$ respectively, although we do consider systems with a fine collapse ($\epsilon \ll 1$) and a pressure response so fast that $\epsilon \mu^{2/3} \gg 1$ (Section 3.4).

If the pressure response is moderate ($\mu = O(1)$), then requiring that the pressure gradient matches with the incoming Poiseuille pressure gradient introduces the scalings $x = RX$ and $v = R^{-1}V(X, y)$, which in turn imply that the governing equations are the nonlinear boundary layer equations, that is

$$\left. \begin{aligned} u \frac{\partial u}{\partial X} + v \frac{\partial u}{\partial y} &= -p'(X) + \frac{\partial^2 u}{\partial y^2}, \\ \frac{\partial u}{\partial X} + \frac{\partial V}{\partial y} &= 0, \end{aligned} \right\} (3.1)$$

from conservation of momentum and mass respectively. The boundary conditions are

$$\left. \begin{aligned} u = V = 0 \text{ at } y = \pm y_w(p), \\ u \rightarrow U_0(y) \text{ and } V \rightarrow 0 \text{ as } X \rightarrow -\infty \end{aligned} \right\} (3.2)$$

from no slip at the walls and matching to the incoming Poiseuille flow in turn. As usual, we assume that $p = 0$ at $X = 0$. No evidence is found in Section 3 of any significant upstream adjustment of the flow, and in practice we can apply the upstream matching in (3.2) at $X = 0$.

If the flow is assumed to be symmetric the no slip condition at one of the walls can be replaced by a symmetry condition, viz.

$$V = \frac{\partial u}{\partial y} = 0 \text{ at } y = 0. \quad (3.2a)$$

In general we do not assume symmetry. In fact, some nonsymmetric local solutions are found (Section 3.3).

We assume throughout Section 3 that the tube law is given by (1.4) and (1.6), that is

$$y_w = \begin{cases} 1 & p \geq 0 \\ 1 - \varepsilon + \varepsilon (1 + \mu^2 p^2)^{-q/2} & p < 0 \end{cases} \quad (3.3)$$

In Section 3.2 we study channel-fluid systems with a severe or total collapse, a moderate pressure response and $q \leq 1/3$, and those with a moderate pressure response and moderate collapse. Section 3.3 concerns systems with a moderate pressure response, a severe or total collapse and $q > 1/3$. Systems with a fast pressure response and $\varepsilon \mu^{2/3} \gg 1$ are studied in Section 3.4, and those with a slow pressure response and $\varepsilon = O(1)$ in Section 3.5.

3.2 Channel flows with the collapse extending far downstream

Let us assume first that a complete collapse of the channel is possible ($\varepsilon = 1$), that the pressure response is moderate ($\mu = O(1)$), and that the tube law has the algebraic form (3.3). Close to the origin, where $0 < X \ll 1$ and $0 < -\mu p \ll 1$, the tube law is given by

$$y = 1 - \frac{q}{2} \mu^2 X^2 + o(X^2),$$

and the core flow takes the form of an inviscid rotational perturbation of the Poiseuille flow, viz.

$$\left. \begin{aligned} u &= U_0(y) + X^{7/3} U_1(y) + o(X^{7/3}), \\ v &= X^{4/3} V_1(y) + o(X^{4/3}), \\ p &= -X + p_1 X^{7/3} + o(X^{7/3}), \end{aligned} \right\} \quad (3.6)$$

where p_1 is a constant. The solution of (3.6) is similar in form to (2.2), the core solution for $\varepsilon \ll 1$, and provides similar nonzero matching conditions close to the walls.

Adjacent to the channel walls there are thin viscous layers in the fluid. These layers, which are essentially the same, have width $O(X^{1/3})$

and are governed by the linearized boundary layer equations. In the upper wall layer the stream function ψ takes the form

$$\psi = -\frac{1}{2} X^{2/3} \zeta^2 + \frac{1}{6} X \zeta^3 - X^{7/3} f(\zeta) + o(X^{7/3}), \quad (3.7)$$

where $\zeta = (1 - y)X^{-1/3}$ and $\psi = 0$ at $y = y_w$. The boundary conditions are those of no slip at the wall (given by $\zeta_w = \frac{1}{2} q\mu^2 X^{5/3}$) and matching to (3.6) at the outer edge of the wall layer, which requires $f \rightarrow \text{constant}$ as $\zeta \rightarrow \infty$. The third order ordinary differential equation produced by substituting (3.7) into the streamwise momentum equation is similar to (3.55), the governing equation of the linear similarity problem studied in Section 3.4 below, and can be solved using the same method. Given this solution the boundary conditions can then be applied to determine the constant p_1 , which is $\propto q\mu^2$. The skin friction perturbation is $\propto q\mu^2 X^{5/3}$.

Clearly, near the origin there is a fairly smooth change in the flow and in the wall position, and the effect of increasing q and/or μ is to move this change closer to the origin, as might be expected.

The flow structure outlined above will not be valid when $X = O(1)$, or, more precisely, when $\mu p = O(1)$ and the walls have moved a finite distance into the channel. When this occurs $u - U_0(y)$ is also $O(1)$, and the governing equations are the full nonlinear boundary layer equations (3.1), which apply across the full width of the channel. In general, numerical methods must be used with this problem (see Appendix 5).

Further downstream, where $-\mu p \gg 1$, the tube law (3.3) implies that to leading order

$$y_w = k(-p)^{-q}, \quad (3.8)$$

where $k = \mu^{-q}$ is $O(1)$. As conservation of mass requires that the average streamwise velocity is $O(y_w^{-1})$, the ratio of the pressure gradient to the inertial terms in the momentum equation is $O(y_w^{2-1/q})$. Hence, as $p \rightarrow -\infty$ and $y_w \rightarrow 0$ the pressure gradient will dominate the inertial terms if $q < 1/2$ and the inertial terms the pressure gradient if $q > 1/2$. If $q = 1/2$ then there will be a balance between the inertial and pressure terms as the channel collapses.

For $q < 1/2$ there must eventually be a balance between the pressure gradient and the viscous forces in the fluid, which are of $O(y_w^{-3})$. With an appropriate change of origin this implies that $X = O(y_w^{3-1/q})$ as $y_w \rightarrow 0$. It follows that for $q < 1/3$ the collapse will extend indefinitely for downstream, while for $q > 1/3$ y_w will tend to zero at a finite value (X_0) of X . For the case $q = 1/3$ it is found that the channel will collapse exponentially, i.e. at the fastest rate consistent with a collapse extending to infinity. In this section we restrict our attention to channels with $q \leq 1/3$. Those with $q > 1/3$ are considered in Section 3.3 below.

Suppose first that $q < 1/3$. As $X \rightarrow \infty$ the flow is given to leading order by the viscous similarity structure

$$\left. \begin{aligned} u &= X^{q/m} f(\zeta), \\ p &= -p_0 X^{1/m}, \end{aligned} \right\} (3.9)$$

where $\zeta = y X^{q/m}$, $m = 1 - 3q > 0$, p_0 is a constant to be determined, and an implicit origin shift (which must be determined numerically) has been included. Substitution of (3.9) in the streamwise momentum equation produces

$$f'' + p_0/m = 0. \quad (3.10)$$

In turn, no slip at the walls and conservation of mass require

$$\left. \begin{aligned} f &= 0 \text{ at } \zeta = \pm \zeta_w \\ \int_{-\zeta_w}^{\zeta_w} f(\zeta) d\zeta &= 2/3, \end{aligned} \right\} (3.11)$$

where $\zeta_w = kp_0^{-q}$ gives the position of the upper wall. The solution of (3.10) and (3.11) is

$$f(\zeta) = \frac{1}{2m} p_0 (\zeta_w^2 - \zeta^2), \quad (3.12)$$

where $p_0 = (m/k^3)^{1/m}$. The skin friction is given by

$$\tau = -\frac{1}{m} p_0^{1-q} X^{2q/m}. \quad (3.13)$$

Again (c.f. Sections 2.1, 2.2), we have found a solution without considering any initial conditions. We note, however, that the parabolic form of u in (3.9) is consistent with the incoming Poiseuille flow.

The powers of X in the similarity solution depend only on the value of q , and as might be expected an increase in q brings, with respect to X , a corresponding increase in the order of the pressure, velocity and skin friction, and a decrease in the negative order of the channel width. As $q \rightarrow 1/3$ $q/m \rightarrow \infty$, which suggests formally an exponential structure when $q = 1/3$. Unlike the powers of X , the coefficients p_0 and ζ_w depend on both q and k . The effect on p_0 and ζ_w of varying q depends on the value of k , and an increase in q can result in either an increase or decrease in p_0 and ζ_w . The effect on p_0 and ζ_w of varying k is simpler. With a faster pressure response, i.e. a smaller value of k , there is an increase in the value of p_0 and a decrease in the value of ζ_w . Thus, taking a smaller value of k (a larger value of μ) with the same value of q results in an increase in the absolute values of the pressure and skin friction, and a decrease in the channel width for a given value of X . A larger value of k with the same q has the opposite effect. It should be noted that the size of the implicit origin shift is dependent upon the values of the parameters q and μ and that strictly the values obtained cannot be compared at the same value of X . However, examination of the numerical solution of the problem formed by equations (3.1) with (3.2) shows that this description of the effects of changing the values of the parameters is valid. That is, an increase in q or μ steepens the main part of the collapse and shifts it closer to the origin, with the opposite effect from decreasing q or μ (see Figures 3.1 - 3.4). This is consistent with the expected faster response of the system with larger values of q and/or μ .

With $q < 1/3$ the complete collapse admitted by taking ε as one will be achieved only in the limit as $X \rightarrow \infty$, and the analysis above is valid far downstream.

Let us assume now that the collapse is severe but not complete, i.e. $0 < 1 - \varepsilon \ll 1$. Then, on taking the transverse scaling $y = \varepsilon Y$, it is clear that the analysis given above is valid until Y_w is $O(1 - \varepsilon)$.

When this occurs it is appropriate to rescale the problem. Let

$$\left. \begin{aligned} u &= (1 - \epsilon)^{-1} \bar{u}(\bar{X}, \bar{Y}), \\ p &= (1 - \epsilon)^{-1/q} \bar{p}(\bar{X}), \end{aligned} \right\} \quad (3.14)$$

where $y = (1 - \epsilon)\bar{Y}$ and $x = (1 - \epsilon)^{-m/q} R\bar{X}$. To leading order the upper wall is given by

$$\bar{Y}_w = 1 + \epsilon k(-\bar{p})^{-q}. \quad (3.15)$$

The flow remains viscous in nature throughout the collapse, the boundary conditions are the familiar ones of no slip at the walls and conservation of mass, and the solution for \bar{u} is

$$\bar{u} = \frac{1}{2} \bar{Y}_w^{-3} (\bar{Y}_w^2 - \bar{Y}^2), \quad (3.16a)$$

which again has a parabolic form. The pressure can be found in terms of \bar{X} from

$$\bar{p}' = -\bar{Y}_w^{-3}(\bar{p}). \quad (3.16b)$$

In practice the starting point for the integration of (3.16b) must be found numerically. It is easily shown that this solution matches with the upstream solution of (3.9) and (3.12). Note that a relationship similar to (3.16b) holds upstream where (3.9) is valid. Clearly (3.16a,b) takes the expected form far downstream, i.e. undisturbed Poiseuille flow in the limit as $\bar{X} \rightarrow \infty$ and $\bar{Y}_w \rightarrow 1$. For $-\bar{p} \gg 1$ (3.16) can be expanded in negative powers of $\bar{X} \gg 1$. This expansion is similar to that given in Section 2.4 for a collapse extending far upstream. We omit the details.

Suppose now that $q = 1/3$ and $\epsilon = 1$. If $-\mu p \gg 1$ then to leading order the tube law is given by (3.8), and the necessary balance between the viscous force and the pressure gradient in the fluid implies that $X = O(\ln y_w)$ as $y_w \rightarrow 0$. Thus the collapse has an exponential form, as predicted. The flow, which is viscous in nature, is given by

$$\left. \begin{aligned} u &= e^{ax} g(\eta), \\ p &= -e^{3ax}, \end{aligned} \right\} (3.17a)$$

where

$$g(\eta) = \frac{3a}{2} (k^2 - \eta^2), \quad (3.17b)$$

$\eta = ye^{ax}$, $a = \frac{1}{3k^2}$, the walls are given by $\eta = \pm \eta_w = \pm k$, and an implicit origin shift has been included. Again (c.f. $q < 1/3$ above), a smaller value of k (larger μ) results in a faster (rate of) collapse, and a larger k in a slower collapse.

If the collapse is severe ($0 < 1 - \epsilon \ll 1$) rather than complete, then the analysis above is valid while $Y_w = \epsilon^{-1} y_w \gg 1 - \epsilon$. It is necessary to rescale the problem when Y_w is $O(1 - \epsilon)$. Although X is $O(\ln(1 - \epsilon))$ when this happens, both the pressure p and the pressure gradient dp/dX are then of $O((1 - \epsilon)^{-3})$ and it is not appropriate to adopt a new streamwise length scale. The analysis for y_w of $O(1 - \epsilon)$ proceeds as for $q > 1/3$ above, and the solution is given by (3.14) and (3.16a,b) with a suitable change of origin.

The governing equations (3.1) - (3.3) were solved numerically (see Appendix 5) for various q with $\epsilon = \mu = 1$. The results are shown in Figure 3.4. The solutions given above for $-\mu p \gg 1$ are not shown, as the numerical and analytical solutions are graphically indistinguishable for values of X greater than about two. However, we note that for $q = 1/3$ the pressure, pressure gradient and skin friction curves take the predicted form, i.e. on a logarithmic scale the curves are straight lines except in the region of the origin.

When both the final channel width and the pressure response are moderate, i.e. ϵ , $1 - \epsilon$ and μ are $O(1)$, then the flow close to the origin is given by (3.6), and a far downstream analysis as a perturbation of Poiseuille flow is possible (c.f. Section 2.3). However, over the main part of the collapse the solution must be found numerically. The results for various values of μ with fixed ϵ and q , various q with fixed ϵ and μ and various ϵ with fixed μ and q are shown in Figures 3.1 - 3.3 respectively.

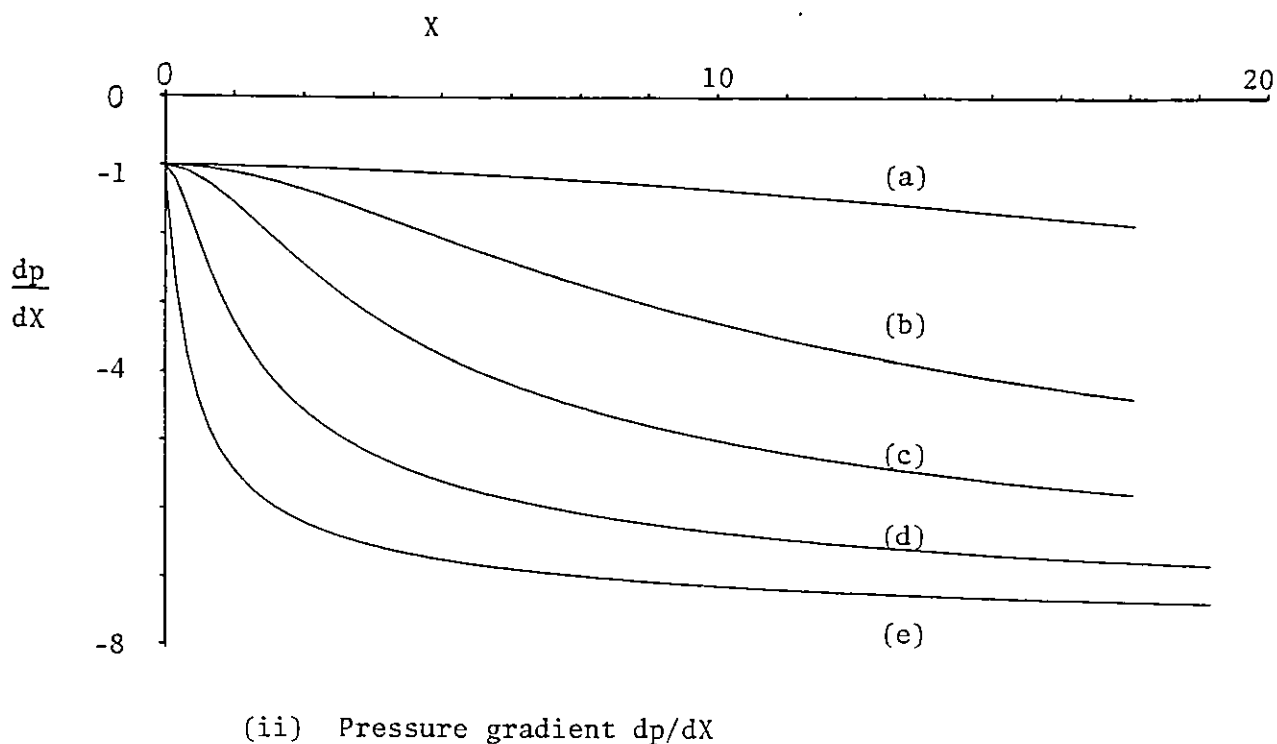
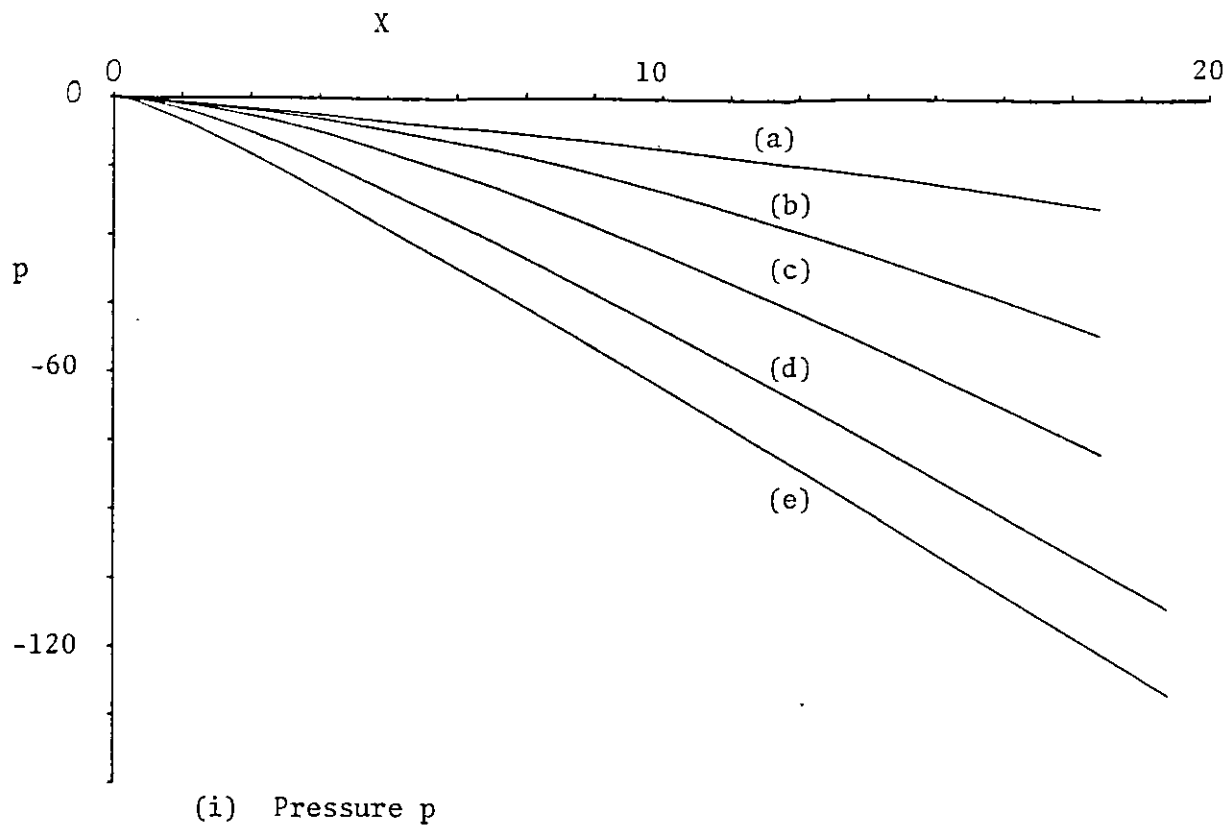


Figure 3.1. Results against distance for a channel with $\epsilon = 1/2$, $q = 1/2$ and varying μ : (a) $\mu = .1$, (b) $\mu = .4$, (c) $\mu = 1.0$, (d) $\mu = 3.0$, (e) $\mu = 10.0$.

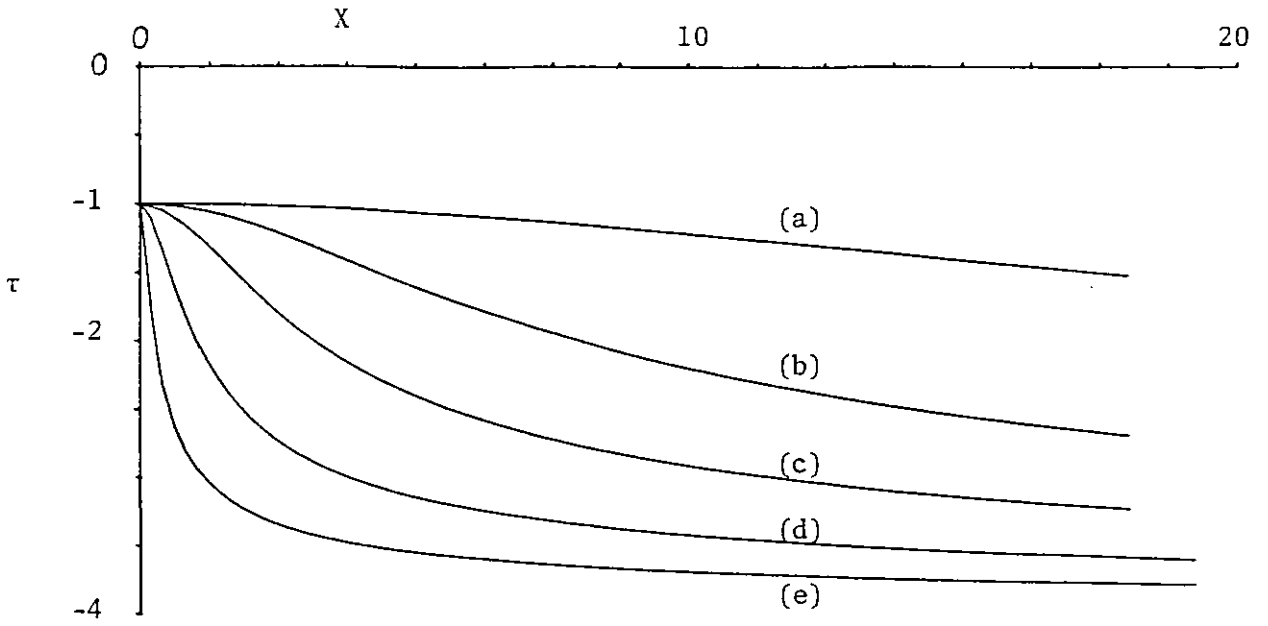
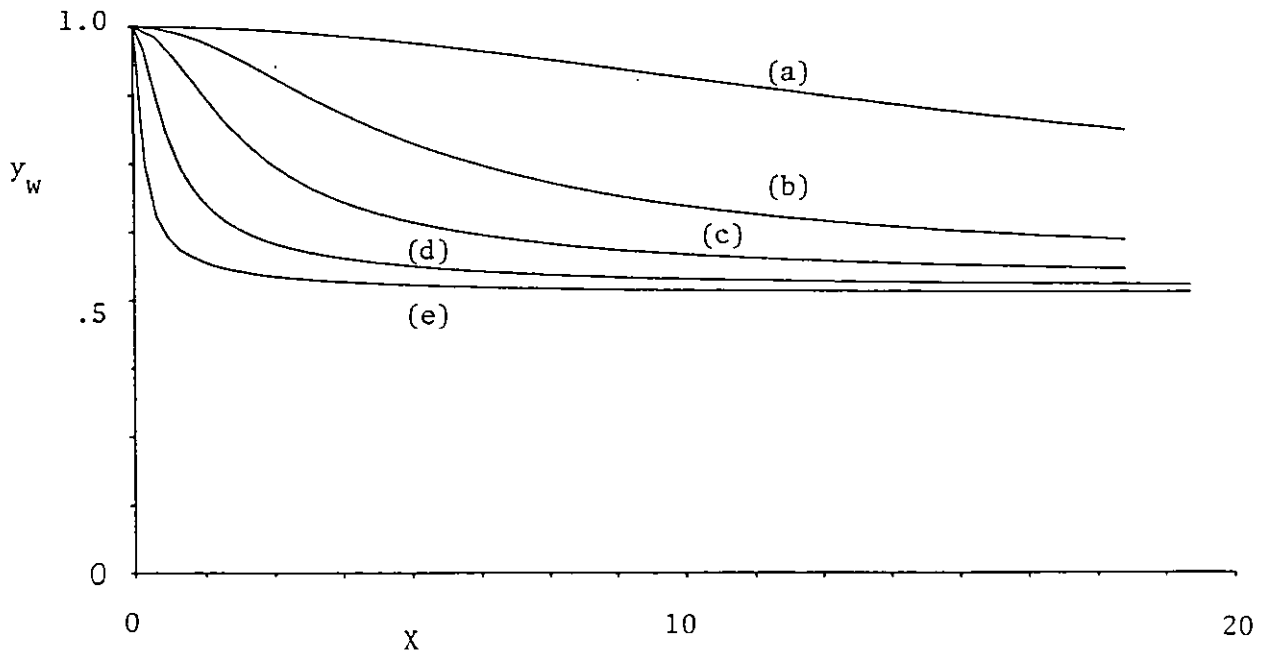
(iii) Upper wall skin friction τ (iv) Channel half-width y_w .

Figure 3.1 (cont.).

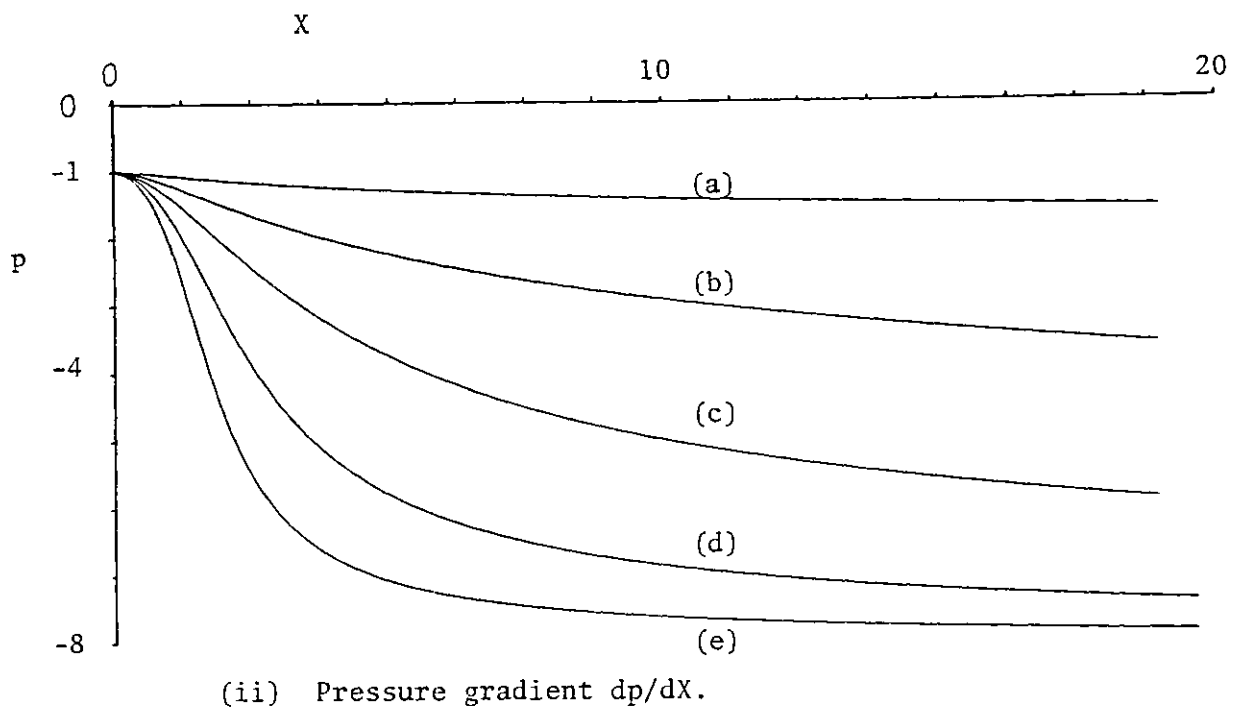
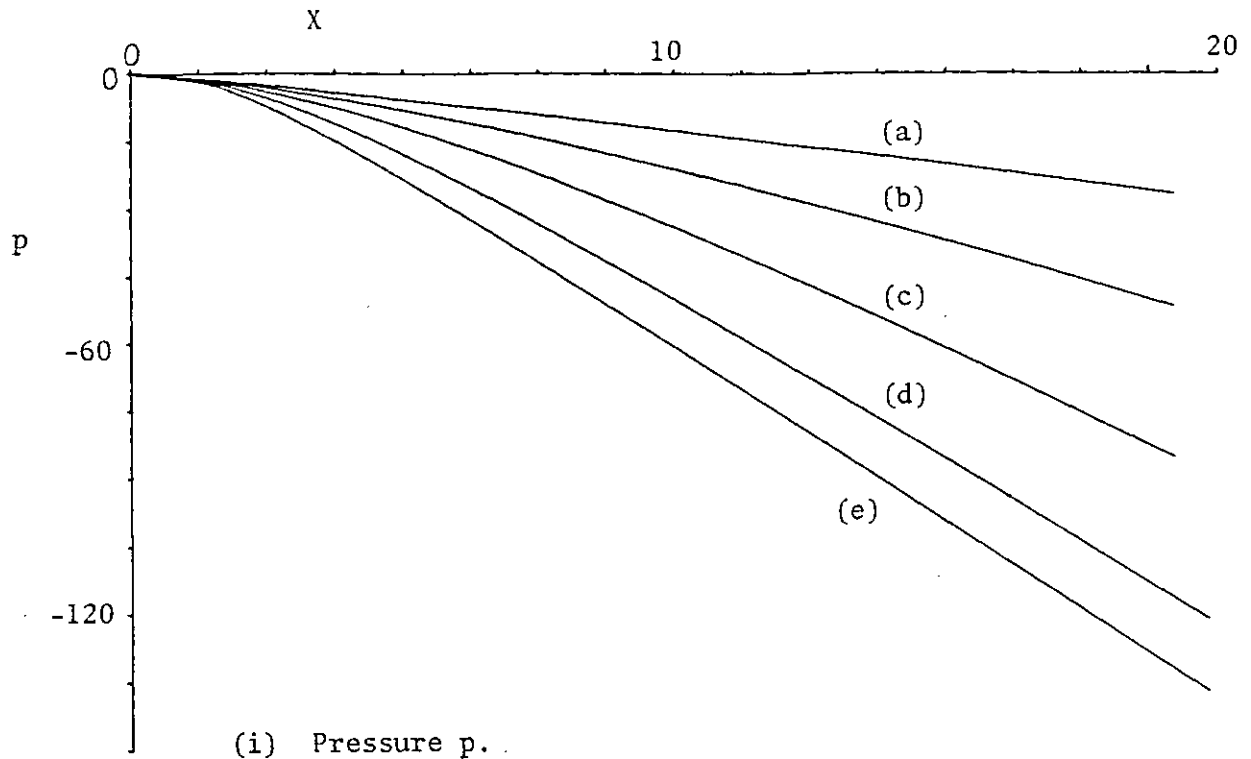
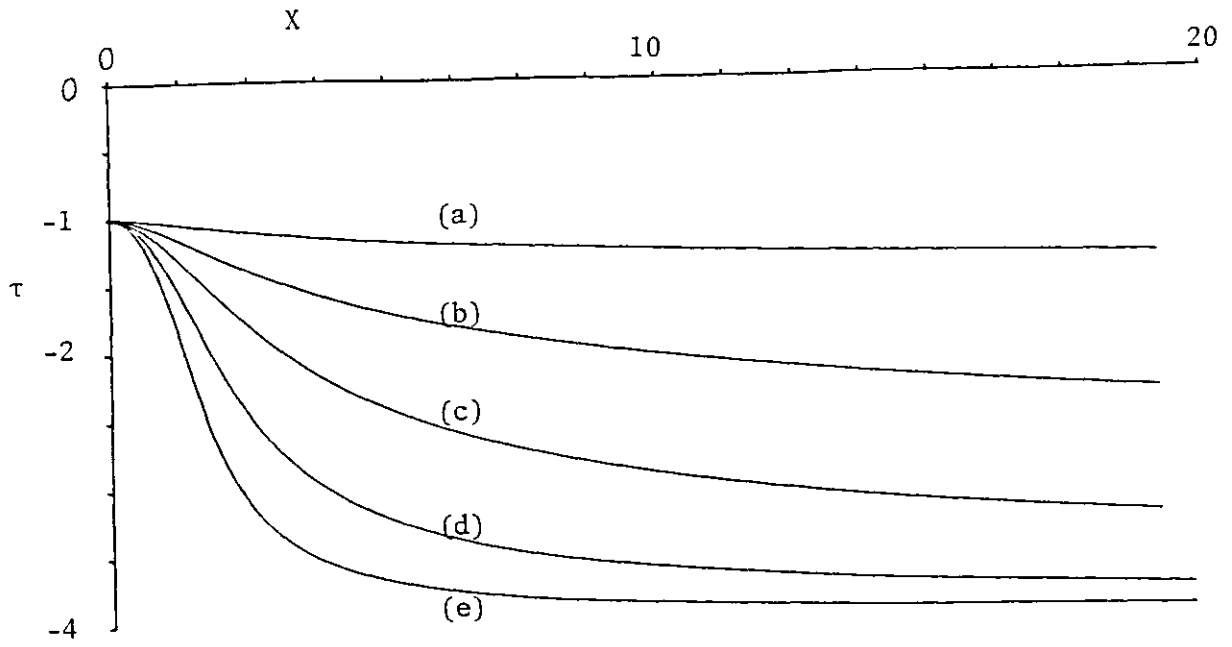
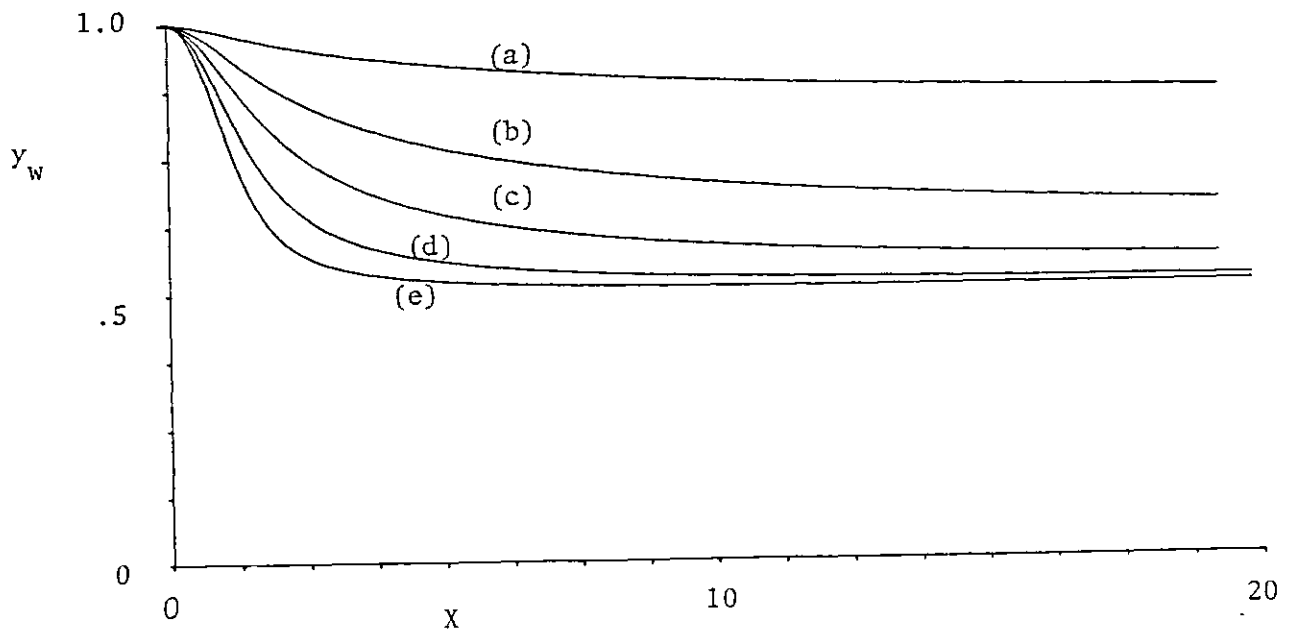


Figure 3.2. Results against distance for a channel with $\epsilon = 1/2$, $\mu = 1$ and various q : (a) $q = .1$, (b) $q = .3$, (c) $q = .5$, (d) $q = .75$, (e) $q = 1.0$.

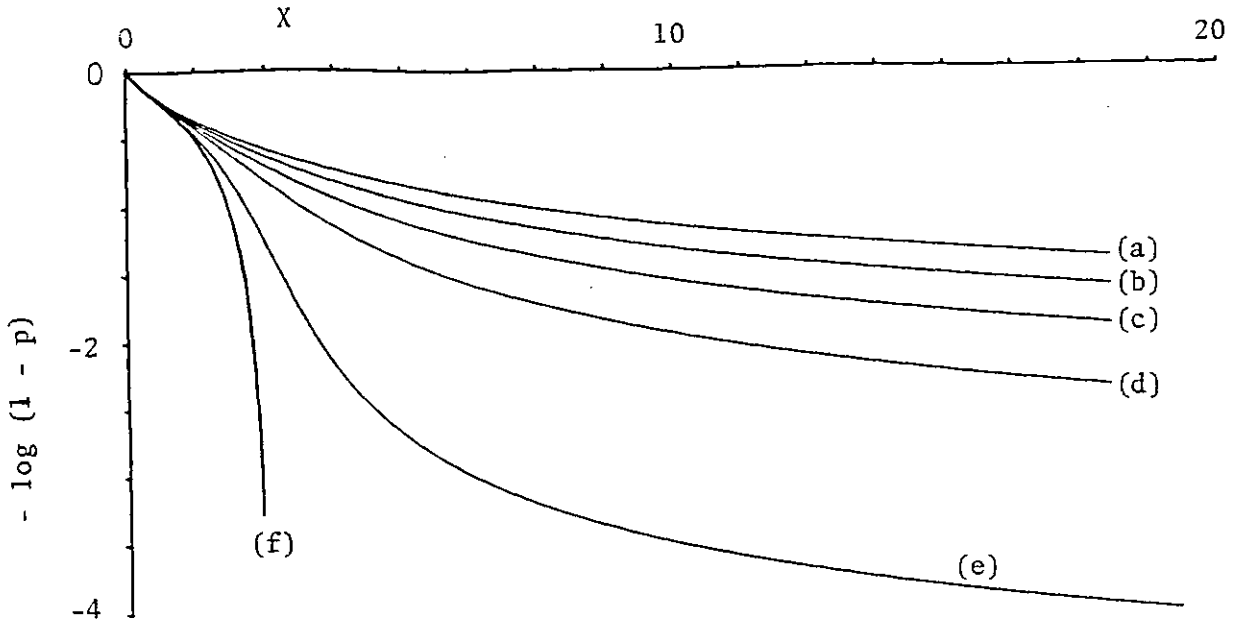


(iii) Upper wall skin friction τ .

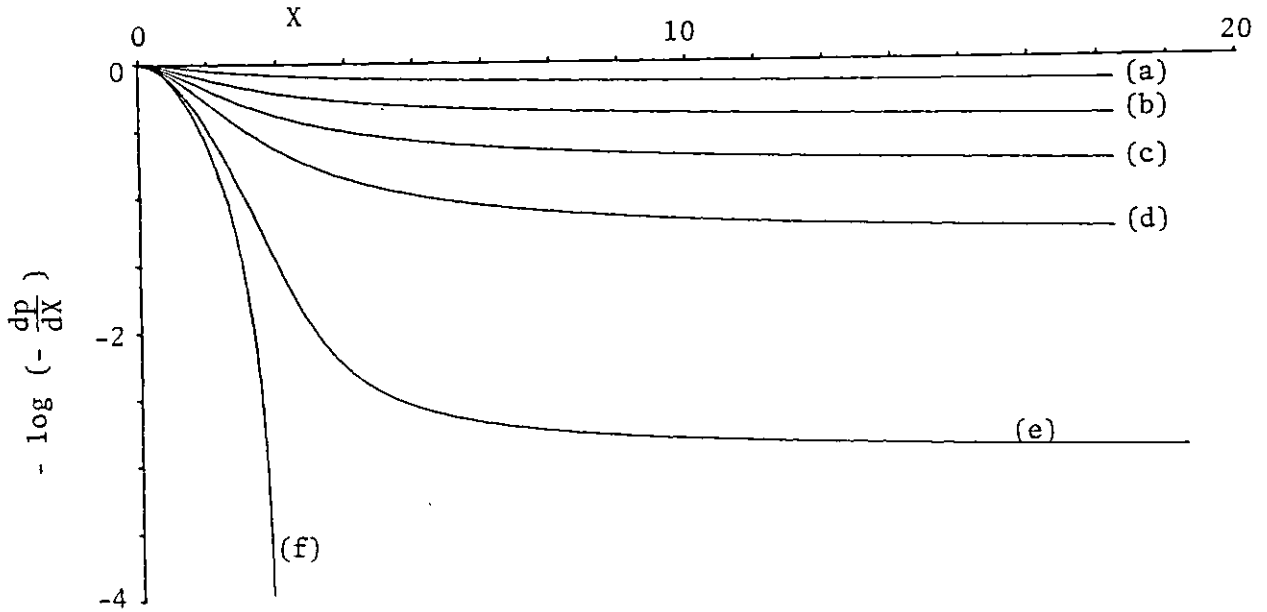


(iv) Channel half-width y_w .

Figure 3.2 (cont.).



(i) Pressure p (on a logarithmic scale).



(ii) Pressure gradient dp/dX (on a logarithmic scale).

Figure 3.3. Results against distance for a channel with $q = 1/2$, $\mu = 1$, and various ϵ : (a) $\epsilon = .1$, (b) $\epsilon = 1/3$, (c) $\epsilon = 1/2$, (d) $\epsilon = 2/3$, (e) $\epsilon = .9$, (f) $\epsilon = 1.0$.

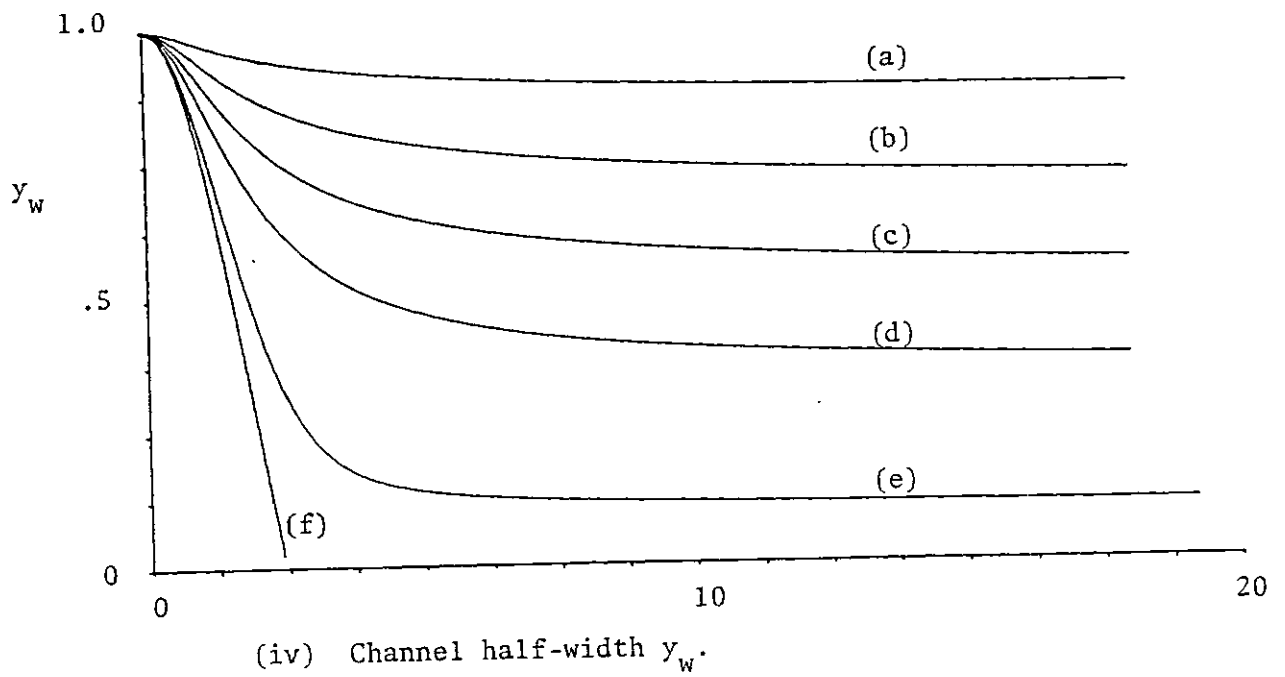
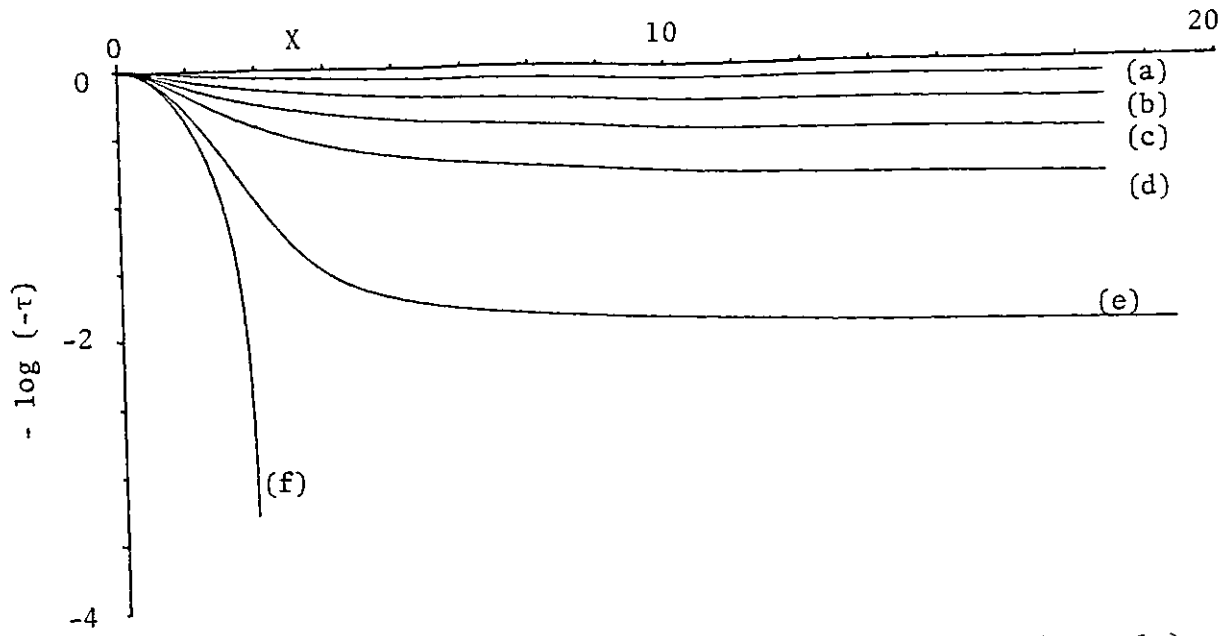
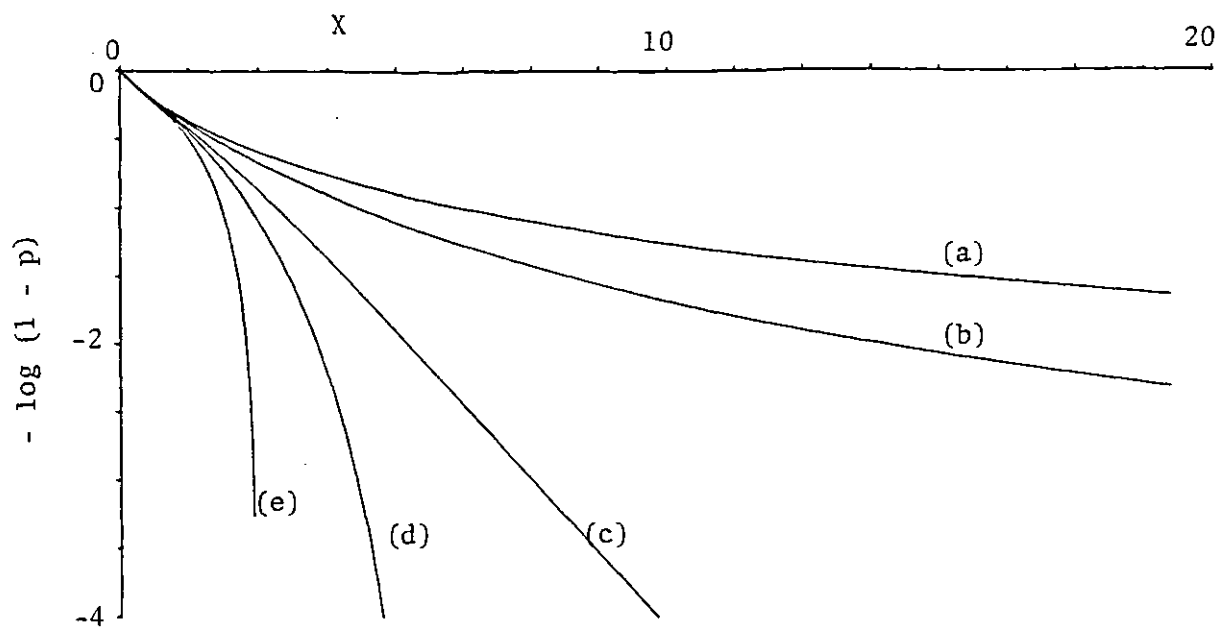
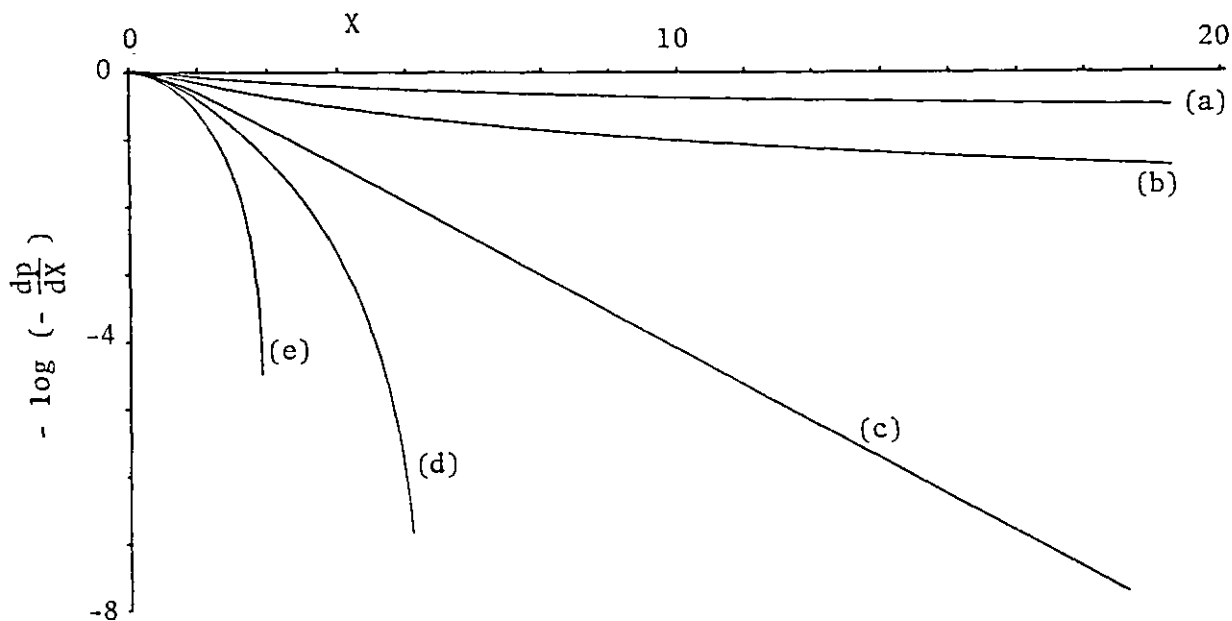


Figure 3.3 (cont.).

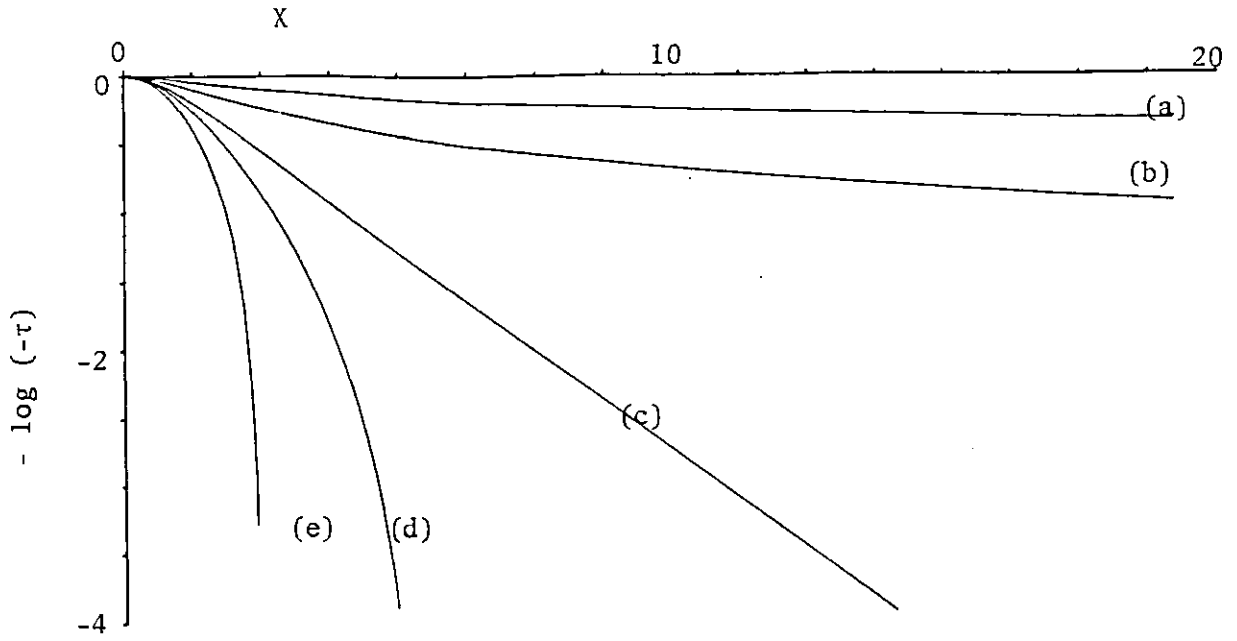


(i) Pressure p (on a logarithmic scale).

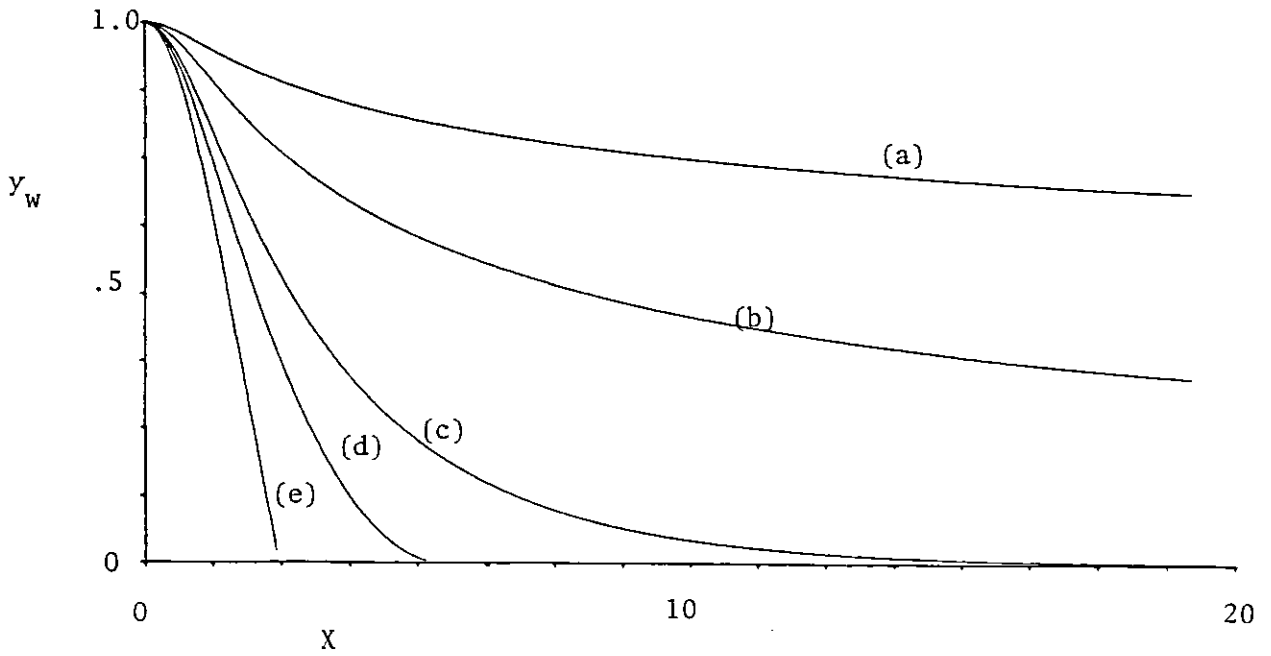


(ii) Pressure gradient dp/dX (on a logarithmic scale).

Figure 3.4. Results against distance for a channel with $\epsilon = \mu = 1$ and various q . The asymptotic solutions for $-p \gg 1$ are graphically identical. (a) $q = .1$, (b) $q = .2$, (c) $q = 1/3$, (d) $q = .4$, (e) $q = 1/2$.

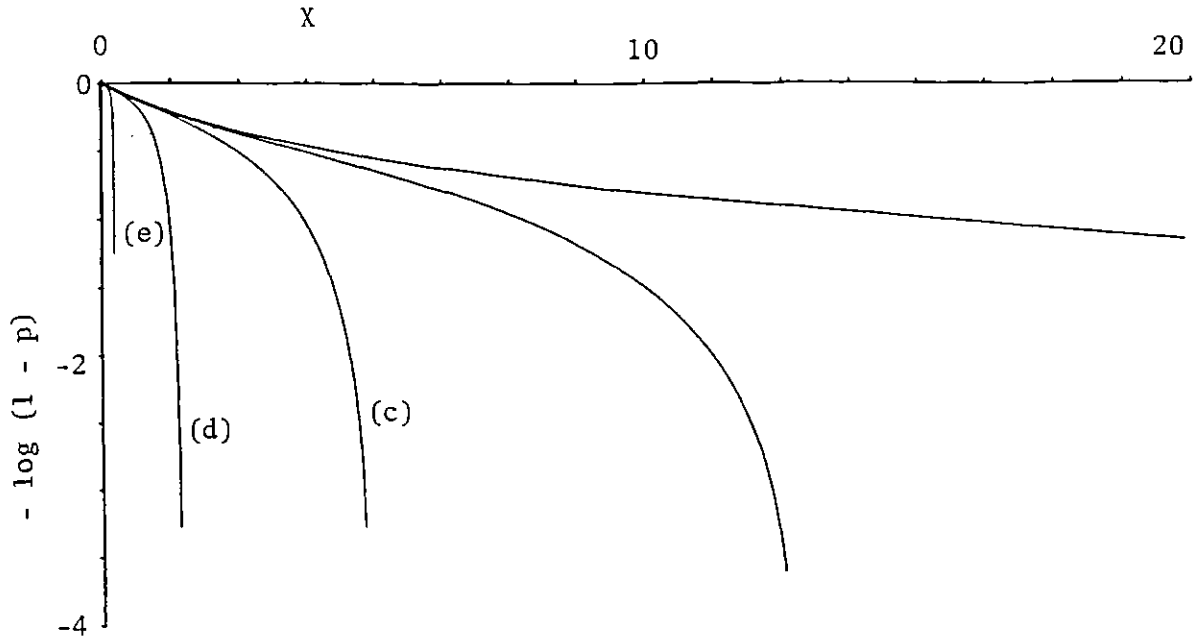


(iii) Upper wall skin friction τ (on a logarithmic scale).

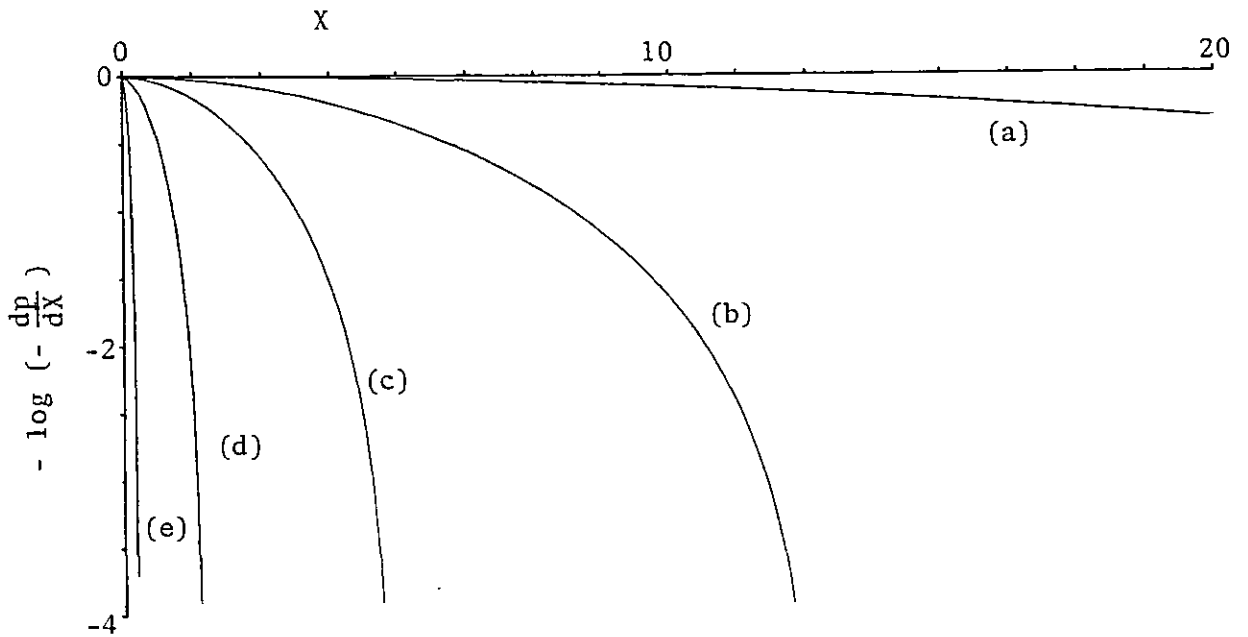


(iv) Channel half-width y_w .

Figure 3.4 (cont.).

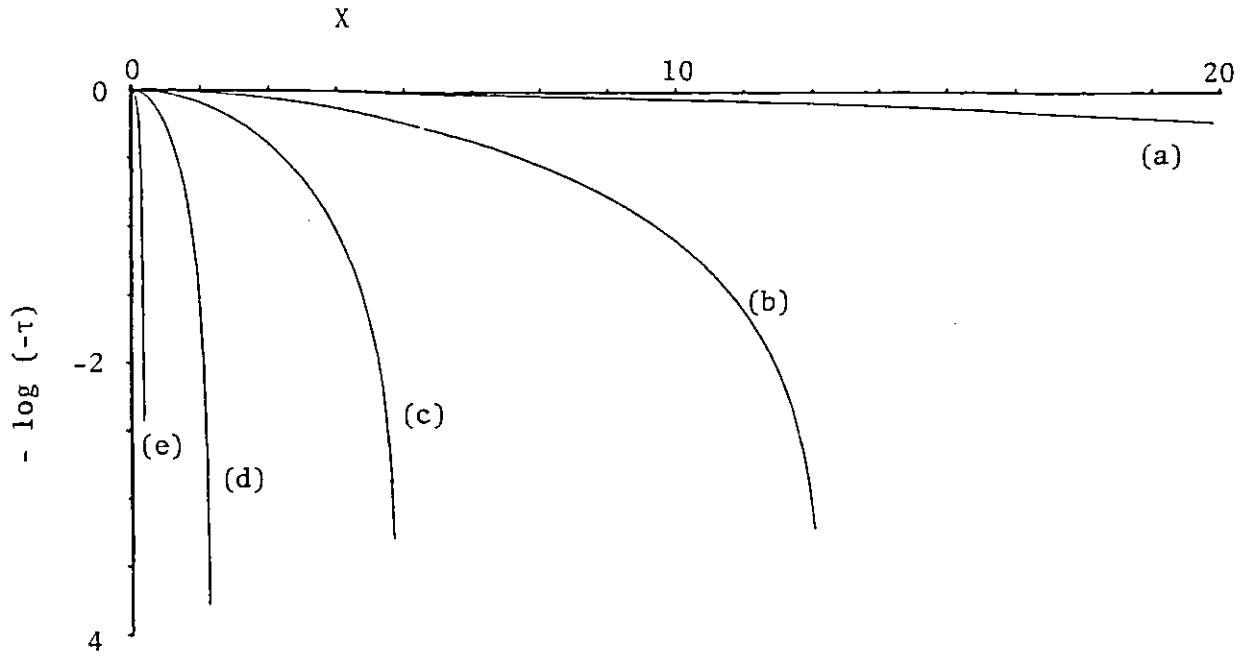


(i) Pressure p (on a logarithmic scale).

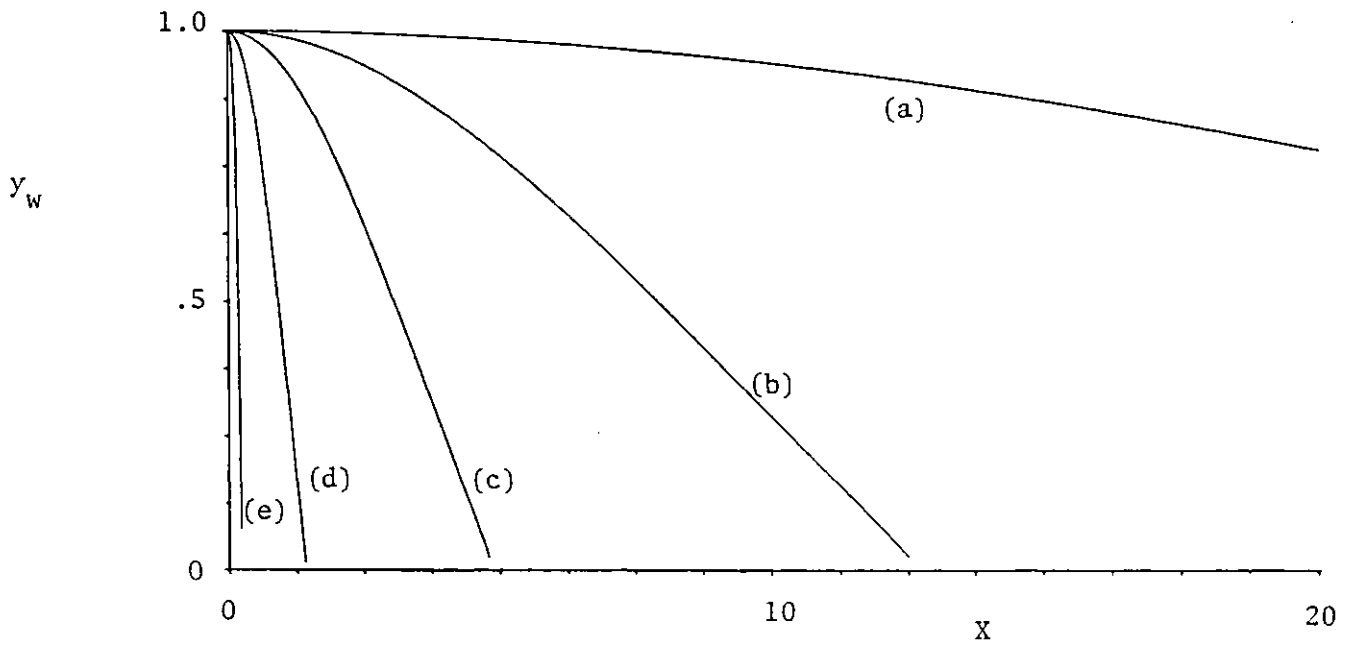


(ii) Pressure gradient dp/dX (on a logarithmic scale).

Figure 3.5. Results against distance for a channel with $\epsilon = 1$, $q = 1/2$ and various μ . The asymptotic solutions for $-\mu p \gg 1$ are graphically identical. (a) $\mu = .1$, (b) $\mu = .4$, (c) $\mu = 1.0$, (d) $\mu = 3.0$, (e) $\mu = 10.0$.



(iii) Upper wall skin friction τ (on a logarithmic scale)



(iv) Channel half-width y_w .

Figure 3.5 (cont.).

It is seen from Figures 3.1 and 3.2 that when the collapse is moderate the effect on the solution of the value of q and μ is qualitatively similar. We could in a sense regard $q = 1/2$ and $\mu = 1$ as intermediate values below which the collapse proceeds relatively slowly downstream, and above which the main part of the collapse occurs close to the origin and there is a sharp change in the pressure gradient, the channel width and the skin friction in this region.

Clearly, for $\mu \gg 1$ it will be necessary to investigate the flow structure close to the origin on a streamwise length scaling shorter than $O(R)$. This will be done in Section 3.4 below. We note that even with the larger values of q and μ the pressure gradient and skin friction tend monotonically towards their respective downstream limit values of $-(1 - \varepsilon)^{-3}$ and $-(1 - \varepsilon)^{-2}$. This also appears to hold for a severe collapse with moderate pressure response, as can be seen from Figure 3.3.

3.3 Channels which collapse at a finite distance downstream

Let us assume now that a complete collapse is possible ($\varepsilon = 1$), that the pressure response is moderate ($\mu = O(1)$), and that the tube law has the algebraic form (3.3) with $1/3 < q < 1/2$. As with $q \leq 1/3$, close to the origin the flow is given by (3.6). We know from Section 3.2 above that further downstream, where the tube law takes the form (3.8), the pressure gradient will dominate the inertial forces in the fluid as the channel collapses, and that the channel width tends to zero at a finite value X_0 of $X = R^{-1}x$. That is, as $y_w \rightarrow 0$ the flow is viscous dominated and acts as if there is a sink at $X = X_0$. For $0 < X_0 - X \ll 1$ the flow has a self-similar structure, viz. $u = (X_0 - X)^{q/m} g(\eta)$ and $p = p_0 (X_0 - X)^{1/m}$, where $\eta = y(X_0 - X)^{q/m}$, $m = 1 - 3q < 0$, $p_0 = (-m/k^3)^{1/m}$, $g(\eta) = -(p_0/m)(\eta_w^2 - \eta^2)$, and the tube law has the local form $\eta = \eta_w$ where $\eta_w = kp_0^{-q}$ (c.f. equations 3.9 and 3.12). The pressure gradient is $p' = -y_w^{-3}$, where y_w is given by (3.8). Integrating,

$$X - X_1 = \frac{\mu^{-3/q}}{3q - 1} [(-p_1)^{1-3q} - (-p)^{1-3q}],$$

where $X < X_1$ and $p = p_1$ at $X = X_1$. It follows that

$$X_0 = X_1 + \frac{\mu^{-3/q}}{1-3q} (-p_1)^{1-3q}. \quad (3.17c)$$

Rubinow and Keller (1972) assumed that Poiseuille flow is valid locally and produced a simple model of steady flow in a collapsible tube. Their model predicts that as the outlet transmural pressure tends to infinity the mass flow tends to an upper limit, a result which depends on the existence of a certain integral. For our present problem this integral is

$$\int_{-\infty}^0 y_w^{-3}(p) dp = \int_{p_1}^0 y_w^{-3}(p) dp + \int_{-\infty}^{p_1} y_w^{-3}(p) dp,$$

which exists if $q > 1/3$. In effect, Rubinow and Keller assume that a complete collapse to a given point (the outlet) is possible and calculate the mass flow consistent with this collapse. For our problem, this is equivalent to assuming that $q > 1/3$, X_0 , X_1 , and p_1 are known, and hence calculate μ from (3.17c). In contrast, we assume a particular mass flow in a given tube, i.e. values of μ and q , and calculate the point (X_0) the channel will collapse to.

Figure 3.5 displays graphically the effect on the solution of varying μ with $q = 1/2$ and $\epsilon = 1$, and Figure 3.4 the effect of varying q with fixed μ and $\epsilon = 1$. The effect of varying μ with fixed q and $\epsilon = 1$ is qualitatively the same for $1/3 < q < 1/2$ as for $q = 1/2$, and we see from Figures 3.4 and 3.5 that, as for $q \leq 1/3$, an increase in q or μ steepens the main part of the collapse and shifts it closer to the origin. We note also that the slope of the channel walls tends to zero as $X \rightarrow X_0^-$. It is easily shown that the flow structure given above remains mathematically valid until the limit as $X \rightarrow X_0^-$ is reached. Clearly, our model must, in some physical sense, break down before this limit is reached.

If the collapse is severe rather than complete, i.e. $0 < 1 - \epsilon \ll 1$, then the analysis continues as for $q < 1/3$ (Section 3.2) with similar results. Figure 3.6 shows the channel half width against X , as obtained from the numerical solution of (3.1) - (3.3) with $\epsilon = .99$, $\mu = 1$ and $q = .4$. Also shown are the theoretical results for the main part of the collapse, and for far downstream where (3.15) and (3.16) imply $\bar{Y}_w = 1 + \epsilon k\bar{X}^{-q} + O(\bar{X}^{-2q})$. We see from Figure 3.6 that there is an excellent agreement between the numerical and theoretical solutions.

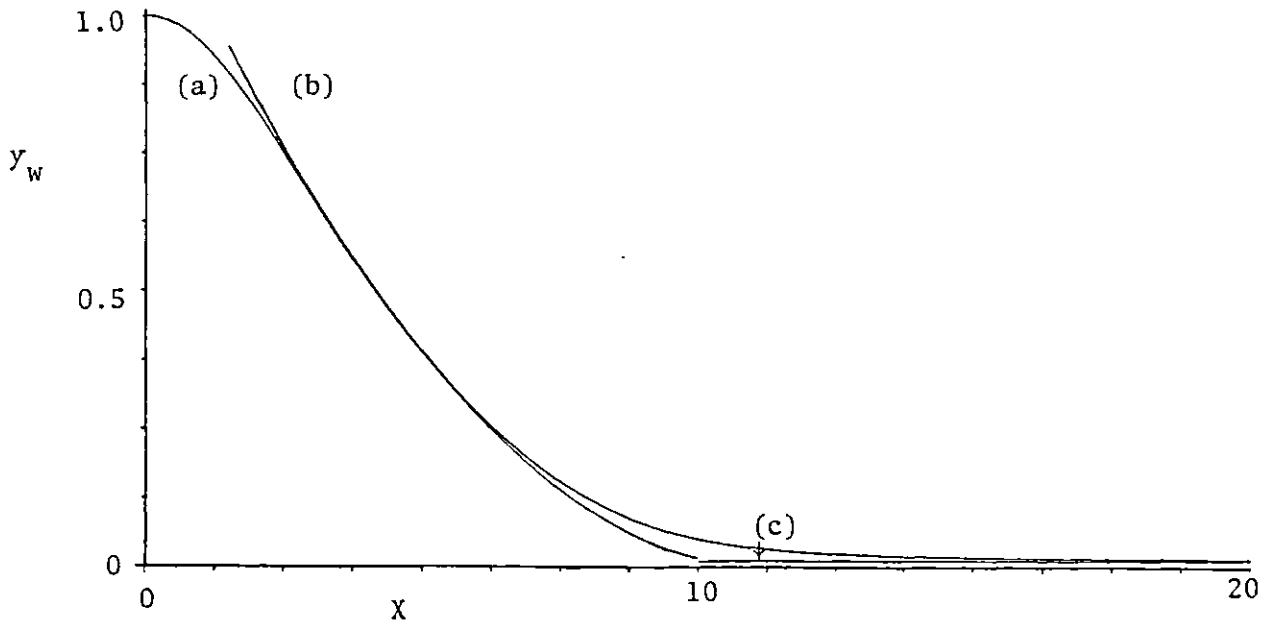


Figure 3.6. Half-width y_w against distance for a channel with $q = .4$, $\mu = 1$ and $\varepsilon = .99$. From (a) Numerical solution of the full problem (equations 3.1 - 3.3), (b) Similarity solution valid when $y_w \sim k(-p)^{-.4}$, (c) Far downstream analysis with $y_w \sim \varepsilon + k\bar{x}^{-.4}$.

Further, a numerical solution for far downstream based on (3.15) and (3.16) is indistinguishable from the full numerical solution to at least three significant figures.

Suppose now that $q = 1/2$, $\mu = O(1)$ and $\epsilon = 1$. As we shall see, $q = 1/2$ is a "critical" value in the sense that it is the largest value of q for which a complete steady solution has been found for the problem with $\epsilon = 1$. Further, it appears possible that there may be no steady solution for the problem with $q > 1/2$, $\mu = O(1)$ and $\epsilon = 1$. Also, with $q = 1/2$ there is an upper limit on the pressure response of $\mu < 18$ for which a steady solution of the form we assume exists (see below).

Again, the flow close to the origin is given by (3.6). It was shown in Section 3.2 that when $q = 1/2$ the inertial force and the pressure gradient are of the same order of magnitude when the tube law takes the form (3.8). Assuming a balance with the viscous force implies that y_w is $O(X_0 - X)$ for some finite X_0 as $X_0 - X \rightarrow 0+$. Making the transformation

$$\left. \begin{aligned} \psi &= (2p_0)^{1/4} f(\zeta), \\ p &= -p_0(X_0 - X)^{-2}, \end{aligned} \right\} (3.18)$$

for the stream function and the pressure, where $\zeta = (2p_0)^{1/4} y (X_0 - X)^{-1}$, the streamwise momentum equation becomes

$$g'' + 1 - g^2 = 0, \quad (3.19)$$

where $g = f'$ gives the streamwise velocity component in the similarity solution. The wall relationship has the local form $\zeta_w = k(2/p_0)^{1/4}$. Conservation of mass and no slip at the walls require

$$\left. \begin{aligned} \int_{-\zeta_w}^{\zeta_w} g(\zeta) d\zeta &= \frac{2}{3}(2p_0)^{-1/4}, \\ g &= 0 \text{ at } \zeta = \pm \zeta_w, \end{aligned} \right\} (3.20)$$

in turn.

Equation (3.19) is similar to that for flow between nonparallel plane walls, first studied by Jeffery (1915) and Hamel (1917), with comprehensive treatments given by Rosenhead (1940) and Millsaps and Pohlhausen (1953). Jeffery-Hamel flows are not in general unique. In fact, there is an infinite number of solutions, although the number that are valid can be restricted severely under certain conditions (see Fraenkel 1962). The Jeffery-Hamel solutions can be found in terms of elliptic integrals. There is also an infinite number of solutions of the present problem, as will now be shown, following Whitham (1963). Equation (3.19) can be integrated to give

$$\frac{1}{2} (g')^2 + g - \frac{1}{3} g^3 = g_0 - \frac{1}{3} g_0^3, \quad (3.21)$$

where g_0 is a value of g for which $g' = 0$. A more convenient form of (3.21) is

$$\frac{1}{2} (g')^2 - \frac{1}{3} (g_0 - g)(a - g)(g - b) = 0, \quad (3.22)$$

where $a = \frac{1}{2}[-g_0 + (12 - 3g_0^2)^{1/2}]$

and $b = -\frac{1}{2}[g_0 + (12 - 3g_0^2)^{1/2}]$

are the other two solutions of $g' = 0$. If a, b and g_0 are all real, then let $b \leq g_0 \leq a$, otherwise let b be the single real solution of $g' = 0$.

Consider a particle of unit mass moving along a straight line with $g(\zeta)$ its distance from the origin at time ζ . Equation (3.22) is the energy equation for a motion in which the potential energy of the particle is given by

$$V(g) = -\frac{1}{3} (g_0 - g)(a - g)(g - b)$$

and the total energy is zero. $V(g)$ must be negative throughout the motion, and the particle must start at $g = 0$ at $\zeta = -\zeta_w$ and return to $g = 0$ at $\zeta = \zeta_w$. From inspection of the graph of $V(g)$ (Figure 3.7), we see that the maximum possible value of g_0 is unity, that the particle will never reach the point $g = a$ unless $g_0 = a = 1$, and that there are two basic motions, a completely forward motion, which can

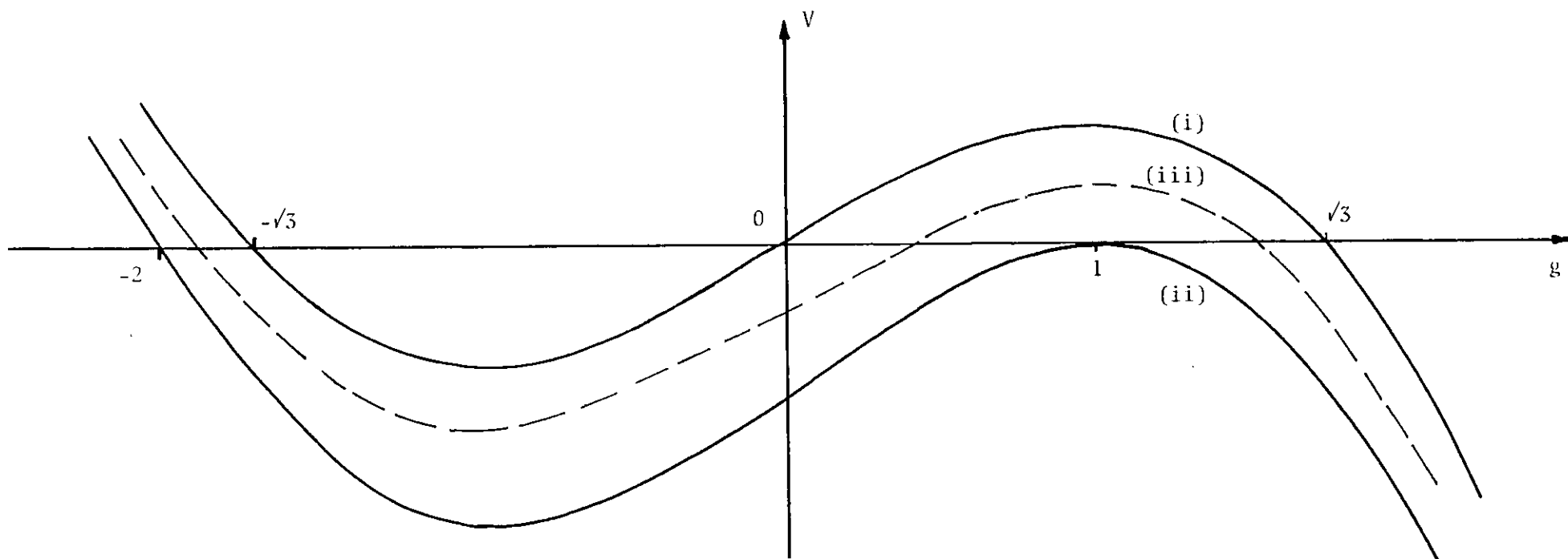


Figure 3.7. The energy function $V(g)$: (i) has $g_0 = 0$, $a = \sqrt{3}$ and $b = -\sqrt{3}$, (ii) has $g_0 = a = 1$ and $b = -2$, and (iii) has $g_0 = 2/3$, $a = (6\sqrt{2} - 1)/5$ and $b = (6\sqrt{2} + 1)/5$. All curves with $0 < g_0 < 1$ lie between (i) and (ii), and unless $0 \leq g_0 \leq 1$ either $V(0) > 0$ or $V(g) < 0$ for all $g > 0$.

exist if $0 < g_0 \leq 1$, and a completely reversed motion with $g \leq 0$, which can exist if $b \leq -\sqrt{3}$. In the former, the particle starts at $g = 0$, moves to g_0 and then returns to $g = 0$, and in the latter moves from $g = 0$ to b and returns to $g = 0$. Clearly, the flow corresponding to the second basic motion cannot satisfy mass conservation. However, if $0 < g_0 \leq 1$ there may be a number of composite motions, in which the particle reaches both g_0 and b , such that the corresponding flow, which will have regions of both forward and reversed flow, can satisfy conservation of mass. We will show later that at least one such composite flow can be constructed, and hence that our problem does not have a unique solution.

Before doing this, let us examine the completely forward flow outlined above. This flow is symmetric (as is the completely reversed flow) and the velocity is monotonic in the upper and lower halves of the channel. Thus the no slip condition at the lower wall can be replaced by the symmetry condition $g'(0) = 0$, which is automatically satisfied as $g(0) = g_0$ in (3.22). In the upper half of the channel g' is negative, and (3.22) and the no slip condition imply that

$$\zeta_w - \zeta = \sqrt{\frac{3}{2}} \int_0^g \frac{dt}{\sqrt{(g_0-t)(a-t)(t-b)}} \quad (3.23)$$

At $\zeta = 0$ this gives

$$k(2/p_0)^{1/4} = \sqrt{\frac{3}{2}} \int_0^{g_0} \frac{dt}{\sqrt{(g_0-t)(a-t)(t-b)}} \quad (3.24)$$

which with the condition from conservation of mass,

$$\frac{1}{3} (2p_0)^{-1/4} = \sqrt{\frac{3}{2}} \int_0^{g_0} \frac{tdt}{\sqrt{(g_0-t)(a-t)(t-b)}} \quad (3.25)$$

determines the values of g_0 and p_0 for a given value of the known parameter k . In practice, it proves easier to take a particular value of g_0 and determine the values of k and p_0 consistent with this g_0 . In turn (3.24) and (3.25) can be written as

$$\zeta_w = (6/\alpha)^{1/2} F(\delta, \gamma) \quad (3.24a)$$

and

$$\frac{1}{3}(2p_0)^{-1/4} = (6/\alpha)^{1/2} (g_0 - a) \Pi(\delta, \gamma^2, \gamma) + a\zeta_w, \quad (3.25a)$$

where F and Π are respectively the elliptic integrals of the first and third kind, as defined by Gradshteyn and Ryzhik (1965). Here

$$\alpha = a - b, \quad \gamma^2 = (g_0 - b)/(a - b) \quad \text{and} \quad \sin^2 \delta = g_0/(\gamma^2 a).$$

It was shown above that $g_0 \leq 1$. We will now examine in detail the solution when g_0 is close to unity. It can be shown that if $1 - g_0 \ll 1$ then $F(\delta, \gamma) \sim -\frac{1}{2} \ln(1 - g_0)$ and $\Pi(\delta, \gamma^2, \gamma) \sim -\frac{1}{4} \ln(1 - g_0)$. It follows from (3.24a) and (3.25a) that $\zeta_w \sim -\frac{1}{\sqrt{2}} \ln(1 - g_0) \rightarrow \infty$ and $k \rightarrow k_0$ as $g_0 \rightarrow 1^-$, where $k_0 = \frac{1}{3\sqrt{2}}$. The behaviour of g , and of the constants g_0 , p_0 , and ζ_w , as $k \rightarrow k_0$ can be deduced directly from the momentum equation (3.19) and conservation of mass. Equation (3.19), the monotonicity of g in $0 \leq \zeta \leq \zeta_w$, and $\zeta_w \gg 1$ imply that, to leading order,

$$g = 1 \quad (3.26)$$

in the core where $\eta = \zeta_w - \zeta \gg 1$. Further, the next term in the expansion of g in the core must be exponentially small in ζ_w . Likewise $1 - g_0$ must be exponentially small. If, for η of $O(1)$, i.e. close to the wall, we write $g(\zeta)$ as $\hat{g}(\eta)$, then $\hat{g}(\eta)$ must satisfy (3.19) and the boundary conditions $\hat{g}(0) = 0$ (no slip at the wall) and $\hat{g} \rightarrow 1$ as $\eta \rightarrow \infty$ (matching to the core flow). This Falkner-Skan problem is the same as that arising in the flow in a converging channel with intersecting plane walls, first studied by Pohlhausen (1921). The solution, from Jones and Watson (1963), is

$$\hat{g}(\eta) = 3 \tanh^2(\eta_0 + \eta/\sqrt{2}) - 2, \quad (3.27)$$

where $\eta_0 = \tanh^{-1} \sqrt{2/3} = 1.146216$.

Conservation of mass and (3.26) imply that

$$3\sqrt{2}k - (162p_0)^{1/4} \int_0^{\infty} (1 - g) d\eta = 1, \quad (3.28)$$

and that $\zeta_w = (162p_0)^{-1/4}$ to leading order.

This suggests that for ζ_w large we expand p_0 and k as

$$\left. \begin{aligned} k &= k_0 + k_1 \zeta_w^{-1} + \dots, \\ p_0 &= \frac{1}{162} \zeta_w^{-4} + p_{01} \zeta_w^{-5} + \dots \end{aligned} \right\} (3.29)$$

Equation (3.28) and the wall relationship $\zeta_w = k(2/p_0)^{1/4}$, which must hold exactly, can be used to determine the k_i and p_{0i} in (3.29). In particular, we find that $k_0 = 1/3\sqrt{2}$ (as above), $k_1 = 1 - \sqrt{2/3}$, and $p_{01} = \frac{2\sqrt{2}}{27} (1 - \sqrt{2/3})$. There is an implicit assumption here that higher order terms in the boundary layer expansion are insignificant to the orders calculated in (3.29). It is easily shown that if g is expanded in terms of ζ_w^{-1} then the leading order term is given by (3.27) and that the values of k_0 , k_1 and p_{01} are as given. Hence, we conclude that there is no serious omission at the present order of working.

Figure (3.8) shows the values of g_0 and ζ_w against μ as calculated from (3.24) and (3.25) (see Appendix 5 for the method). Also shown are the theoretical values of μ against ζ_w obtained from the first two terms in the expansion for k in (3.29). Agreement is excellent in the region for which $1 - g_0$ is small, i.e. for $\mu > 13$ approximately.

Some important features of the local behaviour of the flow and the channel can now be deduced. The tube law implies that $y_w = k p_0^{-1/2} (X_0 - X)$ locally, and hence that the slope of the channel walls will become infinite as $\mu \rightarrow 18$ and $p_0 \rightarrow 0$. This was confirmed by solving the full problem (equations 3.1 - 3.3) numerically for various μ with $\varepsilon = 1$ and $q = 1/2$ (see Figure 3.5(iv)). Also confirmed (Figure 3.5) was the predicted linear relationship between y_w and X as $y_w \rightarrow 0$, and that, as expected, X_0 is smaller with larger μ . Figure 3.9 displays the shape of the velocity profile for various μ , as determined from (3.23). Clearly, $g(\zeta)$ takes the predicted mainly inviscid form as $\mu \rightarrow 18^-$. By expanding for $0 < g_0 \ll 1$ in (3.24) and (3.25), it can be shown that $g_0 \rightarrow 0$ and $p_0 \rightarrow \infty$ as $\mu \rightarrow 0$. It follows, as might be expected and as is clearly displayed in the results from the numerical

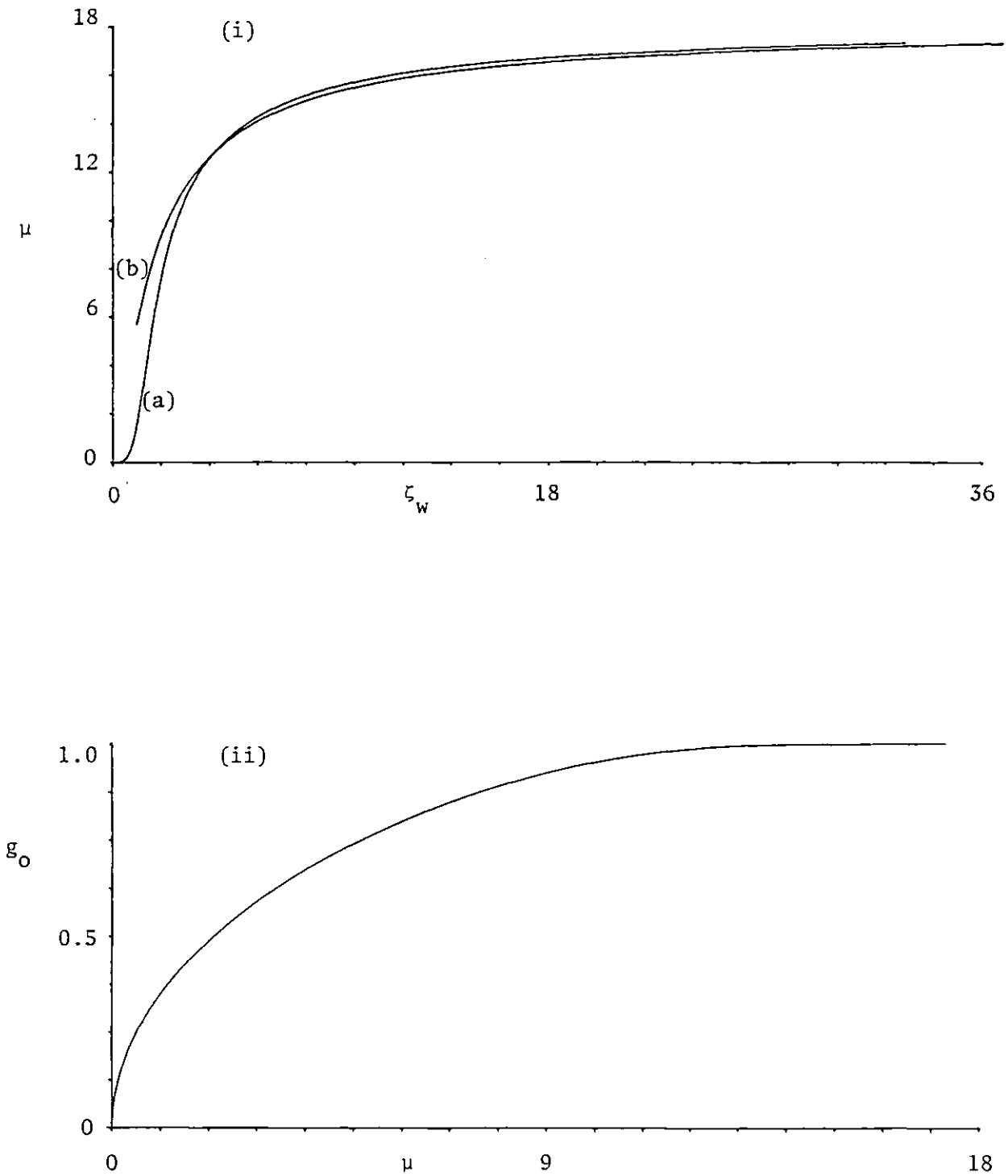


Figure 3.8. Coefficients of the asymptotic solution for $-\mu \gg 1$ with $\epsilon = 1$ and $q = 1/2$.

(i) μ against ζ_w . (a) from (3.24) and (3.25), (b) from the first two terms of (3.29), (ii) g_0 against μ (from (3.24) and (3.25)).

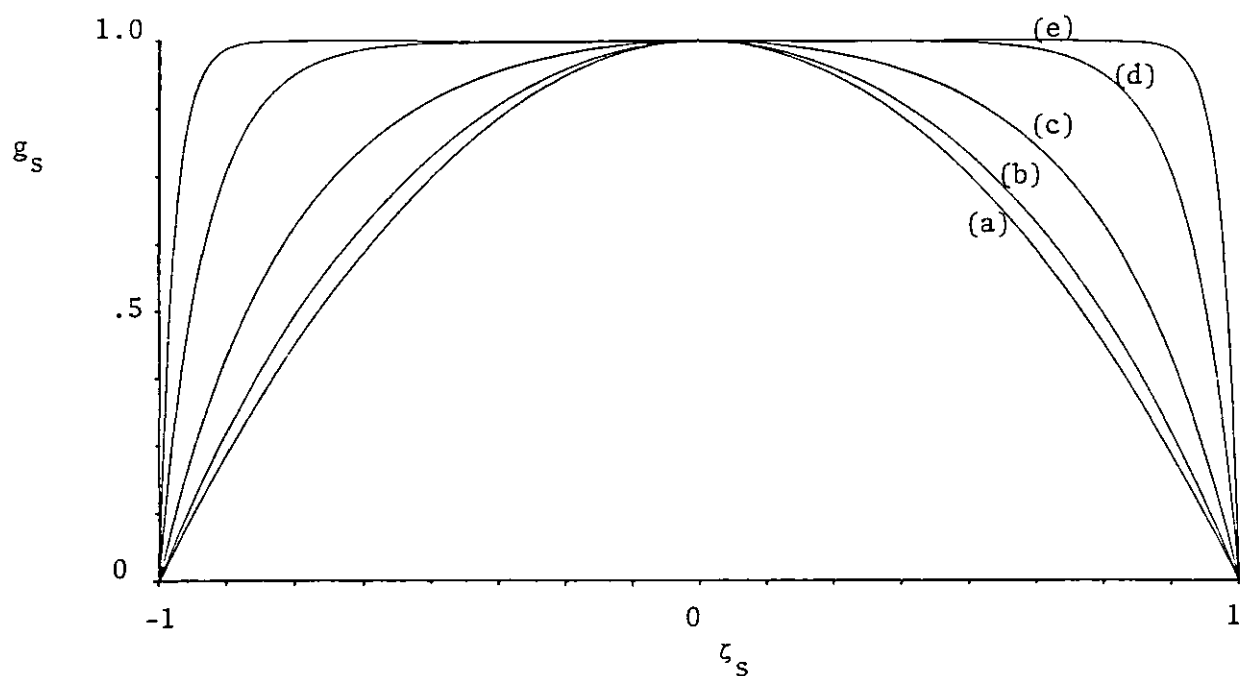


Figure 3.9. Velocity profiles for $q = 1/2$, $\epsilon = 1$, and various μ , where $g_s = g/g_0$ and $\zeta_s = \zeta/\zeta_w$.
(a) $\mu = .1$, (b) $\mu = 4.0$, (c) $\mu = 10.0$, (d) $\mu = 15.0$,
(e) $\mu = 17.0$.

solution (Fig. 3.5), that locally the slope of the channel wall tends to zero as $\mu \rightarrow 0$. The ratio of the inertial terms to the pressure gradient in the streamwise momentum equation is of $O(g_o^2)$. Thus, the flow will become viscous in nature as $\mu \rightarrow 0$, and the velocity profile should be parabolic in form for small μ . That this occurs is evident from Figure 3.9. In fact, the velocity profile is close to the parabolic profile for $\mu \leq 1$ approximately. This is not surprising as $g_o^2 \doteq .1$ for $\mu = 1$. The problem with $\mu \ll 1$ is considered in more detail in Section 3.5 below.

So far we have found a numerical solution of (3.19) and (3.20) valid for $\mu < 18$, and a limit solution valid as $\mu \rightarrow 18$. That the completely forward flow considered above cannot provide a solution of (3.19) and (3.20) for $\mu > 18$ is evident immediately from (3.24) and (3.25). Since $g_o \leq 1$ then $k(2/p_o)^{1/4} > \frac{1}{3}(2p_o)^{-1/4}$, which implies that $\mu < 18$. As will be shown soon, this restriction on μ holds for composite flows as well, and indeed there is no solution of the form (3.18) for $\mu \geq 18$. We see from (3.29) that

$$\zeta_w \sim \frac{k_1}{k - k_o} \quad (3.30)$$

as $\mu \rightarrow 18$. Since $k_1 > 0$, k must be greater than k_o for ζ_w to be positive. Thus the limit solution is valid only as $\mu \rightarrow 18$ from below, and strictly we do not have a solution for $\mu = 18$. An attempt, basically unsuccessful, was made to find an alternative limit structure valid for $\mu = 18$ (see Appendix 1).

Conservation of mass requires that $\bar{u}y_w = \frac{1}{3}$, where \bar{u} is the mean fluid velocity, which suggests that u is $O(y_w^{-1})$. Assuming this and a balance between the viscous and inertial forces in the fluid when $y_w \ll 1$ introduces $y_w = O(X_o - X)$. It appears therefore that a local steady solution balancing these forces as $y_w \rightarrow 0$ should have the similarity form (3.18) regardless of the exact value of μ . This in turn suggests that there is no local steady solution with this balance of forces for $\mu \geq 18$. Alternatively, we could assume that the inertial forces dominate the viscous forces as $y_w \rightarrow 0$. With this assumption the governing equations are given locally by

$$\left. \begin{aligned} u \frac{\partial u}{\partial X} + V \frac{\partial u}{\partial y} &= -p'(X), \\ \frac{\partial u}{\partial X} + \frac{\partial V}{\partial y} &= 0. \end{aligned} \right\} (3.31)$$

Following Cole and Aroesty (1968), the solution of (3.31) downstream of a given point $X = X^*$ is

$$y = \int_0^{\psi} \{ u^{*2}(t) + 2 [p^* - p(X)] \}^{-1/2} dt, \quad (3.32)$$

where $u^*(y)$ and p^* are respectively the streamwise velocity and pressure at $X = X^*$, and $\psi = 0$ at $y = 0$. As $p \rightarrow -\infty$, (3.32) implies that $y_w \sim \frac{1}{3\sqrt{2}} (-p)^{-1/2}$, and hence that this solution is valid only for $\mu = 18$. Thus we are led tentatively to the conclusion that there is no essentially inviscid solution for $\mu > 18$, or, more strictly, unless $|18 - \mu| \ll 1$. We note that the leading order term in the expansion of (3.32) for $p/p^* \gg 1$ gives exactly the inviscid core part of the limit solution studied above. Further, mass conservation implies that such an essentially inviscid uniform flow can arise only if $|18 - \mu| \ll 1$ (see Section 5)

A detailed comparison showed that there is excellent agreement between the numerical solution of the full problem (equations 3.1 - 3.3) with $q = 1/2$, $\varepsilon = 1$, and μ of $O(1)$, and the values obtained from the solution of the local problem (equations 3.18 - 3.20), and it is clear that the similarity solution provides a valid local description of the flow for μ of $O(1)$. However, a complete numerical solution of the full problem could not be obtained by the method used (see Appendix 5) for μ greater than about 13, a value of μ consistent with $1 - g_0 \ll 1$ (see Figure 3.8) and $g(\zeta)$ approaching the limit form discussed above.

For $\mu > 18$ we have neither an analytical self-similar solution of the local problem nor a complete numerical solution of the full problem. There are two possible explanations of this: first, a steady solution exists but our present methods are inadequate; second, no steady solution exists for the problem as formulated above. If a steady solution exists for $\mu > 18$, then our results indicate that while the viscous force in the fluid must be important at leading order, the solution cannot have the similarity form (3.18) which

arises naturally from assuming that the inertial and viscous forces are of the same order. This, and the consistency between the numerical and analytical results, lend support to the second explanation above, i.e. that there is no solution of (3.1 - 3.3) with $\varepsilon = 1$, $q = 1/2$, $\mu > 18$ and $y_w \ll 1$.

If indeed there is no steady solution of this particular problem, then a basic assumption used in formulating the problem must be invalid. One possibility is that a shorter streamwise length scale is necessary, and another that significant upstream effects have been ignored. These points are considered, with respect to the problem with $\mu \gg 1$, in Section 3.4 below, and we will not pursue them here, but note merely that neither appears to provide any reasonable explanation of our failure to find a full solution for $\mu \geq 18$. A further possibility is that the channel-fluid system with $\varepsilon = 1$ and $q = 1/2$ is necessarily unsteady if $\mu \geq 18$, i.e. that there is no complete steady solution on any streamwise length scale. Some experimental and theoretical evidence supports this last possibility. In particular, there is evidence that this fluid-channel system will spontaneously destabilize if $\mu \geq 18$. This is discussed in Section 5 below.

We wish now to examine another solution of (3.19) that can satisfy (3.20). Consider a symmetric flow with one region of reversed flow centred on the midpoint of the channel. Proceeding as before, we find that

$$\zeta_w = \int_b^0 I(t) dt + 2 \int_0^{g_0} I(t) dt, \quad (3.33)$$

where $I(t) = \sqrt{3/2} \{(t - b)(g_0 - t)(a - t)\}^{-1/2}$. Here g_0 is the maximum value attained by g and $b = g(0) < 0$. We see from Figure 3.7 that $-2 \leq b \leq -\sqrt{3}$. The mass flow in the channel is given by $2(2p_0)^{1/4}Q$ where

$$Q = \int_b^0 tI(t) dt + 2 \int_0^{g_0} tI(t) dt. \quad (3.34)$$

Conservation of mass will be satisfied if

$$Q = \frac{1}{3} (2p_0)^{-1/4}. \quad (3.35)$$

Clearly, we require Q to be positive. Numerical experimentation showed that $Q > 0$ if $-2 \leq b \leq b_0$, where $b_0 \doteq -1.9845$. It follows that this solution of (3.19) can provide a valid solution for our local problem. However, since $0 < g_0 \leq 1$ and $b < 0$ then $Q < \zeta_w$, which implies that $\mu < 18$ in this case also. It was found that $\zeta_w \rightarrow \infty$ as $\mu \rightarrow 18^-$ and that $b \rightarrow b_0^-$ as $\mu \rightarrow 0$. Thus the restrictions on μ are the same here as for the completely forward flow studied previously. Proceeding as above, we find that as $\mu \rightarrow 18^-$ the solution tends to a limit form given by (3.26), (3.27), and a reversed jet at the centre of the channel. The velocity profile of this centre jet is given by $\mathfrak{g}(\zeta)$ from (3.27) with $\eta_0 = 0$. Expansions of k and p_0 in powers of $\zeta_w \gg 1$ can be made. They have the same leading order terms as those in (3.29).

Generalising, we can construct a solution of (3.19) which satisfies no slip at the walls and has an arbitrary finite number of regions of reversed flow, including possibly reversed flow adjacent to either or both of the walls. Such a solution will have a limit form of $g = 1$ over most of the channel and the appropriate number of reversed jets interspersed across the channel. Clearly mass conservation can be satisfied by this limit form. Hence there is a range of $g_0 < 1$ for which this generalised solution can satisfy (3.20). Expansions of k and p_0 for $\zeta_w \gg 1$, similar to (3.29), can be made. The expansion for k would imply that

$$\zeta_w \sim \frac{k'_1}{k - k_0}$$

as $\mu \rightarrow 18$, where $k'_1 > 0$ and $k'_1 \neq k_1$ (c.f. equation 3.30). Requiring $0 < \zeta_w < \infty$ implies that $\mu < 18$, as above. More formally, for any particular solution of (3.19) and (3.20) we can construct expressions of the form of (3.33) and (3.34), which with (3.35) imply that $\mu < 18$. We conclude therefore that if $\mu \geq 18$ then there is no local solution with the similarity form (3.18). We note that, in common with our problem, a solution of the Jeffery-Hamel problem does not exist for all values of the parameters (Rosenhead 1940).

On comparing values from the numerical solution of the full problem (equations 3.1 - 3.3) with those from the local solution given by the completely forward flow (equations 3.23 - 3.25), we found excellent agreement. Further, there was no evidence in the numerical solution of the full problem of the concavities or reversals in the

flow field which must occur with any other solution of (3.19). Accordingly, we conclude that, when it exists, the correct similarity solution is that given by the completely forward flow.

The analysis for a severe collapse ($0 < 1 - \varepsilon \ll 1$) with $q = 1/2$ and $\mu = 0(1)$ is easily deduced from the above and the results of Section 3.2.

Finally in this section we study the channel with $q > 1/2$, $\varepsilon = 1$ and $\mu = 0(1)$. As $y_w \rightarrow 0$ the inertial terms in the momentum equation will dominate the pressure gradient, and the local problem does not appear to be well posed, in the sense the positions of the walls (and therefore the boundary conditions) depend on the pressure but the pressure gradient does not appear in the leading order governing equations. If we assume a balance between the viscous and inertial forces, then, as with $q = 1/2$, y_w is $O(X_0 - X)$, and it can be shown, using a dynamical argument similar to that found above, that there is no similarity solution for the local problem which can satisfy both no slip at the walls and conservation mass. Alternatively, if it is assumed that the flow is inertia dominated, then the solution takes the form $u(X,y) = A(X)V(X,y)$, where $A(X)$ is to be determined. It follows that the flow must be nonsymmetric unless there is a concavity in the flow field at $y = 0$, and unless $V(X,y)$ is unidirectional there must be reversed flow over part of the channel. Although concavities have been reported for flows through constricted tubes (Smith 1979, Deshpande et al. 1976, Forrester and Young 1970), there is no evidence in the numerical solutions of the full problem, as far as they could be obtained, for any such occurrence here. A larger value of q is expected to force a faster response from the system, and, considering the flow structure for $q \leq 1/2$, it is natural to assume that $p \propto (X_0 - X)^{-n}$, where $nq < 1$. This implies that $u \propto (X_0 - X)^{-nq}$ as $X \rightarrow X_0^-$ which suggests that $A(X) = (X_0 - X)^{-nq}$ and a self-similar flow structure for which there is no solution. The numerical procedure applied to the full problem (equations 3.1 - 3.3) diverged when the walls moved a finite distance into the channel, i.e. no complete numerical solution was found. It is possible that no complete steady solution exists (c.f. $q = 1/2$, with $\mu \geq 18$ above). This possibility is discussed briefly in Section 5 below.

As for a complete collapse ($\varepsilon = 1$), we could not find a full solution for the channel-fluid system with a severe collapse ($0 < 1 - \varepsilon \ll 1$), $q > 1/2$ and μ of $O(1)$.

3.4 Channel flows with a fast pressure response

The basic problem we study in this section is that of a channel obeying (3.3) with a fast pressure response, a total collapse possible, and q of $O(1)$. That is, unless otherwise stated we assume that

$$\left. \begin{aligned} q &= O(1), \quad \varepsilon = 1 \\ 1 &\ll \mu^2 \ll R. \end{aligned} \right\} (3.39)$$

Later in this section we investigate the effects of $q \ll 1$ and/or $\varepsilon \neq 1$. The upper limit on μ in (3.39) ensures that the pressure remains independent of y .

If $0 < -\mu p \ll 1$, then from (3.3) the position of the upper wall is given by

$$y_w = 1 - \frac{1}{2} q u^2 p^2 + O(\mu^4 p^4). \quad (3.40)$$

We propose that as the flow passes the origin thin viscous layers form adjacent to the walls, and that it is the flow in these boundary layers that determines the pressure, and thus the position of the walls, while the core flow responds passively to changes in the boundary layers (c.f. $\mu^{2/3} \varepsilon \leq O(1)$, Section 2.1). The boundary layers have, at least initially, a linear flow structure. Let $x = \delta^3 R \bar{X}$ and $y = 1 - \delta \bar{Y}$, where $\delta = \mu^{-1/2}$. To match with the incoming Poiseuille pressure gradient, the pressure scaling must be $p = \delta^3 P$. At this stage the pressure will be uniform across the channel if $\delta^3 R \gg 1$. The necessity for the tighter restriction $\delta^4 R \gg 1$ will become apparent later in the analysis. With these scalings the flow structure in the boundary layer adjacent to the upper wall is given by

$$\left. \begin{aligned} u &= \delta \bar{Y} + \delta^2 u_1(\bar{X}, \bar{Y}) + o(\delta^2), \\ v &= -R^{-1} v_1(\bar{X}, \bar{Y}) + o(R^{-1}), \end{aligned} \right\} (3.41)$$

and to leading order the equations of motion reduce to the linearised boundary layer equations, viz.

$$\left. \begin{aligned} \bar{Y} \frac{\partial u_1}{\partial \bar{X}} + v_1 &= -P' + \frac{\partial^2 u_1}{\partial \bar{Y}^2}, \\ \frac{\partial u_1}{\partial \bar{X}} + \frac{\partial v_1}{\partial \bar{Y}} &= 0. \end{aligned} \right\} (3.42)$$

The tube law becomes

$$\bar{Y}_w = \begin{cases} 0 & P > 0, \\ \frac{q}{2} \delta P^2 & P < 0, \end{cases} \quad (3.43)$$

and the boundary conditions are

$$\left. \begin{aligned} v_1 &= 0 \text{ and } u_1 = -\bar{Y}_w \text{ at } \bar{Y} = 0, \\ u_1 &\sim -\frac{1}{2} \bar{Y}^2 \text{ as } \bar{Y} \rightarrow \infty, \\ u_1 &\rightarrow 0 \text{ as } \bar{X} \rightarrow -\infty, \end{aligned} \right\} (3.44)$$

from no slip at the wall, and matching to Poiseuille flow at the outer edge of the layer and upstream in turn.

The transform solution of this boundary layer problem can be found using the method applied to a similar problem in Section 2.1.

Again, no evidence is found for any significant upstream influence. Thus there is a definite starting point, $\bar{X} = 0$, for the change in the flow from the incoming Poiseuille flow. The pressure downstream of the origin is given by the solution of the integro-differential equation

$$-\frac{q}{2} p^2 = \frac{-1}{3Ai'(0)\Gamma(2/3)} \left\{ \int_0^{\bar{X}} (\bar{X} - t)^{-1/3} \frac{dP}{dt} dt + \frac{3}{2} \bar{X}^{2/3} \right\}. \quad (3.45)$$

The skin friction perturbation is given by the solution of (3.45) and

$$\tau_1 = \frac{-Ai(0)}{\Gamma(\frac{1}{3})Ai'(0)} \left\{ \int_0^{\bar{X}} (\bar{X} - t)^{-2/3} \frac{dP}{dt} dt + 3\bar{X}^{1/3} \right\}, \quad (3.46)$$

where $\bar{X} > 0$ and $\tau = \partial u / \partial y$ ($y = y_w$) = $-1 + \delta\tau_1 + o(\delta)$. As $\bar{Y} \rightarrow \infty$

$$v_1 \sim -(P' + 1),$$

which provides a matching condition for the core flow at the outer edge of the wall layer. As for the fine collapse with $\varepsilon = 0(\mu^{-2/3})$ (Section 2.1), it is the matching of u_1 to the second order term from the Poiseuille flow at the outer edge of the layer that forces the inclusion of the $\bar{X}^{2/3}$ term in (3.45), and thus ensures a nontrivial solution for the pressure.

Before discussing the behaviour of the wall solution in detail, it is convenient to present the core solution. The core flow takes the form of an inviscid rotational perturbation to the Poiseuille flow (c.f. $\varepsilon \ll \mu^{-2/3}$, Section 2.1) and is given by

$$\left. \begin{aligned} u &= U_0(y) + \delta^3 \bar{u}_1(\bar{X}, y) + o(\delta^3), \\ v &= R^{-1} \bar{v}_1(\bar{X}, y) + o(R^{-1}), \end{aligned} \right\} \quad (3.47)$$

where

$$\left. \begin{aligned} \bar{u}_1 &= -\frac{P + \bar{X}}{U_0(y)} \left\{ 1 + U_0(y) U_0'(y) \int_0^y U_0^{-2}(t) dt \right\}, \\ \bar{v}_1 &= (P' + 1) U_0(y) \int_0^y U_0^{-2}(t) dt. \end{aligned} \right\} \quad (3.47a)$$

Note that $(\bar{u}_1, \bar{v}_1) \equiv 0$ for $\bar{X} < 0$. By expanding (3.47a) for $1 - y \ll 1$, it can be shown that (u, v) match to the boundary layer solution as $y \rightarrow 1$. Also the behaviour of \bar{u}_1 as $y \rightarrow 1$ suggests that the next term in the boundary layer expansion is of $0(\delta^3 \ln \delta)$.

Applying the transformations $P = \alpha \hat{P}$ and $\bar{X} = \frac{2}{3} \alpha \hat{X}$, where $\alpha = (\frac{2}{3})^{1/2} [-qAi'(0)\Gamma(\frac{2}{3})]^{-3/4}$, to (3.45) produces

$$-\hat{P}^2 = \int_0^{\hat{X}} (\hat{X} - t)^{-1/3} \frac{d\hat{P}}{dt} dt + \hat{X}^{2/3}. \quad (3.48)$$

Close to the origin ($0 < \hat{X} \ll 1$) the pressure is given by the series

$$\hat{P} = \mu_0 \hat{X} + \mu_1 \hat{X}^{7/3} + O(\hat{X}^{11/3}), \quad (3.49)$$

where $\mu_0 = -2/3$, $\mu_1 = -\frac{3}{7} \mu_0^2 / B(7/3, 2/3)$ etc., and $B(m,n)$ is the Beta function as defined by Abramowitz and Stegun (1965). The first term in (3.49) comes from the Poiseuille flow, and the others from the balance of the integral term with $-\hat{P}^2$ in (3.48). Numerical methods (see Appendix 5) are necessary to obtain a full solution of (3.48). This solution is shown in Figure 3.10, as is \hat{P} from (3.49). Clearly \hat{P} has a singularity at a finite value \hat{X}_0 (≈ 1.047) of \hat{X} . Assuming that \hat{P} can be written as

$$\hat{P} = -\lambda_1 (\hat{X}_0 - \hat{X})^{-1/3} + \hat{P}_1(\hat{X}), \quad (3.50)$$

where $(\hat{X}_0 - \hat{X})^{1/3} \hat{P}_1(\hat{X}) \rightarrow 0$ as $\hat{X} \rightarrow \hat{X}_0^-$, the integral in (3.48) can be written as

$$-\frac{\lambda_1}{3} I_1(\hat{X}) + I_2(\hat{X}),$$

where $I_1(\hat{X}) = \int_0^{\hat{X}} (\hat{X} - t)^{-1/3} (\hat{X}_0 - t)^{-4/3} dt$ and

$I_2(\hat{X}) = \int_0^{\hat{X}} (\hat{X} - t)^{-1/3} \frac{d\hat{P}_1}{dt} dt$. Clearly, as $\hat{X}_0 \rightarrow \hat{X}$ the leading order term from I_1 must balance with $-\lambda_1^2 (\hat{X}_0 - \hat{X})^{-2/3}$, the leading order term from $-\hat{P}^2$. Let $\Delta = \hat{X}_0 - \hat{X} \ll 1$. If θ is chosen such that $\theta \gg \Delta$ then

$$\begin{aligned} \int_{\hat{X}-\theta}^{\hat{X}} (\hat{X} - t)^{-1/3} (\hat{X}_0 - t)^{-4/3} dt &= -\frac{3}{2} \hat{X}^{-2/3} + \frac{4}{5} \Delta \hat{X}^{-5/4} - \\ &\frac{7}{12} \Delta^2 \hat{X}^{-8/3} + \dots \\ &+ \frac{3}{2} \theta^{-2/3} - \frac{4}{5} \Delta \theta^{-5/3} + \frac{7}{12} \Delta^2 \theta^{-8/3} + \dots, \end{aligned}$$

and

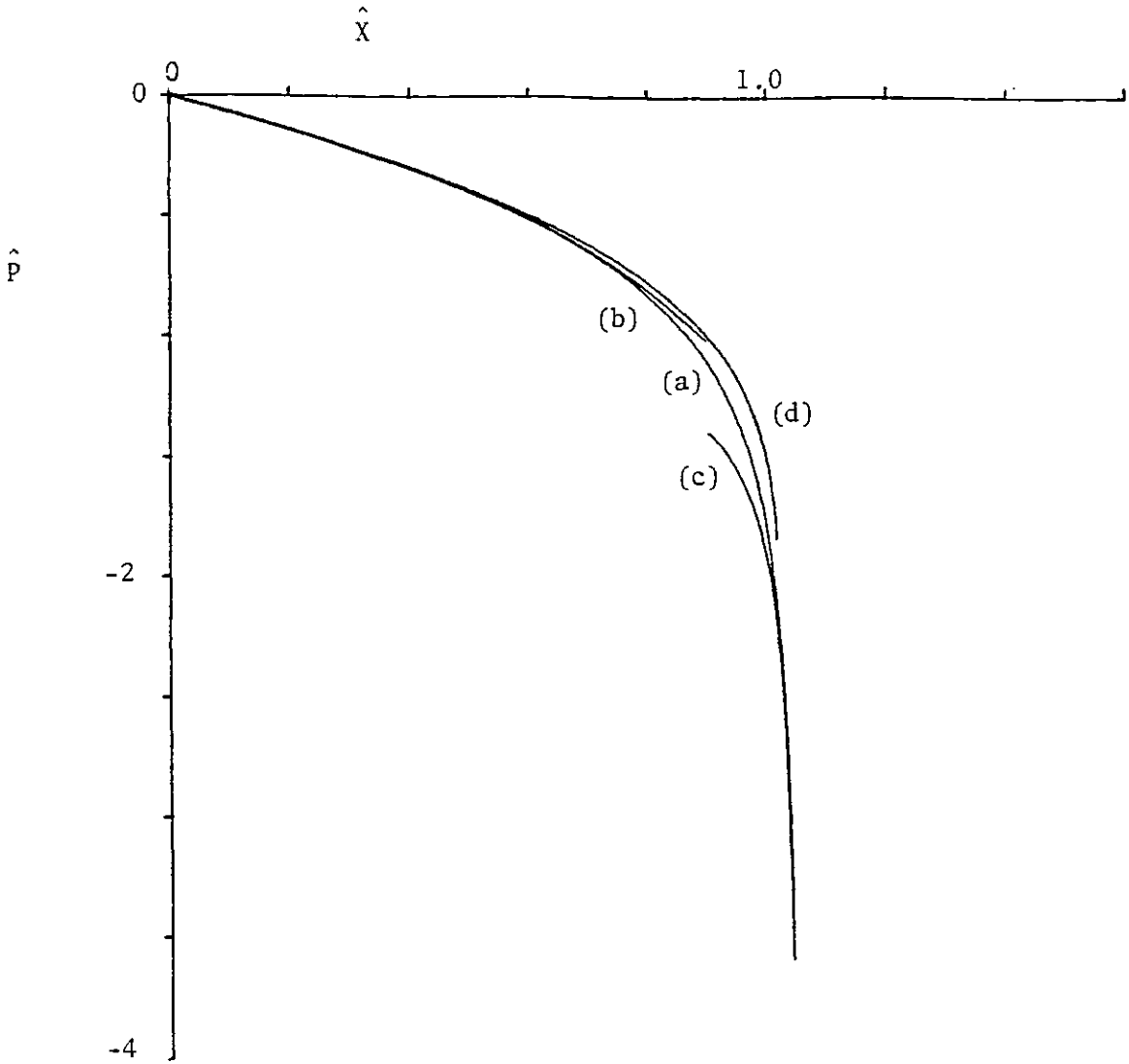


Figure 3.10. The pressure in a channel with a fast pressure response.

From (a) the numerical solution of (3.48), (b) the series for $\hat{X} \ll 1$ (equation 3.49), (c) the asymptotic expansion for $\hat{X}_0 - \hat{X} \ll 1$ (equation 3.50), and (d) the numerical solution of the full problem (equations 3.1 - 3.3) with $\epsilon = 1$, $q = 1/2$, and $\mu = 100$.

$$\int_0^{\hat{X}-\theta} (\hat{X}-t)^{-1/3} (\hat{X}_0-t)^{-4/3} dt = \Delta^{-2/3} B\left(\frac{2}{3}, \frac{2}{3}\right) \\ - \frac{3}{2} \theta^{-2/3} + \frac{4}{5} \Delta \theta^{-5/3} - \frac{7}{12} \Delta^2 \theta^{-8/3} + \dots,$$

which imply that

$$I_1(\hat{X}) = (\hat{X}_0 - \hat{X})^{-2/3} B\left(\frac{2}{3}, \frac{2}{3}\right) - \frac{3\hat{X}^{-2/3}}{2} + \frac{4}{5} (\hat{X}_0 - \hat{X}) \hat{X}^{-5/3} + \dots,$$

hence that

$$\lambda_1 = \frac{1}{3} B\left(\frac{2}{3}, \frac{2}{3}\right). \quad (3.51)$$

We could not find a solution or a leading order term for \hat{P}_1 directly from (3.48). However, by a process similar to the above, it can be shown that there are no terms of order $\Delta^m \ln \Delta$ or Δ^m in the expansion for \hat{P} , where $-\frac{1}{3} < m < \frac{1}{3}$. This suggests that I_2 is bounded as $\hat{X} \rightarrow \hat{X}_0$.

We will now investigate the flow structure as $\bar{X} \rightarrow \bar{X}_0^-$, where $\bar{X}_0 = \alpha \hat{X}_0$. If the stream function ψ is zero at $y = y_w$ then

$$\psi = -\delta^2 Y^2/2 - \delta^3 \psi_1(\bar{X}, \bar{Y}) + o(\delta^3) \quad (3.52)$$

in the viscous layer adjacent to the upper wall. A similarity solution for ψ_1 can be obtained from the expansions

$$\left. \begin{aligned} \psi_1 &= (\bar{X}_0 - \bar{X})^{-1/3} f_0(\zeta) + (\bar{X}_0 - \bar{X}) f_1(\zeta) + o(\bar{X}_0 - \bar{X}) \\ P &= -P_0 (\bar{X}_0 - \bar{X})^{-1/3} - P_1 (\bar{X}_0 - \bar{X}) + o(\bar{X}_0 - \bar{X}) \end{aligned} \right\} (3.53)$$

where $\zeta = \bar{Y}(\bar{X}_0 - \bar{X})^{-1/3}$, $P_0 = \frac{2}{q} g^{-1/3} \Gamma\left(\frac{2}{3}\right)$ and P_1 is a constant. This value for P_0 was obtained from (3.51), but it can also be found from the solution for $f_0(\zeta)$, as will be shown below. The $O(\bar{X}_0 - \bar{X})$ terms in (3.53) are required by the matching to Poiseuille flow at the outer edge of the layer, and it has been assumed that they are the second order terms in the expansions. This matching implies that $P_1 = 1$, and hence from (3.50) that

$$\hat{P}_1(\hat{X}) = -\frac{2}{3}(\hat{X}_0 - \hat{X}) + o(\hat{X}_0 - \hat{X}). \quad (3.54)$$

From (3.42), $f_0(\zeta)$ must satisfy

$$f_0'''' - \frac{1}{3}\zeta^2 f_0'' - \frac{1}{3}\zeta f_0' + \frac{1}{3}f_0 = -\frac{1}{3}P_0, \quad (3.55a)$$

The boundary conditions

$$\left. \begin{aligned} f_0(0) &= 0, \\ f_0'(0) &= -\frac{q}{2}P_0^2, \\ f_0'(\infty) &= 0, \end{aligned} \right\} (3.55b)$$

come from $\psi = 0$ at the wall, no slip at the wall and matching to the core flow in turn.

A particular solution of (3.55a) is $f_0 = -P_0$, and $f_0 = \zeta$ is one solution of the homogeneous equation. Taking $f_0 = \zeta g(\zeta)$, $h = dg/d\zeta$ and $s = \zeta^3$, the homogeneous form of (3.55a) becomes

$$9sh'' + (15 - s)h' - h = 0$$

where the prime now denotes differentiation with respect to s . The method of integral transforms (Burkill 1975) can be used to determine $h(s)$. Taking $h = \int_c e^{\omega s} \phi(\omega) d\omega$, we find that if c is chosen such that

$$[e^{\omega s} (1 - 9\omega) \omega \phi]_c = 0,$$

then

$$\phi(\omega) = (1 - 9\omega)^{-1/3}.$$

The paths c_1 ($-\infty < \omega \leq \frac{1}{9}$) and c_2 ($-\infty < \omega \leq 0$) provide two independent solutions for h . The solution from c_1 , which can be found explicitly, must be excluded as it grows exponentially in s as $s \rightarrow \infty$. Hence the solution for f_0 is

$$f(\zeta) = -P_0 + a\zeta + b\zeta \int_{\zeta}^{\infty} dt \int_0^{\infty} (1 + 9\omega)^{-1/3} \exp(-\omega t^3) d\omega \quad (3.56)$$

where a and b are arbitrary constants and the bar denotes the finite part of the integral. To leading order the integral in (3.56) is proportional to ζ^{-2} as $\zeta \rightarrow \infty$. Thus a must be zero to satisfy the outer matching condition from (3.55b). When $\zeta \ll 1$

$$\int_0^{\infty} (1 + 9\omega)^{-1/3} \exp(-\omega \zeta^3) d\omega = 9^{-1/3} \Gamma\left(\frac{2}{3}\right) \zeta^{-2} + 0(1)$$

and

$$\begin{aligned} & \int_{\zeta}^{\infty} dt \int_0^{\infty} (1 + 9\omega)^{-1/3} \exp(-\omega t^3) d\omega \\ &= 9^{-1/3} \Gamma\left(\frac{2}{3}\right) \zeta^{-1} - 9^{-2/3} \Gamma^2\left(\frac{2}{3}\right) + 0(\zeta). \end{aligned}$$

Therefore, the boundary conditions at the wall are satisfied by taking $b = 2/q$ and $P_0 = \frac{2}{q} 9^{-1/3} \Gamma\left(\frac{2}{3}\right)$. As required, this is the value of P_0 implied by (3.51).

The solution for \hat{P} obtained numerically from the integral equation (3.48) is displayed in Figure 3.10. Also shown in Figure 3.10 are the values of \hat{P} obtained from the first six terms of the Taylor series for \hat{X} small (equation 3.49), from the first two terms of the expansion of \hat{P} as $\hat{X} \rightarrow \hat{X}_0$ (equations 3.50 and 3.54), and from the numerical solution of the full problem (equations 3.1 - 3.3) with $\varepsilon = 1$, $q = 1/3$ and $\mu = 100$. The value of \hat{X}_0 used here is 1.047, a value obtained from the numerical solution of (3.48). As can be seen from Figure 3.10, the values for the pressure obtained from the series for $\hat{X} \ll 1$ and the asymptotic structure as $\hat{X} \rightarrow \hat{X}_0$ show excellent agreement with the solution of the integral equation (3.48), as do the values obtained from the solution of the full problem. Thus it appears that the flow structure given above provides a valid description of the flow as it passes the origin and the channel begins to collapse.

Immediately downstream of the origin, where $0 < \bar{X} \ll 1$ and (3.49) is valid, a similarity solution for the perturbation to the flow in the upper wall layer can be obtained. Here, to leading order,

$u_1 + \frac{1}{2} \bar{Y}^2 \propto \bar{X}^2$, $P + \bar{X} \propto \bar{X}^{7/3}$, $\tau_1 \propto \bar{X}^{5/3}$, $\bar{Y}_w = \frac{1}{2} \delta q \bar{X}^2$, and the boundary layer thickness is $O(\bar{X}^{1/3})$. Hence, as the flow passes the origin the change from the Poiseuille flow, and of the wall from $y_w = 1$ ($\bar{Y}_w = 0$), is fairly smooth, with the wall layers increasing in thickness downstream. Note that the leading term in \bar{Y}_w represents the effect on the wall position of the Poiseuille pressure, and that the leading terms in u_1 and P are from the Poiseuille flow while the lower order terms are forced by the nontrivial change in the wall position. Thus, in $0 < \bar{X} \ll 1$ the changes in the flow and the wall positions are initiated and driven by the pressure from the Poiseuille flow.

When \bar{X} and $\bar{X}_0 - \bar{X}$ are both $O(1)$ numerical methods must be used to complete the solution.

When $0 < \bar{X}_0 - \bar{X} \ll 1$, the leading term in the expansion for u_1 is the first term forced by the nontrivial \bar{Y}_w , and in (3.45) the P^2 term, which gives the change in the wall position, dominates the $\bar{X}^{2/3}$ term from the Poiseuille flow. Thus, in $0 < \bar{X}_0 - \bar{X} \ll 1$ the interaction between the change in the flow and the change in the wall position dominates the change forced by the Poiseuille flow and the collapse is self-sustaining. The singularity in the solution arises naturally from the dominance of this interaction: if the P^2 term in (3.45) balances with the integral term as $P \rightarrow -\infty$, then $P \propto (\bar{X}_0 - \bar{X})^{-1/3}$ as $\bar{X} \rightarrow \bar{X}_0$ follows directly. To leading order $\tau_1 \propto (\bar{X}_0 - \bar{X})^{-1}$ as $\bar{X} \rightarrow \bar{X}_0$. It follows that the asymptotic flow structure becomes invalid when $\bar{X}_0 - \bar{X} = O(\delta)$. This suggests that an $O(\delta^4 R)$ streamwise length scaling be adopted close to \bar{X}_0 in an attempt to smooth out the singularity.

Before doing this, we consider the effects on the solution of altering the parameters. The value of the pressure response μ has a direct effect on the length scalings but not on the solution as such. If μ is increased, the streamwise length scaling is decreased, the boundary layers are concentrated closer to the walls, and magnitude of the core perturbation is smaller. Decreasing μ has the opposite effect. Unlike that of μ , the value of q has a direct effect on the solution, but not on the length scalings. In particular, α is proportional to $q^{-3/4}$. Thus, if q is increased then \bar{X}_0

is decreased, and if q is decreased \bar{X}_0 is increased. We see therefore that increasing the value of q or μ has the expected effect of moving the collapse closer to the origin, with the opposite effect from decreasing these values. The direct dependence on q of the solution to the boundary layer problem could be removed by taking δ as $(q\mu^2)^{-1/4}$ instead of $\mu^{-1/2}$. This would be appropriate if $q \gg 1$ or $q \ll 1$. If $1 \ll q\mu^2 \ll R$ and $q \neq 0(1)$ then the structure of the flow immediately downstream of the origin will be similar to that given above for $q = 0(1)$.

We will now investigate the flow for $\bar{X}_0 - \bar{X} = 0(\delta)$. If $x = \delta^4 R \bar{X} + \delta^3 R \bar{X}_0$, $\tilde{Y} = 1 - \delta^{4/3} y$, $p = \delta^{8/3} \tilde{P}$ and $\psi = -\delta^{8/3} \tilde{\psi}$ then the governing equations in the viscous layer adjacent to the upper wall are

$$\left. \begin{aligned} \tilde{u} \frac{\partial \tilde{u}}{\partial \tilde{X}} + \tilde{v} \frac{\partial \tilde{u}}{\partial z} &= -\tilde{p}' + \frac{\partial^2 \tilde{u}}{\partial z^2}, \\ \frac{\partial \tilde{u}}{\partial \tilde{X}} + \frac{\partial \tilde{v}}{\partial z} &= 0, \end{aligned} \right\} (3.57)$$

where the Prandtl transformation $\tilde{Y} = z + \frac{q}{2} \tilde{P}^2(\tilde{X})$ has been applied, $\tilde{u} = \partial \tilde{\psi} / \partial z$ and $\tilde{v} = -\partial \tilde{\psi} / \partial \tilde{X}$. The boundary conditions are

$$\left. \begin{aligned} \tilde{u} = \tilde{v} = 0 &\text{ at } z = 0, \\ \tilde{u} \sim z + \frac{q}{2} \tilde{P}^2 &\text{ as } z \rightarrow \infty, \end{aligned} \right\} (3.58)$$

from no slip at the wall and matching to the Poiseuille flow at the outer edge of the layer. We note the nonlinearity of outer condition on \tilde{u} , which arises from the form of the tube law. Also, far upstream the solution of (3.57) and (3.58) must match with the asymptotic flow structure for $\bar{X}_0 - \bar{X} \ll 1$ given above. This upstream condition is satisfied (see Appendix 2). The core flow takes the form of an inviscid rotational perturbation to the Poiseuille flow, i.e. $u = U_0(y) + 0(\delta^{8/3})$, and is given by (3.47a) with $P + \bar{X}$ replaced by \tilde{P} .

Let us now seek an asymptotic solution of (3.57) and (3.58) valid as $\tilde{P} \rightarrow -\infty$. Suppose that $\tilde{P} \propto \tilde{X}^n$ as $\tilde{X} \rightarrow \infty$, where $n > 0$. Then the necessary balance between the terms in the momentum equation requires that $n \geq 1/6$. With $\eta = z\tilde{X}^{n-1/2}$ the flow is given by

$$\tilde{\psi} = \tilde{X}^{n+1/2} F(\eta) + o(\tilde{X}^{n+1/2}),$$

$$\tilde{P} = \tilde{P}_0 \tilde{X}^n + o(\tilde{X}^n),$$

where $F(\eta)$ must satisfy the Falkner-Skan equation

$$F'''' + (n + \frac{1}{2}) FF'' - 2nF'^2 = 0. \quad (3.59)$$

If $n > 1/6$ the boundary conditions, from (3.58), are

$$\left. \begin{aligned} F(0) = F'(0) = 0, \\ F'(\infty) = \frac{q}{2} \tilde{P}_0^2 \end{aligned} \right\} (3.60)$$

Clearly, the boundary conditions are not consistent with the Falkner-Skan equation, and there is no non-trivial solution for F when $n > 1/6$. Suppose now that $n = 1/6$. The condition at infinity in (3.60) must be replaced by

$$F' \rightarrow \eta + \frac{q}{2} \tilde{P}_0^2 \text{ as } \eta \rightarrow \infty. \quad (3.60a)$$

On differentiating (3.59) it is seen that

$$F'''' = a \exp[-\frac{2}{3} \int_0^\eta F(t) d(t)]$$

where a is an unknown constant. Equation (3.59) and the boundary conditions imply that both $F''''(0)$ and $F''''(\infty)$ must be zero, which is possible only if a is zero, that is $F'''' \equiv 0$. It follows that when $n = 1/6$ there is no solution for F such that \tilde{P}_0 is non-zero. Further, it can be shown that there are no satisfactory solutions of the Falkner-Skan problems with $\tilde{P} \propto (\tilde{X}_0 - \tilde{X})^{-n}$, $\tilde{X}^n \ln \tilde{X}$, or $(\tilde{X}_0 - \tilde{X}) \ln (\tilde{X}_0 - \tilde{X})$, nor is there any linearised similarity solution for (3.57) and (3.58) such that $\tilde{P} \rightarrow -\infty$.

Our inability to find a suitable asymptotic structure does not, of course, imply that one does not exist. However, if a nonlinear structure exists as $\tilde{P} \rightarrow -\infty$, then $\tilde{u} \propto \tilde{P}^2$, and it follows that the pressure gradient will not appear in the leading order momentum equation. Thus, as the boundary conditions are pressure dependent, it seems possible that the boundary layer problem (equations 3.57 and 3.58)

is not well posed for $-\tilde{P} \gg 1$. We note the similarity to the problem with a moderate pressure response and $q > 1/2$ (Section 3.3), when, again, we could not find a solution.

A finite difference method of computation was applied to the non-linear boundary layer problem formed by (3.57) and (3.58) (see Appendix 5 for details). Upstream, where $|\tilde{P}| \ll 1$, the numerical solution showed the expected behaviour. That is, \tilde{P} was proportional to $(\tilde{X}_0 - \tilde{X})^{-1/3}$, where \tilde{X}_0 is a constant and $\tilde{X}_0 - \tilde{X} \gg 1$. However, when \tilde{P} approached $O(1)$ the numerical process failed to converge. Variation of the grid size, including changing to a non-uniform grid, had no substantial effect on the results. Close examination revealed that the process had become unstable with an oscillatory type of divergence. Further, attempts to find a solution of the full problem (equations 3.1 - 3.3) using numerical methods were unsuccessful when μ was sufficiently large. As can be seen from Table 3.1, $\bar{\mu}_c$, the value of μ at which the numerical process fails, depends on the value of q (and of ϵ , though it is assumed here that $\epsilon = 1$). These values are approximate, and were obtained by trial and error. As expected, the effect of increasing q (or ϵ) is to decrease $\bar{\mu}_c$.

The methods used above have been consistently unsuccessful in completing the solution of the problem defined by (3.1) - (3.3) and (3.39). If a solution of the form proposed above exists then the perturbation to Poiseuille flow in the core must be $O(1)$ when p is $O(\mu^{-1})$, since both $1 - y_w$ and y_w are then finite. In the region of the singularity, where the flow in the upper wall layer is controlled by (3.57), $u - U_0(y)$ must be proportional to p in the core if the flow is to be symmetric. This suggests that $u - U_0(y)$ will be $O(\mu^{-1})$ when p is $O(\mu^{-1})$, and hence that there is a basic contradiction between the behaviour of core flow as proposed above, and that required by the tube law. However, if it is assumed that the flow is not significantly disturbed until the pressure falls below zero then the flow structure given above arises naturally. Also, an analysis along these lines is suggested by the results for a fine collapse with a fast pressure response such that $\epsilon\mu^{2/3}$ is large (Section 2.1). In fact, this approach is successful for a channel with $\mu^{-2/3} \ll \epsilon \leq O(\mu^{-1/2})$ (see below).

A possibility worth considering is that the flow is altered significantly ahead of the collapse, although no evidence of this has been found so far.

It was shown in Section 2.2 that small exponential disturbances to the Poiseuille flow can occur far ahead of the collapse on an $O(R)$ streamwise length scale, but also that they decay rapidly downstream. Similar exponential disturbances to the flow upstream of the collapse were investigated on $O(\beta R)$ streamwise length scalings, with $\beta \gg 1$ and $R^{-1} \ll \beta \ll 1$. Again no solutions that could lead to significant changes in the flow were found.

If x is assumed to be $O(1)$, then the pressure cannot be taken to be independent of y . It is known that in a tube with a fixed constriction significant changes to the flow can occur ahead of the constriction if its dimensions are such that the pressure will not be uniform across the tube (see Smith 1976a,b,e; 1977b; 1978a; 1979). In particular, Smith (1979) has found two possible solutions for the flow ahead of a symmetric constriction in a pipe of radius a when the height and length of the constriction are both $O(a)$. In the first solution, Poiseuille flow continues undisturbed until the constriction is reached, while in the second separation occurs a distance $0.087 a \ln R + O(a)$ ahead of the constriction. A similar result holds for the analogous channel flow. The mechanism for the viscous upstream separation is based on an extension of Kirchhoff (1869) free streamline theory, which has been shown (Sychev 1972, Smith 1977a) to provide a rational basis for the description of high Reynolds number flows past bluff bodies in external flows. It is felt that such an upstream separation is unlikely to occur in the steady flow problems that the present study is concerned with. There are several reasons for this belief: first, such a separation requires a strong adverse pressure gradient close to the wall in the region of separation, whereas there must be a favourable pressure gradient at the wall in order for our tubes to collapse; second, the pressure is constant along the free streamline, which implies that a separated flow must remain separated, with a favourable pressure gradient in the region between the wall and the free streamline, or that the flow reattaches at a point where the tube has its original shape (i.e. $y_w = \pm 1$ for a channel). Suppose now that the collapse is severe, not complete, i.e. $0 < 1 - \epsilon \ll 1$. Then, if the flow remains steady, we expect that the tube will eventually collapse to its minimum width, and that the flow will again take a Poiseuille form far downstream. This appears to contradict a permanently detached free streamline, and indicates that a steady flow with an upstream separation must reattach ahead of the

main collapse. Thus the results of Smith's (1979) study of flow in constricted tubes suggest that if the flow remains steady and significant changes occur ahead of the collapse, then the resultant flow pattern must be extremely complicated.

Another possibility worth considering is that there is no steady solution to the basic problem studied in this section, and that the flow in a tube obeying (3.3) and (3.39) will spontaneously destabilise. Support for this hypothesis can be found in a number of theoretical and experimental studies (see Section 1.3). This will be discussed further in Section 5 below.

Suppose now that the collapse is fine, q is $O(1)$, and

$$\mu^{-2/3} \ll \varepsilon \ll \mu^{-1/2}. \quad (3.62)$$

The flow structure in the region where $0 < -\mu p \ll 1$ can be obtained from (3.41) and (3.47) above by replacing δ by $\delta_1 = (\varepsilon \mu^2)^{-1/4}$ throughout. When $-p$ becomes $O(\mu^{-1})$ this solution fails as $S(\mu p)$ cannot be expanded in powers of $-\mu p \ll 1$. However, the skin friction perturbation is still small compared with one, and the general structure of the flow remains the same, i.e. a linear structure in the wall layers and a passive irrotational perturbation to the Poiseuille flow in the core. The wall layers retain their linear structure and grow in thickness downstream until eventually they merge with the mainstream. When this occurs the flow takes the form of an $O(\varepsilon)$ viscous perturbation to the Poiseuille flow, developing on an $O(R)$ streamwise length scale (c.f. $\mu^{2/3} \varepsilon \leq O(1)$, Section 2.1).

A complete solution of the present problem can be obtained using the techniques found in Section 2.1. We omit the details, but make some comments about the behaviour of the flow. As occurred with $\varepsilon = 1$, immediately downstream of the origin the change in the wall positions is initiated and driven by the pressure change from the Poiseuille flow. Again, this is followed by a self-sustained collapse, in which the interaction between the change in the flow and the movement of the walls is dominant. This interaction results in an extremely fast change in the pressure and in $S(\mu p)$ which is terminated when S approaches one. In the limit far downstream the flow again takes a Poiseuille form. As might be expected, the behaviour of the present

fluid-channel system is similar to that found for the system with $\lambda = \mu\epsilon^{3/2}$ large (Section 2.1). Note that the flow structure outlined above for a channel satisfying (3.62) can be regarded as a natural development from the structure found for $\lambda = 0(1)$, in the sense that the former can be obtained from the latter by expanding for large λ .

Suppose now that

$$\epsilon = K \mu^{-1/2} \quad (3.63)$$

where K is an $0(1)$ constant. Again, the flow immediately downstream of the origin has a linear structure, obtained from (3.41) and (3.47) by replacing δ by δ_1 . However, $K = 0(1)$ implies that the skin friction perturbation and $-\mu p$ become $0(1)$ simultaneously, and hence that the flow in the viscous wall layers is nonlinear in form when $p = 0(\mu^{-1})$. If $x = \mu^{-3/2} R\hat{x}$, $y = 1 - \mu^{-1/2} [\hat{y} + KS(\hat{p})]$, $p = \mu^{-1} \hat{p}(\hat{x})$ and $\psi = -\mu^{-1} \hat{\psi}(\hat{x}, \hat{y})$, then $(\hat{\psi}, \hat{p})$ must satisfy the nonlinear boundary layer equations, and the boundary conditions

$$\left. \begin{aligned} \frac{\partial \hat{\psi}}{\partial \hat{y}} = \hat{\psi} = 0 \text{ at } \hat{y} = 0, \\ \frac{\partial \hat{\psi}}{\partial \hat{y}} \rightarrow \hat{y} + KS(\hat{p}) \text{ as } \hat{y} \rightarrow \infty. \end{aligned} \right\} (3.64)$$

Also, $\hat{\psi}$ and \hat{p} must match to the incoming flow. It is easily shown that a satisfactory matching of $(\hat{\psi}, \hat{p})$ to the downstream asymptotic behaviour of (3.41) can be achieved (c.f. Appendix 2). If $K \ll 1$ a linearized solution can be obtained analytically. As expected, this solution is essentially that described above for ϵ satisfying (3.62). If $K \geq 0(1)$ numerical methods of solution are necessary (see Appendix 5). Let us assume that $S(\hat{p})$ has the standard form (1.6), with $q = 4$. The values obtained for $\hat{p}(\hat{x})$, $\hat{\tau} = \partial \hat{u} / \partial \hat{y}$ and $S(\hat{p})$ with $K = 1$ are shown graphically in Figure 3.11. For the problem with $K = 0(1)$ we can distinguish at least three distinct stages in the development of the flow in the wall layers. First, there is a slow upstream development with the boundary layer taking a linear form. Next, the boundary layer becomes nonlinear, and there is a rapid adjustment to the flow, with the major part of the wall collapse occurring over a relatively short distance. In this region the magnitude of both the skin

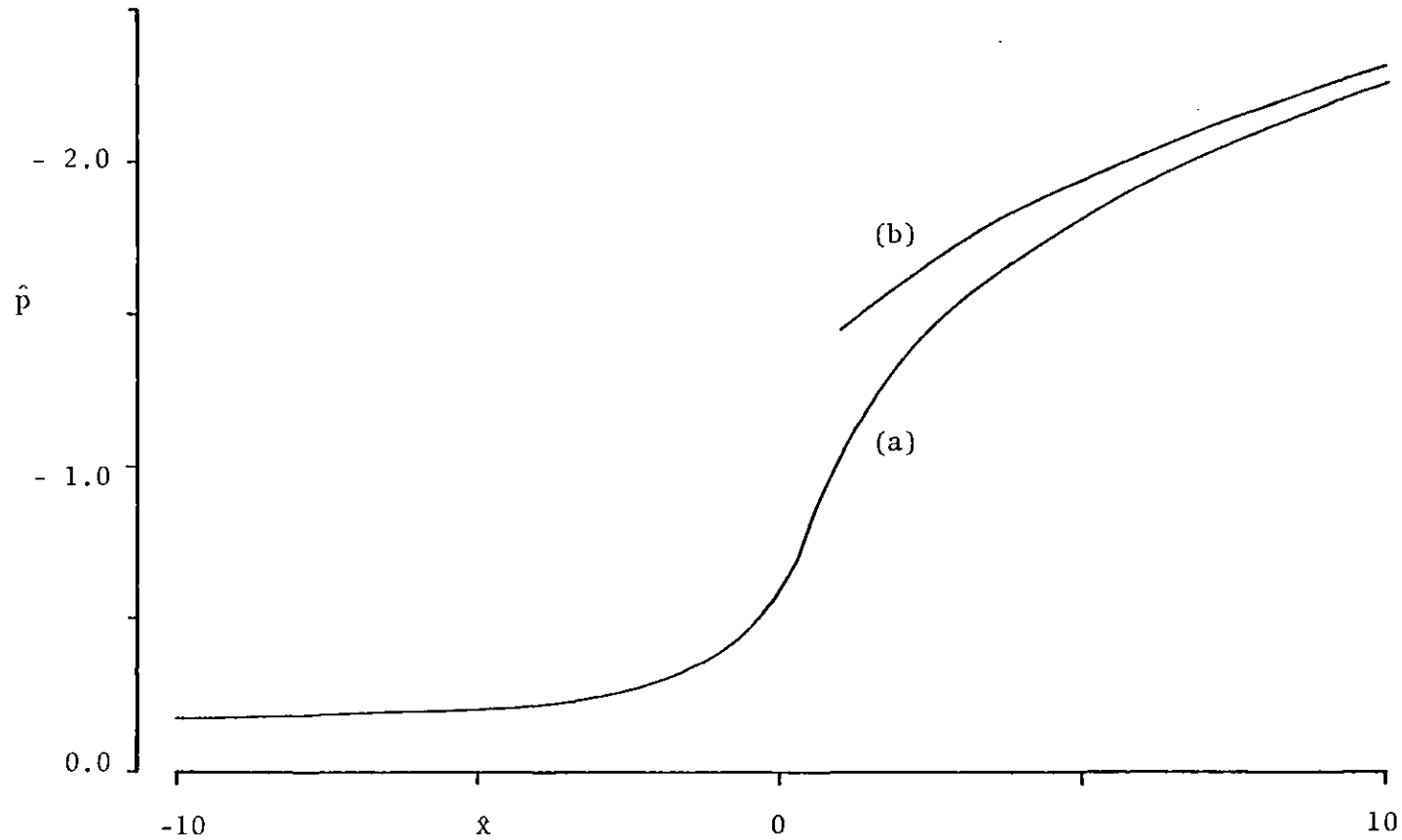


Figure 3.11(i). Pressure \hat{p} against distance \hat{x} for a channel with $S(\hat{p}) = 1 - (1 + \hat{p}^2)^{-2}$, $\mu \gg 1$ and $K = \epsilon\mu^{1/2} = 1$. A change in origin for \hat{x} is included here. From (a) the numerical solution of the boundary layer problem, and (b) the downstream analysis for $-\hat{p} \gg 1$, which gives $\hat{p} = \hat{p}_d + \hat{p}_o (\hat{x} + \hat{x}_d)^{1/3}$, where $\hat{p}_d = -.397$ and $\hat{x}_d = .767$.

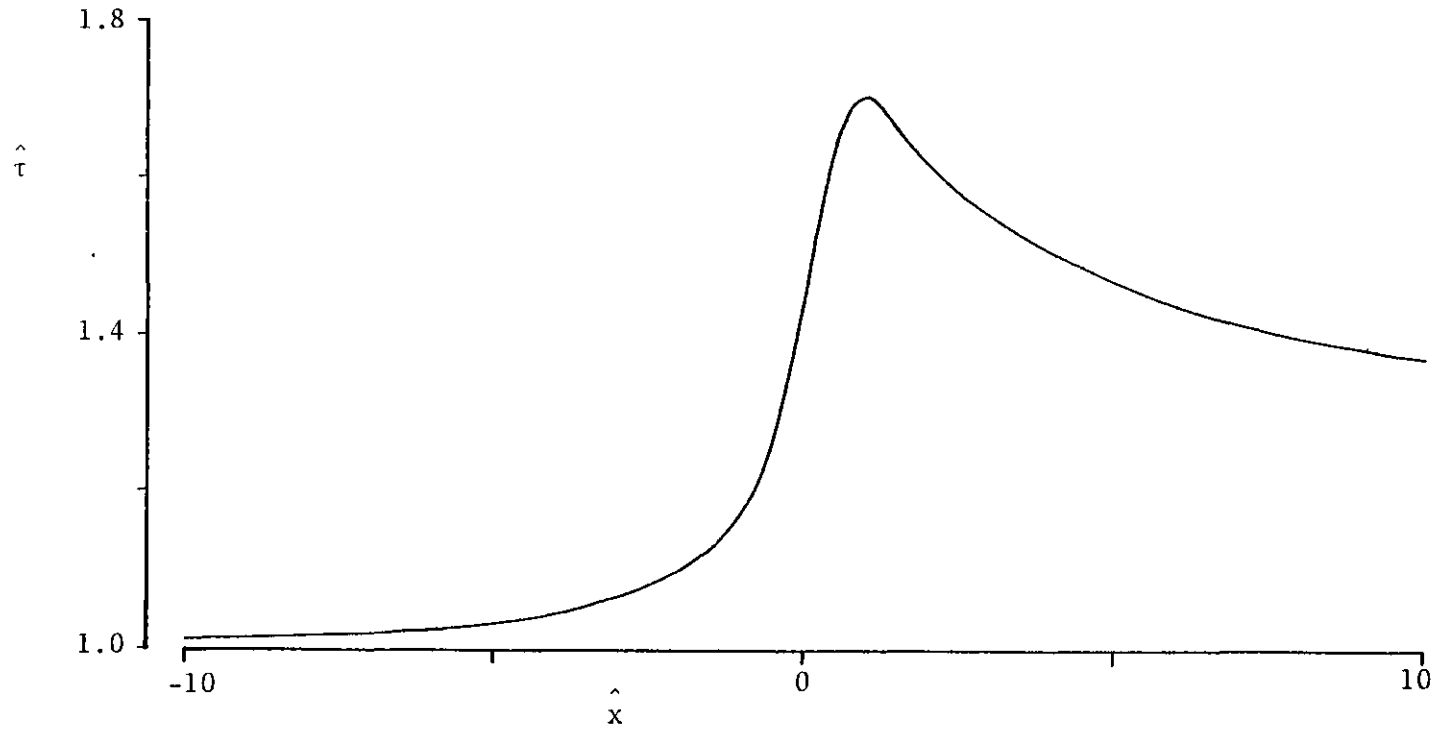


Figure 3.11 (ii). Skin friction $\hat{\tau}$ against distance \hat{x} for a channel with $K = 1$ (see Figure 3.11 (i)). The values are from the numerical solution of the boundary layer problem.

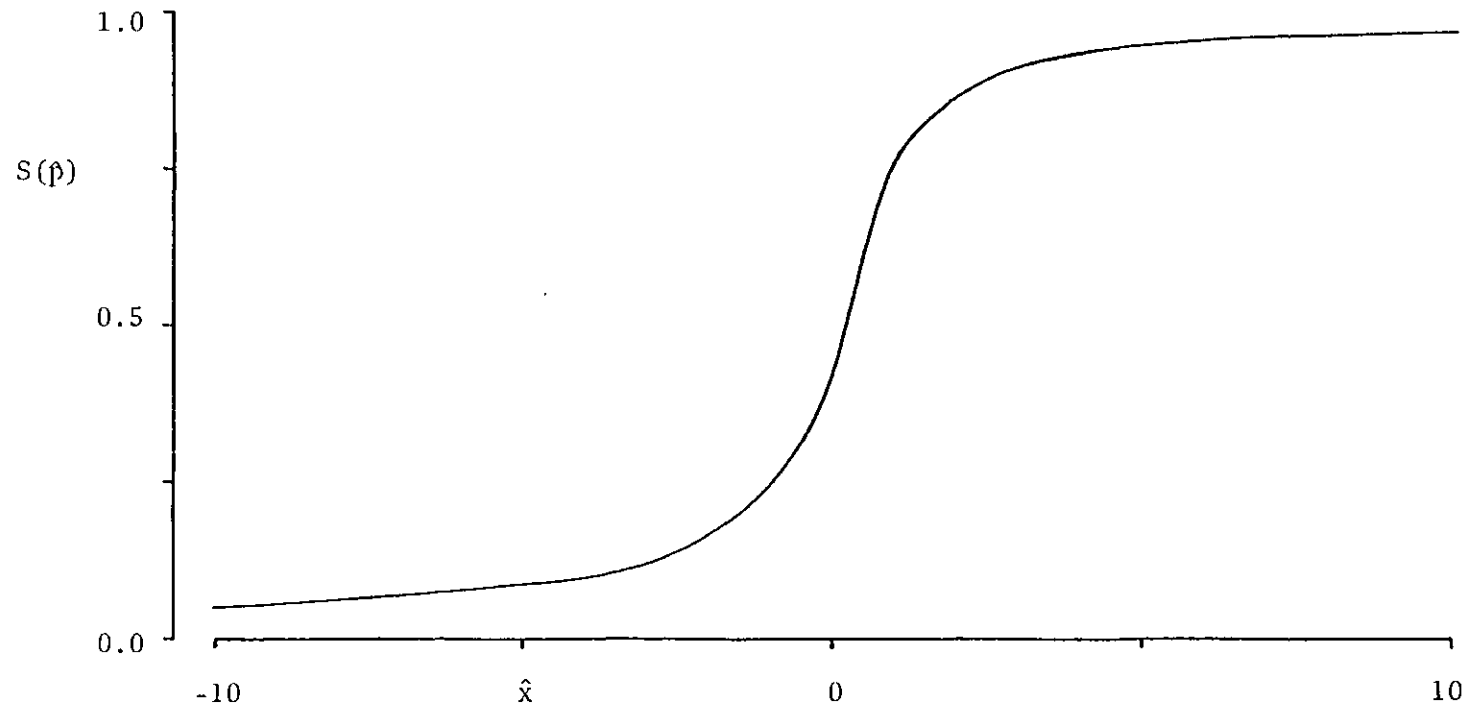


Figure 3.11 (iii). Wall displacement $S(p)$ against distance \hat{x} for a channel with $K = 1$ (see Figure 3.11 (i)). The values are from the numerical solution of the boundary layer problem.

friction $\hat{\tau}$ and the pressure gradient increase rapidly, peak and then begin to fall. Finally, as the flow proceeds downstream the boundary layer again becomes linear in form, with a relatively gradual decrease in the skin friction and increase in the pressure gradient, both tending asymptotically towards zero. An asymptotic flow structure with $\hat{p} \propto \hat{x}^{1/3}$ and $\hat{\psi} - \frac{1}{2} \hat{y}^2 \propto \hat{x}^{1/3}$ can be developed for the downstream region where $1 - S \ll 1$. If $\hat{p} \sim \hat{p}_0 \hat{x}^{1/3}$ as $\hat{x} \rightarrow \infty$ then it can be shown (c.f. the problem defined by (3.53) - (3.55a,b)) that

$$\hat{p}_0 = -K\beta^{5/3}/\Gamma^2(1/3).$$

Note that this result is valid for K of all magnitudes, not just $O(1)$.

Using the above value of \hat{p}_0 and a suitable change in origin, a comparison was made between the asymptotic and numerical pressure solutions for the problem with $K = 1$. Agreement was excellent for large \hat{x} ($\hat{x} > 20$), and as can be seen from Figure 3.11, agreement was good for moderate values of \hat{x} ($5 < \hat{x} < 20$).

The rapid changes in the flow and the wall position which occur with $K = 1$ suggest that it may be necessary to adopt a shorter stream-wise length scale for the problem with K large. However, this would lead to an analysis for $K \gg 1$ essentially the same as that given above for the problem with $\epsilon = 1$ and $\mu \gg 1$, a problem for which we could not find a complete solution. As might be expected from the difficulties encountered with $\epsilon = 1$ and $\mu \gg 1$, the numerical process failed to converge when applied to the present boundary layer problem with values of K substantially greater than one, e.g. for $K = 5$. As before, altering the grid did not noticeably improve convergence. No reason is known for the failure of the numerical method with large K , nor is it known whether a solution exists. We note the natural development between the flow structures for $\epsilon \ll \mu^{-1/3}$, $\epsilon = O(\mu^{-1/2})$ and $\mu^{-1/2} \ll \epsilon \leq 1$.

Suppose now that $\epsilon = 1$, $\mu \gg 1$ and $q \ll 1$. In this case the behaviour of the flow depends greatly on the relative order of μ and q . For example, if $q \ll \mu^{-2}$, then the expansion of y_w for $-\mu p \ll 1$ (equation 3.40) implies that the initial response of the tube to the changing pressure is slow, whereas if $q \gg \mu^{-2}$, then the initial response is fast. Further, if $q \ll \mu^{-2}$, then immediately downstream of the origin the flow is viscous in nature and does not have separate wall

layers, while if $q \gg \mu^{-2}$ then the perturbation to the Poiseuille flow in the core is inviscid, and viscous wall layers form when the flow passes the origin. We will not investigate the flow for $q \ll 1$ in detail, but will comment on some points of particular interest. If $\mu^{-2/3} \ll q \ll \mu^{-1/2}$, then (3.41) and (3.47) are valid if δ is replaced by $\delta_2 = (q\mu^2)^{-1/3}$, and the wall layers retain their linear structure when $-\mu p$ becomes $0(1)$. If $q = 0(\mu^{-1/2})$ then the boundary layer structure becomes nonlinear when p becomes $0(\mu^{-1})$. If $1 \ll q \ll \mu^{-1/2}$ then there is a region in which the flow structure in the wall layers is nonlinear and $S \propto q\mu^2 p^2$. Hence we do not have a full solution for the case with $1 \ll q \ll \mu^{-1/2}$. Nor do we have a numerical solution for the full problem (equations 3.1 - 3.3 with 3.39). In fact the approximate values found for $\bar{\mu}_c$ (the upper limit on μ for convergence of the numerical process used for the full problem) for small q are consistent with $q\bar{\mu}_c^{1/2} = 0(1)$ (see Table 3.1). This suggests that the difficulties encountered in numerically solving the full problem and the nonlinear boundary layer problem (equations 3.57 and 3.58) may be connected. It is stressed that the values obtained for $\bar{\mu}_c$ are approximate, and that further investigation is required to confirm or refute this proposed relationship between q and $\bar{\mu}_c$, and any connection between the failure of the full and boundary layer problems to converge.

The flow in a channel that can collapse completely must adjust in such a way that $u - U_0(y)$ is $0(1)$ when $1 - y_w$ becomes $0(1)$. In Appendix 3 we investigate a channel with the tube law

$$y_w = \begin{cases} 1 & p \geq 0 \\ \left[1 - \frac{\mu^2}{qR} \int_0^x p(t) dt\right]^{-q} & p < 0 \end{cases} \quad (3.65)$$

where $1 \ll \mu^2 \ll R$ and $q = 0(1)$. A solution of the form proposed above for a channel obeying (3.3) and (3.39) is considered, again on an $0(\mu^{-3/2}R)$ streamwise length scale in the region of the origin. It is shown that the flow can develop in such a way that p and $1 - y_w$ become $0(1)$ simultaneously. That is, with (3.65) the flow can adjust so that the core flow becomes nonlinear as the collapse becomes finite. An outline of a complete solution is given in Appendix 3.

q	$\hat{\mu}_c$	$\bar{\mu}_c$	$q\bar{\mu}_c^{-1/2}$
.5	18.0	12	1.7
.4	29.5	25	2.0
.3	45.6	50	2.1
.2	76.4	120	2.2
.1	167.0	450	2.1

Table 3.1. Critical values of μ for a channel obeying (3.3) with $\varepsilon = 1$; $\hat{\mu}_c$ obtained from equation (5.2) and $\bar{\mu}_c$ by numerical experimentation.

3.5 Channel flows with a slow pressure response

Suppose that the collapse is moderate and the pressure response slow, that is $\epsilon = 0(1 - \epsilon)$ and $\mu \gg 1$. It follows that the flow is viscous in nature, the pressure is independent of y to leading order, and with $x = \mu^{-1}R\bar{x}$ and $p = \mu^{-1}\bar{p}(\bar{x})$ the streamwise velocity is given by

$$u(\bar{x}, y) = \frac{1}{2} y_w^{-3} (y_w^2 - y^2) \quad (3.66)$$

where $y_w = y_w(\bar{p})$ and \bar{p} is determined by

$$-\bar{x} = \int_0^{\bar{p}} y_w^3(t) dt. \quad (3.67)$$

Clearly, this solution takes the expected Poiseuille form in the limit far downstream as $\bar{x} \rightarrow \infty$ and $y_w \rightarrow 1 - \epsilon$.

If $\epsilon \ll 1$ then the solution given in Section 1.2 for a channel with a fine collapse and slow pressure response is obtained as the $O(\epsilon)$ term in the expansion of (3.66) and (3.67), as would be expected.

Suppose now that the collapse is total ($\epsilon = 1$) and that y_w is given by (3.3). Then (3.67) implies that to leading order $\bar{p} \propto \bar{x}^n$ as $\bar{x} \rightarrow \infty$ if $q < 1/3$, $\bar{p} \propto (\bar{x}_0 - \bar{x})^n$ as $\bar{x} \rightarrow \bar{x}_0$ if $q > 1/3$, and that $\bar{p} \rightarrow -\infty$ exponentially in \bar{x} if $q = 1/3$. Here $n = 1/(1 - 3q)$ and \bar{x}_0 is finite. Hence, if $q \leq 1/3$ the collapse extends indefinitely far downstream, while if $q > 1/3$ then $y_w \rightarrow 0$ at a finite value of \bar{x} . An asymptotic structure for the flow as $p \rightarrow -\infty$ can be obtained directly from (3.66) and (3.67). For $q < 1/2$, this asymptotic structure is essentially that found for the flow as $p \rightarrow -\infty$ when $\mu = 0(1)$ (Sections 3.2 and 3.3). If $1/3 < q \leq 1/2$ then to leading order the flow remains viscous in nature throughout the collapse, and the asymptotic structure for $\bar{x}_0 - \bar{x} \ll 1$ is mathematically valid for all such $\bar{x} < \bar{x}_0$. It appears then that at least one of the assumptions made in formulating our model must become invalid as $y_w \rightarrow 0$ if $1/3 < q \leq 1/2$. If $q > 1/2$ then the viscous and inertial forces in the streamwise direction and the pressure gradient are all of the same order when $\bar{x}_0 - \bar{x} = O(\mu^{(3q-1)/(2q-1)})$. It is then necessary to reformulate the problem.

Let $m = q/(2q - 1) > 0$. Taking $x = \mu^m R \bar{x} + \mu^{-1} R \bar{x}_0$, $y = \mu^m \bar{y}$, $u = \mu^{-m} \bar{u}(\bar{x}, \bar{y})$, $v = \mu^{-m} R^{-1} \bar{v}(\bar{x}, \bar{y})$, and $p = \mu^{-2m} \bar{p}(\bar{x})$ in the region of the singularity, the governing equations for $(\bar{u}, \bar{v}, \bar{p})$ are the nonlinear boundary layer equations. The boundary conditions are those of no slip at the walls, given by $\bar{y} = \pm \bar{y}_w$ where $\bar{y}_w = (-\bar{p})^{-q}$, and matching upstream to the asymptotic flow structure for $\bar{x}_0 - \bar{x} \ll 1$. It follows from the results of the problem with $\mu = 0(1)$, $q > 1/2$ and $\epsilon = 1$ (Section 3.3) that we do not have an asymptotic solution for this local problem as $\bar{p} \rightarrow -\infty$, nor a numerical solution for $-\bar{p} \gg 1$. Thus, with a channel obeying (3.3), we do not have a complete solution for any value of μ if $q > 1/2$.

If the collapse is severe, then (3.66) and (3.67) are valid throughout the collapse if $q \leq 1/2$, or if $1 - \epsilon$ is $0(\mu^m)$ or greater when $q > 1/2$. If $0 < 1 - \epsilon \ll \mu^m$ and $q > 1/2$, then, again, we encounter the nonlinear problem with $y_w \propto (-p)^{-q}$, and do not have a complete solution for the problem.

Section 4. Pipe flow

4.1 The governing equations

In this section we study a model of flow in collapsible pipes. We assume that the motion of the fluid-pipe system is steady, that the Reynolds number is large, and that far upstream the pipe has a circular cross-section and the flow is fully developed Poiseuille flow. Let (x, r, θ) be standard nondimensional cylindrical coordinates, with associated velocity components (u, v, w) . In the problems studied in this section, the restrictions placed on the parameters are such that the radial and azimuthal momentum equations always imply that the pressure $p = p(x)$ is independent of r and θ . It follows that the governing equations are the streamwise momentum and vorticity equations and the continuity equation. In turn these are

$$\left. \begin{aligned} u \frac{\partial u}{\partial x} + v \frac{\partial u}{\partial r} + \frac{w}{r} \frac{\partial u}{\partial \theta} &= -p'(x) + R^{-1} \nabla^2 u, \\ u \frac{\partial \Omega}{\partial x} + v \frac{\partial \Omega}{\partial r} + \frac{w}{r} \frac{\partial \Omega}{\partial \theta} - \frac{\partial u}{\partial x} \Omega + \\ + \frac{\partial u}{\partial r} \frac{\partial w}{\partial x} - \frac{1}{r} \frac{\partial u}{\partial \theta} \frac{\partial v}{\partial x} &= R^{-1} \nabla^2 \Omega, \\ \frac{\partial u}{\partial x} + \frac{\partial v}{\partial r} + \frac{v}{r} + \frac{1}{r} \frac{\partial w}{\partial \theta} &= 0, \end{aligned} \right\} (4.1)$$

where $\Omega = \frac{\partial w}{\partial r} + \frac{w}{r} - \frac{1}{r} \frac{\partial v}{\partial \theta}$ is the streamwise component of vorticity, $\nabla^2 \equiv \frac{\partial^2}{\partial r^2} + \frac{1}{r} \frac{\partial}{\partial r} + \frac{1}{r^2} \frac{\partial^2}{\partial \theta^2} + \frac{\partial^2}{\partial x^2}$ and R is Reynolds number based on the radius of the pipe far upstream where its cross-section is circular.

As with the channels considered above, it is supposed that the cross-sectional area of the pipe depends on the local pressure only. Thus, if the wall is given by $r = r_w$ then $r_w = r_w(p, \theta)$. Except in Section 4.3, where the collapse extends indefinitely far upstream, we assume that $r_w = 1$ for $p \geq 0$, and that $p = 0$ at $x = 0$ (c.f. the channels studied above).

The boundary conditions are

$$\left. \begin{aligned} u = v = w = 0 \quad \text{at } r = r_w, \\ u \rightarrow U_0(r), \quad v \rightarrow 0 \quad \text{and } w \rightarrow 0 \quad \text{as } x \rightarrow -\infty \end{aligned} \right\} (4.2)$$

where $U_0(r) = \frac{1}{4} (1 - r^2)$ is the incoming Poiseuille velocity profile. Also, we require the solution to be bounded in $r < r_w$. No evidence is found for any significant upstream influence in any of the problems considered below. Thus it would be sufficient to apply the upstream matching to the Poiseuille flow in (4.2) at the point where the wall first varies from $r_w = 1$; that is, except in Section 4.3, at $x = 0$.

An initial scaling on x is obtained by matching the pressure gradient to the incoming Poiseuille pressure gradient, as was done for channel flows above. When the collapse is nonsymmetric the order of the azimuthal velocity w , like that of v , can be fixed by mass conservation. Alternatively, the order of w , or of v , could be fixed by assuming a balance of terms in the streamwise vorticity equation. However, for the fluid-pipe systems studied below it can be shown that there are no valid solutions of the problems generated by assuming a vorticity balance. Thus, all the terms in the continuity equations must be of the same order.

The behaviour of collapsible pipes was discussed in Section 1.2, and nonsymmetric collapses were felt to be of most practical importance. Also, we wish to study (as a first step) a problem that is mathematically tractable. Accordingly, we assume that r_w is given by

$$r_w = 1 - \epsilon S(\mu p) f(\theta), \quad (4.3)$$

where ϵ , S and f are such that r_w describes a non-intersecting curve for all p , $S(\mu p) = 0$ for $p \geq 0$ and S is monotonic decreasing for $p < 0$. With no loss of generality it may be assumed that $f(\theta)$ is $O(1)$ or less for all θ , and is $O(1)$ for at least one value of θ . Where an explicit form of S is required, (1.6) will be used.

The perimeter $P_t(x)$ of the tube is given by

$$P_t(x) = \int_0^{2\pi} \{ r_w^2 + (dr_w/d\theta)^2 \}^{1/2} d\theta.$$

A collapse for which P_t maintains its upstream value of 2π will be called a bending collapse, and one for which P_t varies from 2π a stretching collapse. As will be seen below, the behaviour of the fluid-pipe system for a bending collapse is considerably different

from that for a stretching collapse. In a region where $|\epsilon S(\mu p) f(\theta)| \ll 1$ for all θ , a collapse will be a bending collapse to $O(\epsilon)$ if

$$\int_0^{2\pi} f(\theta) d\theta = 0,$$

which is also the condition that the cross-sectional area remains constant to $O(\epsilon)$.

4.2 Axisymmetric pipe flow

An axisymmetric collapse is essentially a "pure stretching" collapse with $f(\theta)$ in (4.3) set identically equal to one. The governing equations are the continuity and streamwise momentum equations obtained from (4.1) by suppressing all θ dependence.

In general, the analysis for axisymmetric pipe flow is analogous to that given above for symmetric channel flow, as are the results of this analysis. However, there is one major exception to this. Consider a pipe obeying (4.3) with $f(\theta) \equiv 1$ and S given by (1.6). If the pressure response is moderate, $q = O(1)$, and the collapse is total, then to leading order $r_w = k(-p)^{-q}$ when $-\mu p \gg 1$, where $k = \mu^{-q}$ is $O(1)$. It follows that if $q = 1/4$ then the inertial forces in the streamwise direction and the pressure gradient will be of the same order when $-\mu p \gg 1$. If $q < 1/4$ then the fluid motion will be essentially viscous in character when $-\mu p \gg 1$, while if $q > 1/4$ then the inertial forces must dominate the pressure gradient as $p \rightarrow -\infty$. No solution has been found for a pipe with $q > 1/4$. If $q < 1/4$ the necessary balance between the pressure gradient and viscous force in the direction of flow implies that $p \propto X^{1/(1-4q)}$ as $X \rightarrow \infty$, where $X = R^{-1}x$. If $q = 1/4$ a balance of the viscous, inertial and pressure terms in the moment equation implies that $p \rightarrow -\infty$ exponentially in X as $X \rightarrow \infty$. Thus, for $q \leq 1/4$ the collapse of a pipe will extend indefinitely far downstream. There are both similarities and differences between (axi)symmetric pipe and channel flows. If $-\mu p \gg 1$ then the ratio of inertial forces to the pressure gradient is proportional to $(-p)^{-m}$, where $m = 1 - 2q$ for a channel and $1 - 4q$ for a pipe. No solution has been found for a channel or a pipe with $m < 0$. If $0 \leq m < 1$ then the collapse of a

pipe extends indefinitely far downstream, i.e. $r_w \rightarrow 0$ as $X \rightarrow \infty$. For a channel, it has been shown (Section 3.3) that $y_w \rightarrow 0$ as $X \rightarrow X_0$ - if $0 \leq m < 1/3$, where $X_0 = X_0(q)$ is finite, and that $y_w \rightarrow 0$ as $X \rightarrow \infty$ if $1/3 \leq m < 1$.

The flow structure for a pipe with $0 < q < 1/4$ is similar to that for a channel with $0 < q < 1/3$. We omit the details. Suppose now that $q = 1/4$. The flow has an exponential self-similar structure, viz.

$$\left. \begin{aligned} \psi &= (4a)^{-1} f(\zeta), \\ p &= -e^{-4ax}, \end{aligned} \right\} (4.5)$$

where $\psi(x,r)$ is the stream function, $\zeta = (4a)^{1/2} r e^{ax}$ and a is a constant to be determined. With (4.5) the momentum equation in (4.1) becomes

$$g'' + g'/\zeta + 1 - \frac{1}{2} g^2 = 0, \quad (4.6)$$

where $g = f'/\zeta$ gives the streamwise velocity component. The tube law takes the local form

$$\zeta_w = k(4a)^{1/2},$$

where $k = \mu^{-1/4}$. The boundary conditions are that g is regular in $\zeta < \zeta_w$, and that

$$\left. \begin{aligned} g(\zeta_w) &= 0, \\ \int_0^{\zeta_w} \zeta g(\zeta) d\zeta &= a/4, \end{aligned} \right\} (4.7)$$

from no slip at the wall and conservation of mass respectively.

Unfortunately, equation (4.6) cannot be integrated directly, and an analysis similar to that given in Section 3.3 for equation (3.19) (arising in the study of a channel with $q = 1/2$) is not possible. However, we can show that a solution of (4.6) and (4.7) can exist only if $\mu < 128$, and that, if a solution exists when $0 < 128 - \mu \ll 1$, then the flow must be essentially uniform across the pipe, the viscous

effects being restricted to thin layers. This flow structure for $0 < 128 - \mu \ll 1$ is of course the analogue of that for a channel with $q = 1/2$ and $0 < 18 - \mu \ll 1$.

From (4.6) we see that any turning point at which $g > \sqrt{2}$ must be a minimum. Hence, if g and g' are continuous and $g > \sqrt{2}$ at any point, then either g is monotonic or $g > \sqrt{2}$ at all points. Thus $\sqrt{2}$ is the maximum possible value that g can take if no slip at the wall is to be satisfied and the solution is to be smooth. It follows that

$\int_0^{\zeta_w} \zeta g(\zeta) d\zeta < \zeta_w^2/\sqrt{2}$, and hence from (4.7) that mass conservation can

be satisfied only if $k > k_0$, where $k_0 = (128)^{-1/4}$; that is, if $\mu < 128$. Further, if $k - k_0 \ll 1$ then $\sqrt{2} - g \ll 1$ over most of the tube ($0 \leq \zeta \leq \zeta_w$). Thus, as $\mu \rightarrow 128^-$ any solution of (4.6) and (4.7) must have an essentially inviscid uniform mainstream with a viscous boundary layer adjacent to the wall. Note that this limit structure may not be unique. In particular, regions of reversed flow, similar to those described in Section 3.3 for a channel with $q = 1/2$ and $0 < 18 - \mu \ll 1$, may be possible. This limit structure is discussed briefly with reference to experimental results in Section 5 below.

4.3 A nonsymmetric collapse extending far upstream

The analysis below is similar to that of Section 2.4 concerning a channel collapse that extends indefinitely far upstream. As several significant features of nonsymmetric flow in collapsible pipes are illustrated by this analysis, it is presented in some detail. Assume that far upstream, where $p \gg 1$, the tube law takes the form

$$r_w = 1 - f(\theta)p^{-N} + o(p^{-N}), \quad (4.8)$$

where $N > 0$. Thus, if $-X \gg 1$

$$r_w = 1 - f(\theta)|X|^{-N} + o(|X|^{-N}), \quad (4.8a)$$

where $X = R^{-1}x$. The fluid motion, which takes the form of a viscous perturbation to the Poiseuille flow, is given by

$$\begin{aligned}
 u &= U_0(r) + |X|^{-N} u_1(r, \theta) + o(|X|^{-N}), \\
 v &= R^{-1} [|X|^{-N-1} v_1(r, \theta) + o(|X|^{-N-1})], \\
 w &= R^{-1} [|X|^{-N-1} w_1(r, \theta) + o(|X|^{-N-1})], \\
 p &= -X + |X|^{1-N} p_1 + o(|X|^{1-N}),
 \end{aligned}
 \tag{4.9}$$

if $N \neq 1$. Here p_1 is a constant. If $N = 1$ then the $|X|^{1-N} p_1$ term in the pressure expansion must be replaced by $p_1 \ln |X|$. With (4.9) the equations of motion yield

$$\begin{aligned}
 \nabla^2 u_1 &= (N - 1)p_1, \\
 \nabla^2 \phi &= 0, \\
 Nu_1 + \frac{\partial v_1}{\partial r} + \frac{v_1}{r} + \frac{1}{r} \frac{\partial w_1}{\partial \theta} &= 0,
 \end{aligned}
 \tag{4.10}$$

where $\phi = \partial w_1 / \partial r + w_1 / r - (1/r) \partial v_1 / \partial \theta$ and $\nabla^2 = \partial^2 / \partial r^2 + (1/r) \partial / \partial r + (1/r^2) \partial^2 / \partial \theta^2$. In turn these are the momentum, vorticity and continuity equations. The boundary conditions are

$$\begin{aligned}
 v_1 = w_1 = 0 \text{ and } u_1 &= -\frac{1}{2} f(\theta) \text{ at } r = 1, \\
 \int_0^{2\pi} d\theta \int_0^1 r u_1 dr &= 0,
 \end{aligned}
 \tag{4.11}$$

from no-slip at the wall and conservation of mass, respectively. Also we require the velocity components to be regular throughout the pipe ($0 \leq r < 1$).

Given $f(\theta)$, the solution of (4.10) satisfying (4.11) can be obtained by taking Fourier components and solving the resulting system of ordinary differential equations. Suppose that to first order the pipe takes the shape of an ellipse of small eccentricity; that is

$$f(\theta) = a + b \cos 2\theta. \tag{4.12}$$

Note that if $a = 0$, the collapse is a bending collapse and if $b = 0$ it is a pure stretching collapse.

The solution of (4.10) - (4.12) is

$$\begin{aligned}
 u_1 &= \frac{a}{2} (1 - 2r^2) - \frac{b}{2} r^2 \cos 2\theta, \\
 v_1 &= -\frac{Na}{4} (r - r^3) - \frac{Nb}{2} (r - r^3) \cos 2\theta, \\
 w_1 &= \frac{Nb}{2} (r - r^3) \sin 2\theta, \\
 p_1 &= -\frac{4a}{N-1}.
 \end{aligned}
 \tag{4.13}$$

We see from (4.13) that the secondary motion is divided into independent axisymmetric and nonsymmetric parts, and that it is the axisymmetric part of the motion that determines the pressure perturbation. If the collapse is a bending collapse, which implies that the cross-sectional area of the pipe is constant for $|1 - r_w| \ll 1$, then the secondary motion does not have a symmetric part, and to first order the pressure is not disturbed, i.e. it takes the linear Poiseuille form. As will be seen below, this result is common to all the solutions we find for nonsymmetric problems with $|1 - r_w| \ll 1$.

Consider the secondary flow in a cross-sectional plane. If $a > 0$ the axisymmetric part of v is directed towards the centre of the pipe. The nonsymmetric part of the flow is away from the regions in which the nonsymmetric component of the radius decreases into regions in which it increases, with no flow across lines of symmetry of the nonsymmetric part of $f(\theta)$ (see Figure 4.1). If $f(\theta)$ takes a form different to that of (4.12) then this result applies to any Fourier component of $f(\theta)$ and its associated velocity components. Thus the secondary motion is essentially a simple flow which compensates for the change in shape of the pipe. In Section 4.4 below a similar result is found for a nonsymmetric collapse with $\mu \varepsilon^{3/2} \leq 0(1)$.

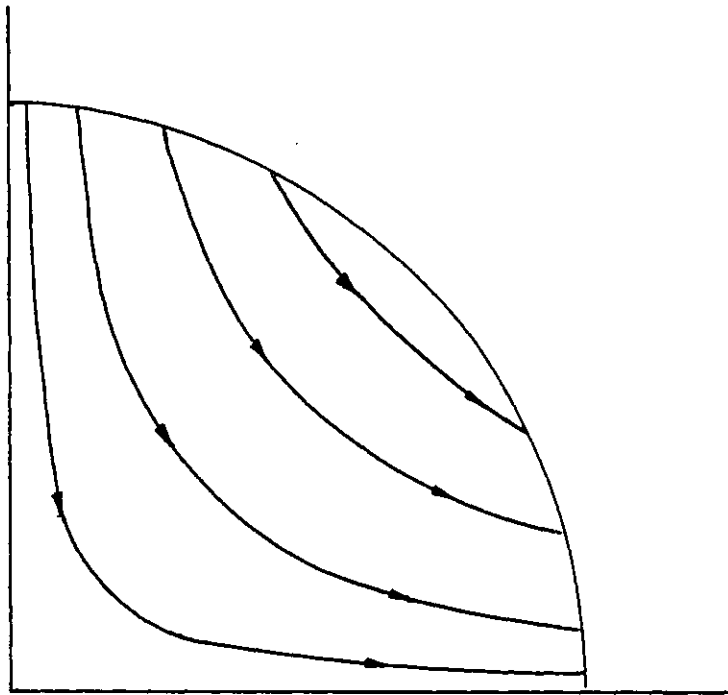


Figure 4.1. Direction of the secondary velocity when the cross-section of the pipe is an ellipse of small eccentricity and the collapse is a bending collapse: obtained from (4.13) with α set to zero.

4.4 Non-symmetric pipe flows with a fast pressure response

We begin by studying the flow in a pipe with a fast pressure response and a small change in radius. In particular, we assume that $1 \ll \mu \ll R$ and that $\lambda = \mu \epsilon^{3/2}$ is $O(1)$. The flow structure is similar to that for the analogous channel flow (Section 2.1). The core flow takes the form of an inviscid $O(\epsilon^{3/2})$ perturbation to the Poiseuille flow, and a viscous layer of thickness $O(\epsilon^{1/2})$ forms immediately adjacent to the wall. Again, it is the flow in this viscous wall layer which determines the pressure. The flow can, as in Section 4.3, be separated into an axisymmetric part and a nonsymmetric part, and again, it is the axisymmetric part that determines the pressure.

In the viscous wall layer we propose that the flow is given by

$$\left. \begin{aligned} u &= \frac{1}{2} \delta y + \delta^2 u_1(X, y, \theta) + o(\delta^2), \\ v &= -R^{-1} v_1(X, y, \theta) + o(R^{-1}), \\ w &= \delta^{-1} R^{-1} w_1(X, y, \theta) + o(\delta^{-1} R^{-1}), \\ p &= \delta^3 P(X) + o(\delta^3), \end{aligned} \right\} \quad (4.14)$$

where $x = \delta^3 R X$, $r = 1 - \delta y$ and $\delta = \epsilon^{1/2}$. We note that mass conservation requires that the azimuthal velocity in (4.14) be much larger than the radial velocity, and that the predominant change in the flow occurs in the axial directions.

Applying (4.14) to (4.1) produces the balances

$$\left. \begin{aligned} \frac{1}{2} y \frac{\partial u_1}{\partial X} + \frac{1}{2} v_1 &= -P' + \frac{\partial^2 u_1}{\partial y^2} - \frac{1}{2}, \\ \frac{\partial^3 w_1}{\partial y^3} - \frac{\partial}{\partial y} \left(\frac{1}{2} y \frac{\partial w_1}{\partial y} \right) &= 0, \\ \frac{\partial u_1}{\partial X} + \frac{\partial v_1}{\partial y} + \frac{\partial w_1}{\partial \theta} &= 0, \end{aligned} \right\} \quad (4.15)$$

from the momentum, vorticity, and continuity equations in turn. The boundary conditions are

$$\left. \begin{aligned}
 v_1 = w_1 = 0 \text{ and } u_1 &= -\frac{1}{2} S(\lambda P) f(\theta) \quad \text{at } y = 0, \\
 u_1 &\rightarrow -\frac{1}{4} y^2 \text{ as } y \rightarrow \infty, \\
 v_1 \rightarrow 0, w_1 \rightarrow 0 \text{ and } u_1 &\rightarrow -\frac{1}{4} y^2 \text{ as } X \rightarrow -\infty,
 \end{aligned} \right\} (4.16)$$

from no-slip at the wall, matching to the core flow, and matching to the incoming Poiseuille flow respectively.

The transform solution of this linear boundary layer problem can be found by a method similar to that used by Smith (1976c) in a study of flow in a curved pipe. Let $w_1^*(s, y, \theta) = \int_{-\infty}^{\infty} w_1(X, y, \theta) e^{-isX} dX$, the generalised transform with respect to s . Then, from the vorticity equation in (4.15),

$$w_1^* = B(s, \theta) \mathcal{L}(\alpha y), \quad (4.17)$$

where $\alpha = (0 + \frac{1}{2} is)^{1/3}$ has a branch cut along the positive imaginary s -axis, $B(s, \theta)$ is a function to be determined,

$$\mathcal{L}(t) = \text{Ai}(t) \int_0^t \frac{d\beta}{\text{Ai}^2(\beta)} \int_{\infty}^{\beta} \text{Ai}(\gamma) d\gamma,$$

and Ai is the Airy function. Let $\hat{u}_1 = u_1 + y^2/4$ and $\hat{P} = P + X$. Then (4.17) and continuity and momentum equations in (4.15) give

$$\hat{u}_1^* = C(s, \theta) \int_{\infty}^y \text{Ai}(\alpha t) dt - \frac{1}{is} \frac{\partial B}{\partial \theta} \mathcal{L}(\alpha y) \quad (4.18)$$

and

$$\left. \begin{aligned}
 v_1^* &= -2is\hat{P}^* + C(s, \theta) \left\{ 2\alpha \text{Ai}'(\alpha y) - \right. \\
 &\quad \left. - isy \int_{\infty}^y \text{Ai}(\alpha t) dt \right\} - \frac{1}{\alpha} \frac{\partial B}{\partial \theta},
 \end{aligned} \right\} (4.19)$$

where the $*$ denotes a transformed variable and $C(s, \theta)$ is a function to be determined. As $\mathcal{L}(t) \rightarrow -t^{-1}$ as $t \rightarrow \infty$, \hat{u}_1^* satisfies the matching to the core flow at the outer edge of the layer, that is $\hat{u}_1^* \rightarrow 0$ as $y \rightarrow \infty$. With (4.19), the condition that v_1 vanishes at the wall becomes

$$- 2is\hat{p}^* + 2\alpha Ai'(0) C(s, \theta) - \frac{1}{\alpha} \frac{\partial B}{\partial \theta} = 0. \quad (4.20)$$

We now take the Fourier expansions

$$\begin{aligned} \hat{u}_1 &= f_0(X, y) + \sum_{n=1}^{\infty} [f_{1n}(X, y) \cos n\theta + f_{2n}(X, y) \sin n\theta], \\ v_1 &= g_0(X, y) + \sum_{n=1}^{\infty} [g_{1n}(X, y) \cos n\theta + g_{2n}(X, y) \sin n\theta], \\ w_1 &= h_0(X, y) + \sum_{n=1}^{\infty} [h_{1n}(X, y) \cos n\theta + h_{2n}(X, y) \sin n\theta], \end{aligned} \quad (4.21)$$

and

$$B(s, \theta) = B_0(s) + \sum_{n=1}^{\infty} [B_{1n}(s) \cos n\theta + B_{2n}(s) \sin n\theta], \quad (4.22)$$

with a similar expansion for $C(s, \theta)$, and expand the shape function $f(\theta)$ as

$$f(\theta) = a_0 + \sum_{n=1}^{\infty} (a_{1n} \cos n\theta + a_{2n} \sin n\theta). \quad (4.23)$$

Immediately, we see from (4.20) that

$$C_0(s) = \frac{is}{\alpha Ai'(0)} \hat{p}^*. \quad (4.24)$$

With (4.23), the no-slip condition for u_1 in (4.16) becomes

$$\left. \begin{aligned} f_0(X, 0) &= -\frac{1}{2} a_0 S(\lambda P), \\ f_{jn}(X, 0) &= -\frac{1}{2} a_{jn} S(\lambda P), \quad j = 1, 2; n = 1, 2, \dots \end{aligned} \right\} \quad (4.25)$$

which, with (4.18) and (4.24) yields

$$\begin{aligned} \frac{a_0}{2} S(\lambda P) &= \frac{2^{2/3}}{3\Gamma(2/3)Ai'(0)} \left\{ \int_0^X (X-t)^{-1/3} \frac{dP}{dt} dt + \right. \\ &\quad \left. + \frac{3}{2} X^{2/3} \right\} \end{aligned} \quad (4.26)$$

The pressure distribution can now be determined from the integro-differential equation (4.26). We see that, as with a collapse extending indefinitely far upstream (Section 3.3), the axisymmetric parts of the fluid motion and the collapse determine the pressure, and

that if the collapse is a bending collapse ($a_0 = 0$), then to leading order the pressure maintains its incoming Poiseuille form ($P = -X$) while (4.26) is valid. For a stretching collapse, numerical methods must be used to solve (4.26) (see Appendix 5 below). The behaviour of the pressure is similar to that for the analogous channel flow, details of which are given in Section 2.1.

With the pressure determined, $S(\lambda P)$ can be regarded as a known function of X , and the Fourier coefficients are then given by

$$\left. \begin{aligned} C_{jn}(s) &= \frac{3}{2} \alpha a_{jn} S^*(s), \\ B_{1n}(s) &= -\frac{3}{n} \alpha^3 a_{2n} \text{Ai}'(0) S^*(s), \\ B_{2n}(s) &= \frac{3}{n} \alpha^3 a_{1n} \text{Ai}'(0) S^*(s), \end{aligned} \right\} \quad (4.27)$$

from (4.18), (4.20) and (4.25). As will be shown below, we require

$$B_0(s) = 0 \quad (4.27a)$$

for the core and boundary layer flows to be consistent. This completes the transform solution of the boundary layer problem formed by (4.15) and (4.16). We note that no evidence was found above for any significant upstream influence, as might be expected from the results for channels (Sections 2 and 3).

We find from the transform solution that

$$\left. \begin{aligned} f_{jn}(X,y) &\sim -a_{jn} y^{-1} I(X), \\ g_0(X) &\rightarrow -2(P'(X) + 1), \\ g_{jn}(X,y) &\rightarrow a_{jn} I'(X), \\ h_{1n}(X,y) &\sim -\frac{1}{n} a_{2n} y^{-1} I'(X), \\ h_{2n}(X,y) &\sim \frac{1}{n} a_{1n} y^{-1} I'(X), \\ &j = 1,2; \quad n = 1,2,\dots \end{aligned} \right\} \quad (4.28)$$

as $y \rightarrow \infty$, where

$$I(X) = \frac{1}{\Gamma^2(2/3)} (3/2)^{2/3} \int_0^X (X-t)^{-2/3} S(\lambda P(t)) dt. \quad (4.29)$$

It remains to be verified that the core flow can act passively and be consistent with the motion at the outer edge of the wall layer. We propose that in the core there is an inviscid perturbation to the Poiseuille flow. In particular, we take

$$\left. \begin{aligned} u &= U_0(r) + \delta^3 \hat{U}(X, r, \theta) + o(\delta^3), \\ v &= R^{-1} \hat{V}(X, r, \theta) + o(R^{-1}), \\ w &= R^{-1} \hat{W}(X, r, \theta) + o(R^{-1}). \end{aligned} \right\} \quad (4.30)$$

It is seen from (4.14) and (4.30) that the radial velocity has constant order throughout the pipe while the azimuthal velocity is much greater in the viscous wall layer than in the core. The wall layer therefore has a jetlike structure. This facet of the boundary layer can occur also in nonsymmetric pipe flows when the wall is fixed (see Smith 1976 c,d,e).

With (4.30) the governing equations (4.1) give

$$\left. \begin{aligned} U_0 \frac{\partial \hat{U}}{\partial X} + U_0' \hat{V} &= -P' - 1, \\ U_0 \frac{\partial \hat{\phi}}{\partial X} + U_0' \frac{\partial \hat{W}}{\partial X} &= 0, \\ \frac{\partial \hat{U}}{\partial X} + \frac{\partial \hat{V}}{\partial r} + \frac{\hat{V}}{r} + \frac{1}{r} \frac{\partial \hat{W}}{\partial \theta} &= 0, \end{aligned} \right\} \quad (4.31)$$

where $\hat{\phi} = R\Omega$. These are in turn the moment, vorticity and continuity equations. The -1 term in the momentum equation represents the viscous effect of the Poiseuille flow. The boundary conditions are that the flow is regular throughout the pipe, matches to the incoming Poiseuille flow, and matches to (4.28) as $r \rightarrow 1^-$.

Taking Fourier series of the form

$$\hat{U}(X, r, \theta) = \hat{U}_0(X, r) + \sum_{n=1}^{\infty} [\hat{U}_{1n}(X, r) \cos n\theta + \hat{U}_{2n}(X, r) \sin n\theta] \quad (4.32)$$

and so on, we find that

$$\left. \begin{aligned}
 \hat{U}_0(X,r) &= -\frac{P+X}{U_0(r)} \left\{ 1 + \frac{U_0(r)U_0'(r)}{r} \int_0^r \frac{t}{U_0^2(t)} dt \right\}, \\
 \hat{V}_0(X,r) &= (P'+1) \frac{U_0(r)}{r} \int_0^r \frac{t}{U_0^2(t)} dt, \\
 \hat{W}_0(X,r) &= 0,
 \end{aligned} \right\} (4.33)$$

is the axisymmetric solution of (4.31) that is regular, matches to the incoming flow, and is consistent with the motion at the edge of the wall layer. The trivial solution is the only regular solution for \hat{W}_0 . Hence consistency with the boundary layer flow requires $B_0(s) = 0$ and $h_0 = 0$. For a bending collapse $P = -X$ and $C_0(s) = 0$, and it follows that \hat{U}_0 , \hat{V}_0 , f_0 and g_0 are all zero; that is, the axisymmetric part of the secondary flow is trivial, as occurred in the problem of Section 4.3. For a stretching collapse \hat{U}_0 in (4.33) is $O(1)$ when $1-r \ll 1$, which suggests that there must be a nontrivial term of $O(\delta^3)$ in the expansion for u in the wall layer.

Let us now separate the variables such that

$$\left. \begin{aligned}
 \hat{U}_{jn}(X,r) &= a_{jn} A_{jn}(X) F_{jn}(r), \\
 \hat{V}_{jn}(X,r) &= a_{jn} A'_{jn}(X) G_{jn}(r), \\
 \hat{W}_{1n}(X,r) &= a_{2n} A'_{2n}(X) H_{1n}(r), \\
 \hat{W}_{2n}(X,r) &= a_{1n} A'_{1n}(X) H_{2n}(r), \\
 j &= 1, 2; \quad n = 1, 2, \dots
 \end{aligned} \right\} (4.34)$$

We require (4.34) to be consistent with (4.28) as $r \rightarrow 1^-$, which suggests that

$$A_{1n}(X) = A_{2n}(X) = -I(X), \quad (4.35)$$

where $I(X)$ is given by (4.29). Equations (4.34), (4.35) and the governing equations (4.31) imply that

$$\begin{aligned}
 G_{1n}(r) &= G_{2n}(r) = G_n(r), \\
 F_{1n}(r) &= F_{2n}(r) = -\frac{U'_0(r)}{U_0(r)} G_n(r), \\
 H_{1n}(r) &= -H_{2n}(r) = \frac{1}{n} \{ (rG_n(r))' - r \frac{U'_0(r)}{U_0(r)} G_n(r) \}, \\
 n &= 1, 2, \dots,
 \end{aligned}
 \tag{4.36}$$

and that the $G_n(r)$ must satisfy

$$r^2 U_0(r) G_n'' + r U_0(r) G_n' + [(1 - n^2) U_0(r) + r^2] G_n = 0.$$

The bounded series solution for $G_n(r)$ in ascending powers of r is

$$G_n(r) = b_n \sum_{k=0}^{\infty} d_{nk} r^{2k+n-1}, \tag{4.37}$$

where $d_{n0} = 1$ and the d_{nk} are determined by

$$k(n+k)d_{nk} - [k(n+k) - (n+2k)]d_{nk-1} = 0 \tag{4.38}$$

for $k \geq 1$. By Weierstrass' test (see e.g. Knopp 1956, p.132) this series is convergent at $r = 1$ and hence is convergent for all $r \leq 1$. Finally, (4.34) will be consistent with (4.28) at the outer edge of the wall layer if $G_n(1) = 1$. Thus taking

$$b_n = 1 / \sum_{k=0}^{\infty} d_{nk} \tag{4.39}$$

completes the solution.

In turn the axial and azimuthal shear stresses can be written as

$$\begin{aligned}
 \hat{\tau} &= -\frac{1}{2} - \delta \tau_1 + o(\delta), \\
 \hat{\tau}_\theta &= -\delta^{-2} R^{-1} \tau_\theta + o(\delta^{-2} R^{-1}),
 \end{aligned}$$

where $\tau_1 = (\partial u_1 / \partial y)_{y=0}$ and $\tau_\theta = (\partial w_1 / \partial y)_{y=0}$. It follows from (4.18) and (4.19) that

$$\left. \begin{aligned} \tau_1 &\propto \int_0^X (X-t)^{-1/3} \frac{dS[\lambda P(t)]}{dt} dt, \\ \tau_\theta &\propto \int_0^X (X-t)^{-1/3} \frac{d^2S[\lambda P(t)]}{dt^2} dt. \end{aligned} \right\} (4.40)$$

Suppose that p is continuous and $S \propto (-\mu p)^m$ for $0 \leq -\mu p \ll 1$, where $m > 0$. Then, at the origin where $p = 0$, S is continuous but has infinite slope if $m < 1$. Assume that the collapse is a bending collapse. Then for $0 \leq X \ll 1$, $P = -X$, $S \propto X^m$, and from (4.40), $\tau_1 \propto X^{m-1/3}$ and $\tau_\theta \propto X^{m-4/3}$. Thus at the origin, the axial shear stress is continuous if $m > 1/3$, but τ_1 has infinite slope if $m < 4/3$. The azimuthal shear stress is more sensitive at $X = 0$ where τ_θ is infinite if $m < 4/3$ and is continuous with infinite slope if $m < 7/3$. Assume now that the collapse is a stretching collapse. The behaviour of pressure and the axial shear stress in $0 \leq X \ll 1$ is similar to that for the analogous channel flow (Section 2.1). Working to leading order, if $m > 2/3$ then for $0 \leq X \ll 1$, $P = -X$ and hence S , τ_1 and τ_θ are the same as for a bending collapse. If $m < 2/3$ and $0 \leq X \ll 1$, it follows from (4.26) that $P \propto -X^\ell$, where $\ell = 1/3(1-m)$, and from (4.40) that $\tau_1 \propto X^{\ell(2m-1)}$ and $\tau_\theta \propto X^{\ell(5m-4)}$. Therefore, P , S , τ_1 and τ_θ have infinite slope at the origin if $m < 2/3$, and τ_1 is infinite at $X = 0$ if $m < 1/2$. Also, the expressions obtained for the core flow may not be continuous at the origin. If $m < 2/3$ then, for both stretching and bending collapses, $I(X)$ is continuous but $I'(X)$ is infinite at $X = 0$, where $I(X)$ is defined by (4.29). Therefore, the nonsymmetric component of the radial velocity and the azimuthal velocity, as given by (4.30) - (4.39), will be discontinuous at the origin if $m < 2/3$. Further, with a bending collapse the symmetric part of the radial velocity will be infinite at $X = 0$ if $m < 2/3$. We will not investigate further, but assume that as the pressure has been determined and is continuous these local irregularities can be smoothed out by an examination on a shorter length scale close to the origin, as is usually the case with boundary layer flows.

Consider now a bending collapse. It follows from (4.28) that at the edge of the wall layer

$$v = -R^{-1}I'(X)f(\theta)$$

to leading order. It can be shown that $I'(X) > 0$ for $X > 0$. Hence, there is a mass flow out of the wall layer in the regions where the tube radius has decreased, and a flow into the layer where the radius has increased. Moreover, it can be shown that this result applies to any particular Fourier component of the collapse and its associated velocity components, and to the nonsymmetric part of the collapse and motion if the collapse is a stretching collapse (c.f. Section 4.3).

Far downstream, where $1 - S \ll 1$, we see from (4.26) and (4.40) that $P + X \propto X^{1/3}$, $\tau_1 \propto X^{-1/3}$, and $\tau_\theta \propto X^{-4/3}$ as $X \rightarrow \infty$. It follows that the wall layer has thickness $\propto X^{1/3}$ for large X , and that where $X = O(\delta^{-3})$ it merges with the coreflow. In this region x is of $O(R)$, $u - U_0(r) = O(\epsilon)$, and $p = O(1)$. As $R^{-1}x \rightarrow \infty$ the flow tends to a limit form in which the radial and azimuthal velocities are zero to leading order, $u - U_0(r)$ is $O(\epsilon)$ and is independent of x , and the $O(\epsilon R^{-1})$ perturbation of $p + R^{-1}x$ is linear in x . This limit flow is given in Section 4.5 below. We note the similarities between the analogous pipe and channel flows far downstream (See Section 2.1).

Suppose that $a_0 = O(1)$ and $|a_{jn}| \ll 1$ for all the a_{jn} . Then to leading order the secondary flow is independent of θ , and is given by the axisymmetric part of the solution given above. If $|a_0| \ll 1$ and at least one of a_{jn} is order $O(1)$, then working to leading order, $P = -X$ and the secondary motion is that for a bending collapse, as given above.

For $\lambda \ll 1$ the problem is similar to that for a channel with $1 \ll \mu \ll \epsilon^{-3/2}$ (see Section 2.1). To leading order, the pressure is $-R^{-1}x$, and the linear boundary layer problem formed is that of shear flow impinging on a fixed nonsymmetric disturbance of the wall. The solution of this problem is straightforward, and the behaviour of the flow can be deduced directly from the results for a channel (Section 2.1) and a nonsymmetric pipe with $\lambda = O(1)$ given above.

For $\lambda \gg 1$ the solution immediately downstream of the origin can be obtained by expanding $S(\mu p)$ for $0 \leq -\mu p \ll 1$ and applying the method used above for $\lambda = O(1)$. If S is given by (1.6) then this procedure yields the integro-differential equation

$$\frac{1}{4} a_0 q \bar{p}^2 = \frac{2^{2/3}}{3\Gamma(2/3)Ai'(0)} \left\{ \int_0^{\tilde{X}} (\tilde{X}-t)^{-1/3} \frac{d\tilde{P}}{dt} dt + \frac{3\tilde{X}^{2/3}}{2} \right\}, \quad (4.41)$$

where $p = \delta_1^3 \tilde{P}$, $x = \delta_1^3 R \tilde{X}$ and $\delta_1 = (\epsilon \mu^2)^{-1/4}$. It is assumed here that

$\delta_1^3 R \gg 1$. Equation (4.41) is similar to (3.45), the equation which determines the pressure immediately downstream of the origin for a channel with S given by (1.6), $\epsilon = 1$ and $\mu \gg 1$. It follows from the analysis of (3.45) in Section 3.4 that, if the collapse is a stretching collapse, then P will have a singularity at some $\tilde{X} = \tilde{X}_0$, where \tilde{X}_0 is finite, and that $\tilde{P} \propto (\tilde{X}_0 - \tilde{X})^{-1/3}$ when $0 < \tilde{X}_0 - \tilde{X} \ll 1$.

Assume now that $\epsilon \gg \mu^{-1/2}$, the collapse is a stretching collapse and $\delta_1^4 R \gg 1$. The behaviour of the flow immediately downstream of the origin can be deduced from the results for a channel (Section 3.4) and for a nonsymmetric pipe with $\lambda = 0(1)$ given above. When $\tilde{X}_0 - \tilde{X} = 0(\delta_1)$ the perturbation to the axial skin friction will be $0(1)$, and the flow structure in the wall layer will not be linear in form. The flow in the boundary layer for $\tilde{X}_0 - \tilde{X} = 0(\delta_1)$ is given by

$$\left. \begin{aligned} u &= \delta_1^{4/3} \bar{U}(\bar{X}, \bar{Z}, \theta) + o(\delta_1^{4/3}), \\ v &= -\delta_1^{-4/3} R^{-1} \{ \bar{V}(\bar{X}, \bar{Z}, \theta) + q \bar{P} \bar{P}' f(\theta) \bar{U} + \\ &\quad + \frac{q}{2} \bar{P}^2 f(\theta) \bar{W} \} + o(\delta_1^{-4/3} R^{-1}), \\ w &= \delta_1^{-8/3} R^{-1} \bar{W}(\bar{X}, \bar{Z}, \theta) + o(\delta_1^{-8/3} R^{-1}), \end{aligned} \right\} \quad (4.42)$$

where $p = \delta_1^{8/3} \bar{P}(\bar{X})$, $x = \delta_1^3 R \tilde{X}_0 + \delta_1^4 R \bar{X}$, and $\bar{Z} = -\frac{q}{2} \bar{P} f(\theta) + \delta_1^{-4/3} (1-r)$.

For $\tilde{X}_0 - \tilde{X} = 0(\delta_1)$ the core flow is given by

$$\left. \begin{aligned} u &= U_0(r) + \delta_1^{8/3} \bar{U}_1(\bar{X}, r, \theta) + o(\delta_1^{8/3}), \\ v &= \delta_1^{-4/3} R^{-1} \bar{V}_1(\bar{X}, r, \theta) + o(\delta_1^{-4/3} R^{-1}), \\ w &= \delta_1^{-4/3} R^{-1} \bar{W}_1(\bar{X}, r, \theta) + o(\delta_1^{-4/3} R^{-1}). \end{aligned} \right\} \quad (4.43)$$

With (4.42) the governing equations (4.1) reduce to

$$\begin{aligned}
 \bar{U} \frac{\partial \bar{U}}{\partial \bar{X}} + \bar{V} \frac{\partial \bar{U}}{\partial \bar{Z}} + \bar{W} \frac{\partial \bar{U}}{\partial \theta} &= -\bar{P}' + \frac{\partial^2 \bar{U}}{\partial \bar{Z}^2}, \\
 \bar{U} \frac{\partial^2 \bar{W}}{\partial \bar{X} \partial \bar{Z}} + \bar{V} \frac{\partial^2 \bar{W}}{\partial \bar{Z}^2} + \bar{W} \frac{\partial^2 \bar{W}}{\partial \theta \partial \bar{Z}} \\
 - \frac{\partial \bar{U}}{\partial \bar{X}} \frac{\partial \bar{W}}{\partial \bar{Z}} + \frac{\partial \bar{U}}{\partial \bar{Z}} \frac{\partial \bar{W}}{\partial \bar{X}} &= \frac{\partial^3 \bar{W}}{\partial \bar{Z}^3}, \\
 \frac{\partial \bar{U}}{\partial \bar{X}} + \frac{\partial \bar{V}}{\partial \bar{Z}} + \frac{\partial \bar{W}}{\partial \theta} &= 0.
 \end{aligned}
 \tag{4.44}$$

The flow in the core is controlled by

$$\begin{aligned}
 U_0 \frac{\partial \bar{U}_1}{\partial \bar{X}} + U_0' \bar{V}_1 &= -\bar{P}', \\
 U_0 \frac{\partial \bar{\Omega}}{\partial \bar{X}} + U_0' \frac{\partial \bar{W}_1}{\partial \bar{X}} &= 0, \\
 \frac{\partial \bar{U}_1}{\partial \bar{X}} + \frac{\partial \bar{V}_1}{\partial r} + \frac{\bar{V}_1}{r} + \frac{1}{r} \frac{\partial \bar{W}_1}{\partial \theta} &= 0,
 \end{aligned}
 \tag{4.45}$$

where $\bar{\Omega} = \delta_1^{4/3} R\Omega$.

The equations in (4.44) and (4.45) are in turn the momentum, vorticity, and continuity equations. The boundary conditions are that the velocity vanishes at the wall, and that (4.42) and (4.43) match at the outer edge of the wall layer. These require

$$\begin{aligned}
 \bar{U} = \bar{V} = \bar{W} = 0 \text{ at } \bar{Z} = 0, \\
 \bar{U} \sim \frac{1}{2} (\bar{Z} + \frac{1}{2} q\bar{P}^2 f(\theta)) \text{ as } \bar{Z} \rightarrow \infty.
 \end{aligned}
 \tag{4.46}$$

Also, (4.42) and (4.43) must be consistent with the incoming flow; that is, for $-X \gg 1$ they must be consistent with the asymptotic flow structure that can be obtained for $\tilde{X}_0 - \tilde{X} \ll 1$. It can be shown, with an analysis similar to that found in Appendix 2, that this initial condition is satisfied.

It is not known whether a solution exists for the boundary layer problem defined by (4.45) and (4.46). Some asymptotic flow structures for $\bar{P} \rightarrow -\infty$ are considered in Appendix 4. It is shown that the matching condition at the outer edge of the layer does not permit a

satisfactory solution to the similarity problem with $\bar{P} \propto (\bar{X}_0 - \bar{X})^{-n}$, where $n > 0$ and \bar{X}_0 is finite, nor to the problem with $\bar{P} \propto \bar{X}^n$, where $n > 0$ but $n \neq 1/6$. If $\bar{P} \propto \bar{X}^{1/6}$ as $\bar{X} \rightarrow \infty$, then the boundary conditions are consistent with the governing equations, and a solution of the similarity problem may exist if $f(\theta) - a_0$ is $O(1)$, but not if $|f(\theta) - a_0| \ll 1$.

Assume now that $\epsilon u^{1/3} \gg 1$, $\delta_1^3 R \gg 1$, and the collapse is a bending collapse. The solution of (4.41) is $\bar{P} = -\bar{X}$, and the perturbation to the axial shear is proportional to $\bar{X}^{5/3}$ for $\bar{X} \gg 1$. It follows that the flow in the boundary layer becomes nonlinear in form where \bar{X} is $O(\delta_1^{-3/5})$. In this region

$$\left. \begin{aligned} u &= \delta_1^{4/5} U(\hat{X}, Y, \theta) + o(\delta_1^{4/5}), \\ v &= -\delta_1^{-4/5} R^{-1} \{V(\hat{X}, Y, \theta) + qp\hat{p}'f(\theta)U + \\ &\quad + \frac{1}{2} q\hat{p}^2 f'(\theta)W\} + o(\delta_1^{-4/5} R^{-1}), \\ w &= \delta_1^{-8/5} R^{-1} W(\hat{X}, Y, \theta) + o(\delta_1^{-8/5} R^{-1}), \end{aligned} \right\} \quad (4.47)$$

in the wall layer, and

$$\left. \begin{aligned} u &= U_0(r) + \delta_1^{8/5} U_1(\hat{X}, Y, \theta) + o(\delta_1^{8/5}), \\ v &= \delta_1^{-4/5} R^{-1} V_1(\hat{X}, Y, \theta) + o(\delta_1^{-4/5} R^{-1}), \\ w &= \delta_1^{-4/5} R^{-1} W_1(\hat{X}, Y, \theta) + o(\delta_1^{-4/5} R^{-1}), \end{aligned} \right\} \quad (4.48)$$

in the core, where $x = \delta_1^{12/5} R \hat{X}$, $Y = -\frac{1}{2} q\hat{p}^2 f(\theta) + \delta_1^{-4/5} (1-r)$, and $p = \delta_1^{12/5} \hat{p}(\hat{X})$. With appropriate changes of variable and \bar{P}' set to zero, the governing equations in the wall layer and the core are given by (4.44) and (4.45) respectively. The boundary conditions of no slip at the wall and consistency between (4.47) and (4.48) at the edge of the layer require

$$\left. \begin{aligned} U = V = W = 0 \text{ at } Y = 0, \\ U \sim \frac{1}{2} \{Y + \frac{1}{2} q \hat{p}^2 f(\theta)\} \text{ as } Y \rightarrow \infty. \end{aligned} \right\} \quad (4.49)$$

Also, (4.47) and (4.48) must be consistent with the incoming flow, that is as $\hat{X} \rightarrow 0+$ they must match with the asymptotic flow structure that can be obtained for $\tilde{X} \rightarrow \infty$. If $\hat{p} = -\hat{X}$ for $\hat{X} \ll 1$, then it can be shown (c.f. Appendix 2) that this upstream matching will be satisfied.

It is not known whether a solution exists for the coupled problem defined by (4.47) - (4.49). However, the problem does not appear to be well posed, in the sense that the boundary conditions (4.49) are pressure dependent but the pressure gradient does not appear in the leading order streamwise momentum equations generated by (4.47) and (4.48). Also, it follows from the analysis of Appendix 4 that there is no satisfactory asymptotic flow structure with $\hat{p} \propto \hat{X}$ as $\hat{X} \rightarrow \infty$, which suggests that if a steady solution exists then, unlike all other fine bending collapses considered in this study, the pressure must deviate from its Poiseuille form in a region in which $|1 - r_w| \ll 1$.

Suppose now that the collapse is a stretching collapse, and

$$\mu^{-2/3} \ll \varepsilon \ll \mu^{-1/2} \ll 1. \quad (4.50)$$

The perturbation to the axial shear stress is still small where p is $O(\mu^{-1})$, and the flow in the wall layer retains its linear form until the boundary layer merges with the core flow far downstream, where the flow is given by an $O(\varepsilon)$ perturbation to the Poiseuille flow on an $O(R)$ streamwise length scale. A full solution can be obtained for the problem satisfying (4.50). The method of solution, and the basic development of the flow, is similar to that outlined in Section 3.4 for the analogous channel flow.

If the collapse is a stretching collapse and $\varepsilon \mu^{1/2} = O(1)$, then the flow in the boundary layer becomes non-linear in form simultaneously with p becoming $O(\mu^{-1})$. A solution has not been found for the non-linear problem which governs the flow in the wall layer when p is $O(\mu^{-1})$. We note that numerical techniques are necessary at this stage.

Consider a bending collapse with

$$\mu^{-2/3} \ll \varepsilon \ll \mu^{-1/3} \ll 1. \quad (4.51)$$

In this case the flow in the wall layer retains a linear structure

until far downstream where the boundary layer merges with the mainstream. A complete solution can be obtained for this problem. The details will be omitted, but an outline of the solution will be given. Immediately downstream of the origin (4.41) is valid and the pressure is given by $\tilde{P} = -\tilde{X}$. Thus if p is $O(\mu^{-1})$, $\tilde{x} = \mu R^{-1}x$ is $O(1)$. In this region, in the wall layer

$$u = \frac{1}{2} \mu^{-1/3} \tilde{z} + \varepsilon \tilde{u}_1(\tilde{x}, \theta, \tilde{z}) - \frac{1}{4} \mu^{-2/3} \tilde{z}^2 + o(\mu^{-2/3}), \quad (4.52)$$

where $\tilde{z} = \mu^{1-3}(1-r)$, and in the core $u - U_0(r) = O(\mu^{-1/3}\varepsilon)$. The boundary conditions of no slip at the wall and matching to the core flow require

$$\left. \begin{aligned} \tilde{u}_1 &= -\frac{1}{4} q S(\tilde{p}) \text{ at } \tilde{z} = 0, \\ \tilde{u}_1 &\rightarrow 0 \text{ as } \tilde{z} \rightarrow \infty, \end{aligned} \right\} \quad (4.53)$$

where $\tilde{p} = \mu p$. The solution for (4.52) subject to (4.53) can be found using the techniques given above. The linear boundary layer equations imply that $\tilde{z}\tilde{x}^{-1/3}$ is $O(1)$ for $\tilde{x} \gg 1$. From (4.53), \tilde{u}_1 is $O(1)$ for $\tilde{x} \gg 1$, and it follows that $\varepsilon \tilde{u}_1$ and $\mu^{-2/3}\tilde{z}^2$ are of the same order if \tilde{x} is $O(\varepsilon^{3/2}\mu)$. In this region the wall layer has thickness $O(\varepsilon^{1/2})$ and axial velocity component is given by

$$u = \frac{1}{2} \varepsilon^{1/2} \hat{y} + \varepsilon \hat{U}_1(\hat{x}, \hat{y}, \theta) + o(\varepsilon), \quad (4.54)$$

where $\hat{y} = \varepsilon^{-1/2}(1-r)$ and $\hat{x} = \varepsilon^{-3/2}R^{-1}x$. In the core $u - U_0(r) = O(\varepsilon^{3/2})$. The boundary conditions for \hat{U}_1 are

$$\left. \begin{aligned} \hat{U}_1 &= -\frac{1}{4} q f(\theta) \text{ at } \hat{y} = 0, \\ \hat{U}_1 &\sim -\frac{1}{4} \hat{y}^2 \text{ as } \hat{y} \rightarrow \infty. \end{aligned} \right\} \quad (4.55)$$

As the flow proceeds downstream the boundary layer continues to expand, with $\hat{y}\hat{x}^{-1/3} = O(1)$, until \hat{x} is $O(\varepsilon^{-3/2})$, where it merges with the mainstream. The final stage in the development of the flow takes the form of an $O(\varepsilon)$ perturbation to the Poiseuille flow on an $O(R)$ streamwise length scale.

For a pipe with $q \ll 1$ the main features of the collapse and the flow can be deduced directly from the above and the results of Section 3.4.

In the present section we have studied a model of a pipe which collapses nonsymmetrically and has a fast pressure response. A summary of our results will now be given. Within the present assumptions no evidence was found for any upstream influence, and the flow retained its incoming Poiseuille form until the origin, where the wall first varies from a circular cross-section. Immediately downstream of the origin a boundary layer forms adjacent to the wall. As for a channel (see Sections 2.1 and 3.4), it is the flow in the wall layer that determines the pressure, and hence the position of the walls, while the core flow responds passively to the changes in the wall layer. The flow in the wall layer has a linear structure initially, but may become nonlinear at some point further downstream. Whether or not this occurs depends on the relative orders of the parameters μ and ϵ . Solutions have been obtained for the linear boundary layer problems, but not for the nonlinear problems, which, we suggest, may well be worthy of further study. The radial velocity is of the same order in the wall layer and the core, but the azimuthal velocity is much larger in the wall layer than the core. Thus, if a boundary layer exists, then the flow has a jetlike form close to the wall. Similar jetlike flow structures can occur in high Reynolds number flows in pipes with fixed nonsymmetric walls, as can a passive core flow (Smith, 1976c, d, e). In regions where the flow in the wall layer takes a linear form the motion can be separated into symmetric and nonsymmetric parts, and it is the symmetric part of the motion that determines the pressure, and hence controls the development of the flow and the collapse, while the nonsymmetric part of the motion responds passively. The type of collapse has a major influence. If the collapse is a stretching collapse, then as far as could be determined the changes in the pressure and the flow are similar to those for a channel with a fast pressure response (see Sections 2.1 and 3.4). With a bending collapse, as far as could be determined, the pressure is given by $p = -R^{-1}x$ throughout the collapse, and the collapse is in all cases more gradual than that for a stretching collapse with the same parameter values. It is stressed that care must be taken in applying any of the above results, as their extension

to pipes with more realistic pressure-area-shape relationships (see e.g. Moreno et al. 1970) is by no means certain.

Finally, we note that the analysis for a symmetric collapse with a fast pressure response can be obtained from the above by setting $f(\theta)$ equal to one.

4.5 Nonsymmetric pipe flows with a slow pressure response

Suppose that the pressure response is slow ($\mu \gg 1$). Taking $x = \mu^{-1}RX$, $p = \mu^{-1}P(X)$, $v = \mu R^{-1}V$, $w = \mu R^{-1}W$, the streamwise momentum equation reduces to

$$\frac{\partial^2 u}{\partial r^2} + \frac{1}{r} \frac{\partial u}{\partial r} + \frac{1}{r^2} \frac{\partial^2 u}{\partial \theta^2} = P'(X). \quad (4.56)$$

The boundary conditions are

$$\left. \begin{aligned} u &= 0 \text{ at } r = r_w(P), \\ \int_0^{2\pi} d\theta \int_0^{r_w} u(r, \theta, X) r dr &= \frac{\pi}{8}, \\ u &\rightarrow U_0(r) \text{ and } P \rightarrow -X \text{ as } X \rightarrow -\infty, \end{aligned} \right\} \quad (4.57)$$

from no slip at the wall, conservation of mass, and matching to the incoming Poiseuille flow in turn. Also it is required that the solution be regular throughout the pipe.

The series solution of (4.56) that is bounded at $r = 0$ is

$$u = \frac{1}{4} r^2 P' + A_0(X) + \sum_{n=1}^{\infty} \{A_{1n}(X) \cos n\theta + A_{2n}(X) \sin n\theta\} r^n, \quad (4.58)$$

where A_0 , A_{1n} and A_{2n} are functions to be determined. It is clear that, in general, no further analytic progress can be made and that numerical techniques are now necessary. However, (4.58) does imply that $u = U_0(r)$, where $r_w = 1$, and hence that there is no upstream influence, as expected.

If ε is small the flow takes the form of a viscous $O(\varepsilon)$ perturbation to the Poiseuille flow, for which a solution can be found.

The radial velocities are both of $O(\epsilon\mu R^{-1})$, and the axial velocity and the pressure are given by

$$\left. \begin{aligned} u &= U_0(r) + \epsilon U_1(r, \theta, X) + O(\epsilon^2), \\ P &= -X + \epsilon P_1(X) + O(\epsilon^2) \end{aligned} \right\} \quad (4.59)$$

The governing equation for (U_1, P_1) is (4.56). From (4.57), the boundary conditions are

$$\left. \begin{aligned} U_1 &= -\frac{1}{2} S(-X) f(\epsilon) \text{ at } r = 1, \\ \int_0^{2\pi} d\theta \int_0^1 U_1(r, \theta, X) r dr &= 0, \\ U_1 &= 0 \text{ as } X \rightarrow -\infty. \end{aligned} \right\} \quad (4.60)$$

The solution of this problem is

$$\left. \begin{aligned} U_1 &= \frac{1}{2} S(-X) \left\{ a_0 (1 - 2r^2) - \right. \\ &\quad \left. - \sum_{n=1}^{\infty} (a_{1n} \cos n\theta + a_{2n} \sin n\theta) r^n \right\}, \\ P_1 &= -4 a_0 \int_0^X S(-t) dt, \end{aligned} \right\} \quad (4.61)$$

where a_0 , a_{1n} and a_{2n} are the coefficients of (4.23), the Fourier expansion of $f(\theta)$. As expected, $a_0 = 0$ implies that $P_1 = 0$. Far downstream where $1 - S \ll 1$, U_1 is independent of X to leading order, and $P_1 \sim -4 a_0 X$ as $X \rightarrow \infty$. In the limit solution referred to in Section 4.4 above, for the problem with $\epsilon\mu^{2/3} = O(1)$ and $\epsilon \ll 1$.

Section 5. Comparison with experimental results

Perhaps the most notable feature of the results presented above is the consistent and unexplained failure to find a complete range of solutions for the tubes studied. In particular, we could not find a complete solution for any tube with $q\epsilon\mu^{1/2} \gg 1$ and tube law given by (1.6) with (1.4) or (4.3).

In Section 1.3 we discussed the phenomenon of "self-excited oscillations" in collapsible tubes, and the possibility of these oscillations being initiated when the mean fluid velocity matches the phase velocity. With respect to our formulation, it was proposed by Brower and Scholten (1975) that

(i) for any given tube there is a critical value of μ , μ_c say, such that the fluid-tube system will spontaneously destabilize for $\mu \geq \mu_c$.

(ii) μ_c is the minimum value of μ for which the mean fluid velocity can match the phase velocity at any stage of the collapse. Here the mean is taken over a cross-section.

We wish now to examine our results with respect to (i) and (ii) above. First, we note that the quasi-steady analysis of Oates (1975) suggests that a necessary condition for the mechanical stability of a system with an inviscid fluid with constant velocity and pressure is that the fluid velocity u be less than the phase velocity c , where c is given by (1.8). In Appendix 6 we find that for this system a small disturbance will propagate both upstream and downstream if $u < c$, but downstream only if $u > c$. Thus the ability of the system to disperse the energy of a small disturbance will be considerably restricted if $u > c$, a factor which could possibly be significant in destabilizing the system. Of course, the applicability of these results to more realistic fluid-tube systems is by no means certain.

It is shown in Appendix 6 that a one-dimensional inviscid flow can exist in a collapsing tube with tube law $A = A(p)$ only if A has the form

$$A(p) = (k - 2p/Q^2)^{-1/2}, \quad (5.1)$$

where A is the cross-sectional area of the tube, $k = 1/A^2$ ($p = 0$) and $Q = Au$ is the constant mass flow rate. Further, for such a flow the fluid velocity must match the phase velocity c given by (1.8). Consider now the channel studied in Section 3.3 with $\epsilon = 1$ and $S(\mu p)$ given by (1.6) with $q = 1/2$. The asymptotic solution found for this problem for $-\mu p \gg 1$ is valid for $\mu < 18$ only. No solution was found for $-\mu p$ of $O(1)$ or greater with $\mu \geq 18$. As $\mu \rightarrow 18^-$ and $p \rightarrow -\infty$ the leading order term of the asymptotic solution takes the form of an inviscid uniform core flow with the viscous effects restricted to thin layers adjacent to the walls. To leading order (5.1) and the tube law (3.3) will match for $-p \gg 1$ if $\mu = 18$, $q = 1/2$ and $\epsilon = 1$. With the results from Appendix 6 this implies that the inviscid core velocity obtained for $0 < 18 - \mu \ll 1$ must be equal to the phase velocity c . It is easily shown from (1.8), (3.18) and (3.26) that this is true. Moreover, it can be shown that the mean fluid velocity $\bar{u} = Q/2y_w$ will be less than c throughout the collapse if and only if $\mu < 18$. Thus our results for this problem are consistent with (i) and (ii) in that a complete steady solution was found for $\mu < 18$ but not for $\mu \geq 18$, and that $\mu = 18$ is the minimum value of μ for which \bar{u} can equal c at any stage of the collapse, albeit in the limit as $p \rightarrow -\infty$. It is stressed that we have not proved that a complete steady solution does not exist for $\mu \geq 18$, nor that (i) and (ii) are valid. However, the above does suggest that (i) and (ii) are valid for this problem, and that the addition of a time dependence and/or a stability analysis of the solution may be a profitable extension to the present theory.

In general, the results given in this study for channels obeying (1.4) and (1.6) are consistent with (i) in the sense that for any particular channel, i.e. values of q and ϵ , there is a $\tilde{\mu}_c$ such that for $\mu \geq \tilde{\mu}_c$ the analytic approach does not provide a complete solution and the numerical process fails to converge at some stage of the collapse.

As noted in Section 1.3, we do not have an expression for the phase velocity when the flow is viscous and the phase and mean fluid velocities are of the same order. This prevents any general comparison between proposal (ii) and our results. However, Brower and Scholten (1975) suggest that the inviscid phase velocity given by (1.8)

can be used to predict the onset of instabilities in the system, that is, that μ_c is the minimum value of μ for which $\bar{u} = c$. For a channel with $\varepsilon = 1$ and $q < 1/2$ we find that $\bar{u} < c$ throughout the collapse if and only if $\mu < \hat{\mu}_c$ where

$$\hat{\mu}_c = \frac{9}{q} 2^{1-q} (1-q)^{1-q} (1-2q)^{q-1/2}. \quad (5.2)$$

Values of $\hat{\mu}_c$ and $\bar{\mu}_c$ (an approximate upper limit on μ for the convergence of the numerical process applied to equations 3.1 - 3.3 with $\varepsilon = 1$) are given in table 3.1. For small q we see that $\bar{\mu}_c - \hat{\mu}_c$ is large, and that while $\hat{\mu}_c \propto q^{-1}$ it appears that $\bar{\mu}_c q^2 = 0(1)$. Clearly, for this problem $\bar{u}/c < 1$ is not a necessary condition for the existence of a steady solution. Although the existence of a steady solution does not imply that the system is stable for $\hat{\mu}_c < \mu < \bar{\mu}_c$, this result suggests that the condition of the mean fluid velocity \bar{u} matching the inviscid phase velocity c may not accurately predict the onset of oscillations in a fluid-tube system if the flow is viscous.

For a channel with $\varepsilon = 1$ and $q > 1/2$, \bar{u}/c will eventually exceed one regardless of the value of μ . In fact, $\bar{u}/c \rightarrow \infty$ as $p \rightarrow -\infty$. If c simply provides an estimate of the phase velocity accurate to order of magnitude, then statements (i) and (ii) would suggest that a complete steady solution would not exist for any channel with $\varepsilon = 1$ and $q > 1/2$. Our results are consistent with this, i.e. a complete solution has not been found for $\mu \gg 1$, $\mu = 0(1)$ or $\mu \ll 1$ (Sections 3.4, 3.3 and 3.5 respectively) for this problem.

The analytical results for axisymmetric pipe-fluid systems (Section 4.2) are consistent with (i) and (ii) in a manner similar to channel-fluid systems as discussed above. In particular, with $-\mu p \gg 1$ and $A \propto (-\mu p)^{-1/2}$ to leading order, the asymptotic flow structure suggested by mass conservation can have a valid solution only if $\mu < 128$, and for $0 < 128 - \mu \ll 1$ this structure must have an essentially inviscid uniform core velocity for the fluid, with the major viscous effects restricted to thin layers. It is easily shown that the tube law for this problem is consistent with (5.1) if $\mu = 128$ and $-\mu p \gg 1$, and that the inviscid core velocity for $0 < 128 - \mu \ll 1$ will match with the inviscid phase velocity in the limit as $p \rightarrow -\infty$.

For nonsymmetric pipe-fluid systems numerical work is necessary before any general comparison with (i) and (ii) can be made. However, we note that if $q\epsilon\mu^{1/2} \gg 1$ and the collapse is a stretching collapse with $0 < |f(\theta) - a_0| \ll 1$, then the leading order problem is simply the analogous axisymmetric problem, for which no satisfactory solution has been found (Section 4.4).

In conclusion, we have found a general consistency between our results and statement (i) above, and also that the ratio of mean fluid velocity to phase velocity is an important parameter for at least some of our tube-fluid systems (c.f. one-dimensional flows, see Section 1.3). The larger question of the validity of (i) and (ii) requires an expression for the phase velocity for viscous flows with the phase and fluid velocities of the same order (which we do not have), the inclusion of time dependence in the analysis, and/or a rigorous analysis of the stability of the system under consideration, all of which are beyond the scope of the present study.

Appendix 1

Consider a channel with tube law

$$y_w = (1 + \mu^2 p^2)^{-1/4} \quad p < 0, \quad (\text{A1.1})$$

and the incoming flow such that the pressure response is moderate. This fluid-channel system was studied in Section 3.3, where it was shown that $p \rightarrow -\infty$ and $y_w \rightarrow 0$ as $R^{-1}x = X \rightarrow X_0^-$, for some finite X_0 . A self-similar flow structure was investigated for $0 < X_0 - X \ll 1$. A solution for this structure was found for $\mu < 18$ only. As $\mu \rightarrow 18^-$ this solution approaches a limit form (equations 3.18, 3.26 and 3.27), which has an essentially inviscid uniform core flow with the major viscous effects restricted to thin layers adjacent to the walls. No solution, either analytical or numerical, was found for $-\mu p \gg 1$ and $\mu \geq 18$. Here we will try to construct an alternative essentially inviscid asymptotic flow structure.

If the core flow is essentially inviscid and uniform with leading order velocity $\bar{u} = \bar{u}(X)$, then the balance between the inertial force and the pressure gradient in the fluid implies that $\bar{u} \sim (-2p)^{1/2}$ as $p \rightarrow -\infty$. To leading order the mass flow is given by $2\bar{u}y_w$, and thus by $2(2/\mu)^{1/2}$ as $p \rightarrow -\infty$. Conservation of mass requires that the mass flow is $2/3$, and hence that $\mu = 18$ to leading order. Thus, the asymptotic flow structures we consider below cannot exist unless $|18 - \mu| \ll 1$. Note that $\mu = 18$ is consistent with the results of Appendix 6, in particular with (A6.5).

Assume that $0 < \tilde{X} \ll 1$, where $\tilde{X} = X_0 - X$. We expand the pressure in the form

$$p = -p_0 \tilde{X}^{-2n} - p_1 \tilde{X}^{-\ell} + o(\tilde{X}^{-\ell}), \quad (\text{A1.2})$$

where $p_0 > 0$ and p_1 are constants, $n > 0$ and $\ell < 2n$. If it is assumed that the wall layers have thickness $\propto \tilde{X}^m$, where $m > n$, then the necessary balance of forces in the viscous layers requires that

$$n = 2m - 1, \quad (\text{A1.3})$$

which implies that

$$\frac{1}{2} < m < 1 \quad (\text{A1.4})$$

since $m > n > 0$. Let

$$y = \gamma \tilde{X}^n - z \tilde{X}^m, \quad (\text{A1.5})$$

where $\gamma = (\mu p_0)^{-1/2}$. Substitution of (A1.2) into (A1.1) produces

$$y_w = \gamma \tilde{X}^n - \frac{1}{2} \gamma \frac{P_1}{P_0} \tilde{X}^{-\ell+2n} - \frac{1}{4} \gamma (\mu p_0)^{-2} \tilde{X}^{5n} + \dots,$$

which with (A1.3) - (A1.5) implies that

$$\frac{5}{9} \leq m < 1 \quad (\text{A1.6})$$

$$\ell = 3n - m, \quad (\text{A1.7})$$

and that the position of the upper wall is given by $z = z_w$, where

$$z_w = \frac{1}{2} \gamma \frac{P_1}{P_0} \quad (\text{A1.8})$$

if $5/9 < m < 1$, and

$$z_w = \frac{1}{2} \gamma \left[\frac{P_1}{P_0} + \frac{1}{2} (\mu p_0)^{-2} \right] \quad (\text{A1.9})$$

if $m = 5/9$.

At the upper wall, where $z - z_w$ is $O(1)$, the stream function ψ can be expanded as

$$\psi = \frac{1}{3} - \tilde{X}^{m-n} (2p_0)^{1/2} \alpha F(y) + o(\tilde{X}^{m-n}), \quad (\text{A1.10})$$

where $y = \alpha^{-1}(z - z_w)$ and $\alpha = (m - n)^{-1/2} (2p_0)^{-1/4}$. The controlling equation for $F(y)$ is the Falkner-Skan equation

$$F'''' - FF'' + \beta(1 - F'^2) = 0, \quad (\text{A1.11})$$

where $\beta = n/(m-n) > 0$. The boundary conditions are

$$F(0) = F'(0) = 0, \tag{A1.12}$$

$$F'(\infty) = 1.$$

From Jones and Watson (1963), a solution for $F(Y)$ exists for all $\beta > 0$ and there is a unique solution such that

$$0 < F' < 1 \tag{A1.13}$$

for $0 < Y < \infty$. It seems desirable on physical grounds to require that (A1.13) be satisfied. The condition $F'(\infty) = 1$ implies that

$$F(Y) = Y + d + q(Y) \text{ as } Y \rightarrow \infty, \tag{A1.14}$$

where d is a constant and $|q(Y)| \ll Y$. Hence, when Y is large (A1.11) approximates to

$$q'' - (Y + d)q' - 2\beta q = 0.$$

From Jones and Watson (1963)

$$q'(Y) \sim A(Y + d)^{-2\beta} \text{ as } Y \rightarrow \infty,$$

where A is a constant which must be non-zero if the boundary condition at infinity is to be satisfied smoothly. Hence

$$q'(Y) \sim AY^{-2\beta} \text{ as } Y \rightarrow \infty,$$

or more precisely as $Y/d \rightarrow \infty$, which suggests that for large Y we consider a power series for $F(Y)$ such that

$$1 - F'(Y) \sim AY^{-2\beta} \text{ as } Y \rightarrow \infty, \tag{A1.15}$$

where A is a non-zero constant.

We will now investigate whether the core and boundary layer flows can be matched successfully for any value of m . First, let us assume that

$$\frac{3}{5} < m < 1.$$

This implies that $1/2 < \beta < \infty$. It follows from (A1.15) that

$$F(Y) \sim Y + D \quad \text{as } Y \rightarrow \infty,$$

where

$$D = \int_0^{\infty} [1 - F'(Y)] dY$$

gives the boundary layer thickness. Hence

$$\psi \sim \frac{1}{3} - \tilde{X}^{m-n} (2p_0)^{1/2} \{z - z_w + \alpha D\} \quad (\text{A1.16})$$

as $z \rightarrow \infty$. Let

$$\psi = (2p_0)^{1/2} \{t + \tilde{X}^{m-n} f_1(t) + o(\tilde{X}^{m-n})\} \quad (\text{A1.17})$$

in the core, where $t = y\tilde{X}^{-n}$. It is easily shown that

$$f_1(t) = \frac{1}{2} \frac{p_1}{p_0} t + k,$$

where k is a constant to be determined. From (A1.5)

$$t = \gamma - z\tilde{X}^{m-n}, \quad (\text{A1.18})$$

which leads to $k = -\alpha D$ if (A1.16) and (A1.17) are to be consistent at the edge of the upper wall layer. However, if (A1.13) is satisfied then the solution for $F(Y)$ is unique, and it follows that the matching of (A1.17) to the flow in the lower viscous layer requires $k = \alpha D$. Also, (A1.13) implies $D > 0$, and hence there is no solution of the problem with $3/4 < m < 1$ such that (A1.13) is satisfied in both the upper and the lower wall layers.

Assume now that

$$m = 3/5,$$

and hence that $\beta = 1/2$. From (A1.15)

$$F(Y) \sim Y + A \ln Y \quad \text{as } Y \rightarrow \infty, \quad (\text{A1.19})$$

which with (A1.10) gives

$$\psi \sim \frac{1}{3} - \tilde{X}^{2/5} (2p_0)^{1/2} \{z - z_w + \alpha A \ln z\} \quad (\text{A1.20})$$

as $z \rightarrow \infty$. Substitution of z from (A1.18) in (A1.20) suggests that in the core

$$\psi = (2p_0)^{1/2} \{t + \tilde{X}^{2/5} (\ln \tilde{X}) f_1(t) + \tilde{X}^{2/5} f_2(t) + o(\tilde{X}^{2/5})\},$$

the solution for which is found to be

$$f_1(t) = k, \quad f_2(t) \text{ arbitrary,}$$

where k is a constant. It follows that for $m = 3/5$ there is no solution that has A non-zero and satisfies (A1.13) in both the upper and lower wall layers (c.f. $3/5 < m < 1$ above).

Suppose now that

$$5/9 < m < 3/5,$$

that is, $1/4 < \beta < 1/2$. Expanding $F(Y)$ in a power series for large Y yields

$$F(Y) \sim Y + c_1 Y^{1-2\beta} + d_1 + c_2 Y^{1-4\beta} + d_2 Y^{-4\beta} \text{ as } Y \rightarrow \infty, \quad (\text{A1.21})$$

where c_1 and d_1 are independent constants,

$$c_2 = -\frac{1}{2} c_1^2 \frac{(1-2\beta)(1+2\beta)}{1-4\beta}, \quad (\text{A1.22})$$

and $d_2 = (1-2\beta) d_1 c_1$.

From (A1.10) and (A1.21)

$$\psi \sim \frac{1}{3} - \tilde{X}^{m-n} (2p_0)^{1/2} \{ z - z_w + c_1 \alpha^{2\beta} z^{1-2\beta} + \alpha d_1 + c_2 \alpha^{4\beta} z^{1-4\beta} + \alpha^{2\beta} [\alpha d_2 - (1-2\beta) c_1 z_w] z^{-2\beta} \} \quad (A1.23)$$

as $z \rightarrow \infty$. Substitution of z from (A1.18) in (A1.23) suggests that

$$\psi = (2p_0)^{1/2} \{ t + \tilde{X}^{2n} f_0(t) + \tilde{X}^{m-n} f_1(t) + \tilde{X}^{4n} f_2(t) + \tilde{X}^{m+n} f_3(t) + o(\tilde{X}^{m+n}) \} \quad (A1.24)$$

in the core. From the governing equations it can be shown that $f_0(t)$ is arbitrary,

$$f_1(t) = \frac{1}{2} (p_1/p_0) t + k, \quad (A1.25)$$

where k is a constant,

$$f_2' = f_0 f_0'' - \frac{1}{2} f_0'^2, \quad (A1.26)$$

and with (A1.25) that

$$f_3' = \frac{1}{2} (p_1/p_0) \{ t f_0'' - f_0' \} + k f_0''. \quad (A1.27)$$

If the solution applies in both the upper and lower wall layers, then $k = d_1 = 0$ (c.f. $3/5 < m < 1$ above) and hence $d_2 = 0$. Matching (A1.23) and (A1.24) requires that

$$f_0(t) \sim -c_1 \alpha^{2\beta} (\gamma - t)^{1-2\beta} \quad (A1.28)$$

as $t \rightarrow \gamma^-$. Equations (A1.22) and (A1.26) - (A1.28) imply that

$$f_2(t) \sim -c_2 \alpha^{4\beta} z^{1-4\beta} \tilde{X}^{m-5n}$$

$$f_3(t) \sim c_1 \alpha^{2\beta} (1-2\beta) z_w z^{-2\beta} \tilde{X}^{-2n},$$

as $t \rightarrow \gamma^-$. Therefore, if $d_1 = 0$ and $f_0(t)$ is any function satisfying

(A1.28) then to the order investigated the core and upper wall layer flows are consistent. Similarly, it can be shown that if

$$f_0(t) \sim c_1 \alpha^{2\beta} (\gamma + t)^{1-2\beta}$$

as $t + \gamma \rightarrow 0+$, then the core and lower wall layer flows are consistent.

Thus, if the unique solution for $F(Y)$ satisfying (A1.12) and (A1.13) has $d_1 = 0$ for any β in the range $1/4 < \beta < 1/2$, then a solution to the problem may exist for that value of β . Unfortunately, it is not known if $d_1 = 0$ for any such β .

Finally, let us assume that

$$m = 5/9,$$

which gives $\beta = 1/4$. The power series for large Y has the form

$$F(Y) \sim Y + c_1 Y^{1/2} - \frac{3}{8} c_1^2 \ln Y \quad \text{as } Y \rightarrow \infty,$$

where $c_1 = 2A$. Hence

$$\begin{aligned} \psi \sim \frac{1}{3} - \tilde{X}^{4/9} (2p_0)^{1/2} \{ z - z_w + c_1 \alpha^{1/2} z^{1/2} - \\ - \frac{3}{8} c_1^2 \alpha \ln z + \frac{3}{8} c_1^2 \alpha \ln \alpha \} \end{aligned} \quad (\text{A1.29})$$

as $z \rightarrow \infty$. If in the core

$$\begin{aligned} \psi = (2p_0)^{1/2} \{ t + \tilde{X}^{2/9} f_0(t) + \tilde{X}^{4/9} (\ln \tilde{X}) f_1(t) + \\ + \tilde{X}^{4/9} f_2(t) + o(\tilde{X}^{4/9}) \}, \end{aligned} \quad (\text{A1.30})$$

where $t = y\tilde{X}^{-1/9}$, then $f_0(t)$ is arbitrary,

$$f_1(t) = k$$

where k is a constant, and

$$f_2'(t) = \frac{1}{2} \frac{p_1}{p_0} + f_0 f_0'' - \frac{1}{2} f_0'^2.$$

Consistency between (A1.29) and (A1.30) requires that

$$f_0(t) \sim c_1 \alpha^{1/2} (\gamma - t)^{1/2}$$

as $t \rightarrow \infty$, which implies that

$$f_2(t) \sim \frac{1}{2} \frac{p_1}{p_0} t + \frac{3}{8} c_1^2 \alpha \ln(\gamma - t) + k_1$$

as $t \rightarrow \infty$, where k_1 is a constant. Thus, the matching of the core and upper wall layer flows requires $k_1 = -\frac{3}{8} c_1^2 \alpha \ln \alpha$ and $k = -\frac{1}{6} \alpha c_1^2$. However, if the flow in the lower wall layer is identical to that in the upper wall, then the matching to the core flow will require $k = \frac{1}{6} \alpha c_1^2$. It follows that there is no solution to the problem with $m = 5/9$ such that (A1.13) is satisfied in both the wall layers.

In summary, it appears that no satisfactory flow structure of the type considered here can exist unless $5/9 < m < 3/5$. Further, it is not known whether a solution exists for the problem even with $5/9 < m < 3/5$.

Appendix 2

The non-linear boundary layer problem posed by

$$\left. \begin{aligned} U \frac{\partial U}{\partial X} + V \frac{\partial U}{\partial Y} &= -P'(X) + \frac{\partial^2 U}{\partial Y^2}, \\ \frac{\partial U}{\partial X} + \frac{\partial V}{\partial Y} &= 0, \end{aligned} \right\} \quad (\text{A2.1})$$

and the boundary conditions

$$\left. \begin{aligned} U = V = 0 \text{ at } Y = 0, \\ U \sim Y + \frac{1}{2} q P^2 \text{ as } Y \rightarrow \infty, \end{aligned} \right\} \quad (\text{A2.2})$$

arose in the study of a channel with a complete collapse and a fast pressure response (equations (3.57) and (3.58), Section 3.4). We will now consider the behaviour of the flow far upstream. In particular, we wish to show that the solution for $-X \ll 1$ is consistent with the incoming flow; that is, with (3.53). If it is assumed that for $-X \gg 1$ P can be expanded as

$$P = -P_0(-X)^n - P_1(-X)^m + \dots, \quad (\text{A2.3})$$

where P_0, P_1 etc. are constants, then the necessary balance of terms in (A2.1) and (A2.2) implies that $n = -1/3$, $m = -4/3$ and that the stream function ψ will have the form

$$\begin{aligned} \psi &= \frac{1}{2}(-X)^{2/3} \eta^2 + (-X)^{-1/3} F_0(\eta) + \\ &+ (-X)^{-4/3} F_1(\eta) + \dots \end{aligned} \quad (\text{A2.4})$$

where $\eta = Y(-X)^{-1/3}$. Substitution of (A2.3) and (A2.4) into (A2.1) and (A2.2) yields the governing equations

$$F_0'''' - \frac{1}{3} \eta^2 F_0'' - \frac{1}{3} \eta F_0' + \frac{1}{3} F_0 = -\frac{1}{3} P_0, \quad (\text{A2.5a})$$

$$\begin{aligned} F_1'''' - \frac{1}{3} \eta^2 F_1'' - \frac{4}{3} \eta F_1' + \frac{4}{3} F_1 = \\ -\frac{4}{3} P_1 + \frac{2}{3} (F_0')^2 - \frac{1}{3} F_0 F_0'', \end{aligned} \quad (\text{A2.5b})$$

and the boundary conditions

$$\left. \begin{aligned} F_0(0) = F_0'(0) = 0, \\ F_0' \rightarrow \frac{1}{2} q P_0^2 \text{ as } \eta \rightarrow \infty, \end{aligned} \right\} \quad (\text{A2.6a})$$

$$\left. \begin{aligned} F_1(0) = F_1'(0) = 0, \\ F_1' \rightarrow q P_0 P_1 \text{ as } \eta \rightarrow \infty. \end{aligned} \right\} \quad (\text{A2.6b})$$

If we write

$$F_0(\eta) = f_0(\eta) + \frac{1}{2} q P_0^2 \eta, \quad (\text{A2.7})$$

then $f_0(\eta)$ must also satisfy (A2.5a). The boundary conditions (A2.6a) become

$$\left. \begin{aligned} f_0(0) = 0, \\ f_0'(0) = -\frac{1}{2} q P_0^2, \\ f_0(\infty) = 0. \end{aligned} \right\} \quad (\text{A2.8})$$

This problem for $f_0(\eta)$ is identical to that for the leading order term of (3.53); that is, with the problem posed by (3.55) and (3.56). Therefore, the upstream matching will be satisfied by (A2.3) and (A2.4).

Unfortunately, we could not find a solution for $F_1(\eta)$. However, we note that the boundary conditions (A2.6a) and (A2.6b) are consistent with the governing equation (A2.5b), which indicates that a solution for $F_1(\eta)$ may exist.

Appendix 3

Consider a channel with the tube law

$$y_w = \begin{cases} 1 & p \geq 0, \\ \left(1 - \frac{\mu^2}{qR} \int_0^x p(t) dt\right)^{-q} & p < 0 \end{cases} \quad (\text{A3.1})$$

where $1 \ll \mu^2 \ll R$ and $p = 0$ at $x = 0$. The channel described by (A3.1) is one for which, at a given point where $p < 0$, it is the total force from the pressure on the channel walls between the origin and that point, rather than the local pressure, which determines the position of the walls. The inclusion of the Reynolds number in (A3.1) ensures that the initial response of the flow and the channel is similar to that found in Section 3.4 when (3.3) with (3.39) was used, i.e. in both cases linear viscous wall layers, with thickness $O(\mu^{-3/2}R)$, form immediately downstream of the origin. However, with (A3.1) there is not a singularity in the pressure in this initial stage, and the change to a nonlinear boundary layer structure is smooth and does not entail a change of scale for x or $1 - y$. Again, the restriction on μ ensures that the pressure is independent of y .

Clearly, the transform technique given in Section 2.1 can be applied here when the boundary layer has a linear flow structure. We omit the details and proceed directly to the nonlinear boundary layer problem that arises at the upper wall. The stream function and pressure can be written as

$$\left. \begin{aligned} \psi &= \frac{1}{3} - \delta^2 \Psi(X, Y), \\ p &= \delta^2 P(X), \end{aligned} \right\} \quad (\text{A3.2})$$

where $x = \delta^3 RX$, $y = 1 - \delta Y$, $\delta = \mu^{-1/2}$, and $\psi = 1/3$ at the upper wall. To leading order the tube law becomes

$$Y_w = - \int_0^X P(t) dt. \quad (\text{A3.3})$$

If the Prandtl transformation $Y = z + Y_w$ is applied then $(U, V) =$

$= (\partial\Psi/\partial z, \partial\Psi/\partial X)$ and P must satisfy the nonlinear boundary layer equations and the boundary conditions

$$\left. \begin{aligned} U = V = 0 \text{ at } z = 0, \\ P = 0 \text{ and } U = z \text{ at } X = 0, \\ u \rightarrow z - \int_0^X P \, dt \text{ as } z \rightarrow \infty \text{ for } X > 0. \end{aligned} \right\} \quad (\text{A3.4})$$

This nonlinear boundary layer problem is essentially the problem for the lower deck of a triple deck structure (see Stewartson and Williams 1969, 1973; Stewartson 1970). The solution applicable here is the one given by Stewartson (1970) which has the pressure falling downstream and the flow remaining attached to the wall. This solution has a singularity at a finite value of X , X_0 say, but is felt to be stable about a basic unique form. If $X_0 - X \ll 1$ then $P \propto (X_0 - X)^{-2}$, $U \propto (X_0 - X)^{-1}$ and the boundary layer thickness is proportional to $X_0 - X$. An interesting point is that this solution was obtained by Stewartson (1970) for the boundary layer flow near a convex corner where there is an inviscid external mainstream, whereas here it applies to a boundary layer flow round a concave corner where the mainstream is viscous and contained. When $X_0 - X = 0(\delta)$ the pressure, velocity in the boundary layer, and $1 - y_w$ are all of $0(1)$. Thus the problem must be reformulated in the region of the singularity on an $0(\delta^4 R)$ streamwise length scale.

When the tube law is given by (A3.3) the core flow takes the familiar form of an inviscid rotational perturbation to the Poiseuille flow which responds passively to changes in the boundary layer (see, for example, Sections 2.1 and 3.4). If in the core

$$u = U_0(y) + \delta^2 U_1(X, y) + o(\delta^2),$$

then $U_1 \propto P$. It follows that $u - U_0(y)$ becomes $0(1)$ when $X_0 - X = 0(\delta)$; that is, when the walls have moved a finite distance into the channel. Thus the proposed boundary layer and core flows are consistent with the behaviour of the tube law (A3.1), unlike those proposed for a channel obeying (3.3) (see Section 3.4).

We will now consider the flow in the region of the singularity. In this region the core flow is basically inviscid, with the major viscous effects occurring adjacent to the channel walls in boundary layers of thickness $O(\delta^2)$. If $x = \delta^4 R \bar{X} + \delta^3 R X_0$ and $v = \delta^{-4} R^{-1} \bar{V}(\bar{X}, y)$ then $(u, \bar{V}, p(\bar{X}))$ must satisfy the continuity equation and inviscid streamwise momentum equation. Following Cole and Aroesty (1968), the solution to the core problem downstream of a given point $\bar{X} = \bar{X}^*$ is

$$y = \int_0^\psi \{u^{*2}(t) + 2(p^* - p(\bar{X}))\}^{-1/2} dt, \quad (\text{A3.5})$$

where $u^*(t) = u(\bar{X}^*, t)$, $p^* = p(\bar{X}^*)$, and the stream-function is taken to be zero at $y = 0$. The tube law (A3.1) becomes

$$y_w = (1 - q^{-1} \int_{-\infty}^{\bar{X}} p(t) dt)^{-q}, \quad (\text{A3.6})$$

where strictly the integration is from $x = 0$ to \bar{X} . As $y = y_w$ when $\psi = 1/3$ the pressure downstream of \bar{X}^* can theoretically be found from (A3.5) and (A3.6). Thus, we see that once the walls have moved a finite distance into the channel it is the core flow, not the boundary layer flow, that determines the pressure to leading order. Further, in this region the boundary layer flow must adjust to match with the core flow, instead of the core flow responding to changes in the boundary layer, as occurs upstream of the singularity.

Equations (A3.5) and (A3.6) imply that if $q < 1/2$ then to leading order $p \propto \bar{X}^n$ as $\bar{X} \rightarrow \infty$, where $n = 2q/(1-2q)$. If $q > 1/2$ then $p \propto (\bar{X}_0 - \bar{X})^n$ as $\bar{X} \rightarrow \bar{X}_0^-$, where \bar{X}_0 is finite. If $q = 1/2$ then $p \rightarrow -\infty$ exponentially in \bar{X} . Thus, the value of q determines whether there is a singularity in the solution as $y_w \rightarrow 0$, with a collapse to a finite value of \bar{X} , or whether the collapse extends indefinitely far upstream. In this respect the flow structure is similar to that given in Section 3.3 for a channel with a moderate pressure response and (3.3) as tube law. A formal asymptotic flow structure can now be constructed for $-p \gg 1$. This would consist of an essentially inviscid uniform mainstream, with boundary layers of thickness $O(\delta^2)$ adjacent to the walls (c.f. Appendix 1).

Appendix 4

Consider the three-dimensional boundary layer problem formed by the equations

$$\begin{aligned}
 U \frac{\partial U}{\partial X} + V \frac{\partial U}{\partial Y} + W \frac{\partial U}{\partial \theta} &= -P'(X) + \frac{\partial^2 U}{\partial Y^2}, \\
 U \frac{\partial^2 W}{\partial X \partial Y} + V \frac{\partial^2 W}{\partial Y^2} + W \frac{\partial^2 W}{\partial \theta \partial Y} \\
 - \frac{\partial U}{\partial X} \frac{\partial W}{\partial Y} + \frac{\partial U}{\partial Y} \frac{\partial W}{\partial X} &= \frac{\partial^3 W}{\partial Y^3}, \\
 \frac{\partial U}{\partial X} + \frac{\partial V}{\partial Y} + \frac{\partial W}{\partial \theta} &= 0,
 \end{aligned}
 \tag{A4.1}$$

and the boundary conditions

$$\begin{aligned}
 U = V = W = 0 \text{ at } Y = 0, \\
 U \sim \frac{1}{2} \left\{ Y + \frac{1}{2} q P^2 f(\theta) \right\} \text{ as } Y \rightarrow \infty, \\
 U \rightarrow \frac{1}{2} Y, \quad P \rightarrow 0 \text{ as } X \rightarrow -\infty.
 \end{aligned}
 \tag{A4.2}$$

The problem defined by (A4.1) and (A4.2) arose in the study of a nonsymmetric pipe with a fast pressure response (Section 4.4). Here we investigate possible asymptotic flow structures for $-P \gg 1$. Suppose that $P \propto X^n$ as $X \rightarrow \infty$, where $n > 0$. The necessary balance of terms in the governing equations (A4.1) requires $n \geq 1/6$, and suggests the self-similar flow structure

$$\begin{aligned}
 U &= X^{2n} F(\eta, \theta) + o(X^{2n}), \\
 V &= X^{\frac{2n-1}{n}} G(\eta, \theta) + o(X^{(2n-1)/2}), \\
 W &= X^{2n-1} H(\eta, \theta) + o(X^{2n-1}), \\
 P &= P_0 X^n + o(X^n),
 \end{aligned}
 \tag{A4.3}$$

where $\eta = YX^{(2n-1)/2}$. Substituting (A4.3) into (A4.1) produces the

governing equations

$$\begin{aligned}
 2nF^2 + \frac{2n-1}{2} \eta F \frac{\partial F}{\partial \eta} + G \frac{\partial F}{\partial \eta} + H \frac{\partial F}{\partial \theta} &= \frac{\partial^2 F}{\partial \eta^2}, \\
 F \frac{\partial}{\partial \eta} \left[(2n-1)H + \frac{2n-1}{2} \eta \frac{\partial H}{\partial \eta} \right] + G \frac{\partial^2 H}{\partial \eta^2} + H \frac{\partial^2 H}{\partial \theta \partial \eta} - \\
 - 2nF \frac{\partial H}{\partial \eta} + (2n-1) H \frac{\partial F}{\partial \eta} &= \frac{\partial^3 H}{\partial \eta^3}, \\
 2nF + \frac{2n-1}{2} \eta \frac{\partial F}{\partial \eta} + \frac{\partial G}{\partial \eta} + \frac{\partial H}{\partial \theta} &= 0.
 \end{aligned}
 \tag{A4.4}$$

These equations are in turn the momentum, vorticity, and continuity equations. If $n > 1/6$ the boundary conditions (A4.5) become

$$\begin{aligned}
 F = G = H = 0 \text{ at } \eta = 0 \\
 F \rightarrow \frac{1}{4} q P_0^2 f(\theta) \text{ as } \eta \rightarrow \infty
 \end{aligned}
 \tag{A4.5}$$

With (A4.5), the momentum and continuity equations of (A4.4) imply that

$$H \rightarrow -\frac{n}{2} q P_0^2 \frac{f(\theta)}{f'(\theta)} \text{ as } \eta \rightarrow \infty.
 \tag{A4.6}$$

Clearly, there must be at least one value of θ such that $f'(\theta) = 0$ but $f(\theta) \neq 0$. Thus, (A4.6) implies that a solution of (A4.4) and (A4.5) cannot be bounded for all θ as $\eta \rightarrow \infty$.

In a manner similar to the above, it can be shown that there is no bounded solution for the asymptotic structure implied by $p \propto (X_0 - X)^{-n}$, where $n > 0$, X_0 is finite, and $X < X_0$.

Suppose now that $n = 1/6$. The boundary conditions (A4.2) become

$$\begin{aligned}
 F = G = H = 0 \text{ at } \eta = 0, \\
 F \sim \frac{1}{2} \left\{ \eta + \frac{1}{2} q P_0^2 f(\theta) \right\} \text{ as } \eta \rightarrow \infty.
 \end{aligned}
 \tag{A4.7}$$

Consider the expansions

$$\begin{aligned}
 F &= \frac{1}{2} \eta + \frac{1}{4} q P_o^2 f(\theta) + \eta^{-1} F_{-1}(\theta) + \dots, \\
 G &= \eta G_1(\theta) + G_o(\theta) + \eta^{-1} G_{-1}(\theta) + \dots, \\
 H &= H_o(\theta) + \eta^{-1} H_{-1}(\theta) + \dots,
 \end{aligned}
 \tag{A4.8}$$

where $\eta \gg 1$. Substitution of (A4.8) into (A4.4) yields

$$\begin{aligned}
 G_1(\theta) &= -\frac{1}{12} q P_o^2 f(\theta), \\
 G_o(\theta) &= \frac{1}{24} \{q P_o^2 f(\theta)\}^2, \\
 H_o(\theta) &= 0.
 \end{aligned}
 \tag{A4.9}$$

Thus if $n = 1/6$, the matching condition at the edge of the layer is consistent with the governing equations, and does not imply an infinite azimuthal velocity. Note that this does not imply that a satisfactory solution exists for the problem with $n = 1/6$, merely that one might exist. Although the analogous problem for a channel is similar in this respect, it has been shown that it has no satisfactory solution (see Section 3.4). If

$$|f(\theta) - a_o| \ll 1 \text{ for all } \theta$$

and a_o is $O(1)$, then to leading order the problem posed by (A4.4) and (A4.5) or (A4.7) reduces to a two-dimensional problem. It follows from the results of Section 3.4 that if the collapse is predominantly symmetric, then there is no solution to the similarity problem with $P \propto X^{1/6}$ as $P \rightarrow -\infty$. We were unable to establish the existence or nonexistence of a solution for the asymptotic problem with $n = 1/6$ and a maximum value of $|f(\theta) - a_o|$ of $O(1)$.

In summary, no satisfactory asymptotic flow structure exists such that $P \propto (X_o - X)^{-n}$ or $P \propto X^n$ as $P \rightarrow -\infty$, where $n > 0$, with the possible exception of $P \propto X^{1/6}$ when $|f(\theta) - a_o|$ has a maximum value of $O(1)$.

Appendix 5. Numerical Methods

The boundary layer equations

The method used in the present study to solve the nonlinear boundary layer equations is essentially that found in Smith (1974) and used by Eagles and Smith (1980). Consider first a channel with fixed nonuniform walls that are symmetric about $y = 0$ and have a rate of change with respect to the axial distance x of $O(R^{-1})$, where $R \gg 1$ is the Reynolds number of the flow in the channel. Taking $x = RX$, the equations of motion for the fluid reduce to the nonlinear boundary layer equations (3.1). If we now take $y = Yh(X)$, where $h(X)$ is the half-width of the channel, and write the stream function ψ as

$$\psi = G(X, Y), \quad (\text{A5.1})$$

then the boundary layer equations (3.1) reduce to the following system of three first order equations:

$$\left. \begin{aligned} C(X, Y) &= \frac{\partial G}{\partial Y}, \\ E(X, Y) &= \frac{\partial C}{\partial Y}, \\ \frac{1}{h} \left[C \frac{\partial C}{\partial X} + \frac{h'}{h} C^2 - E \frac{\partial G}{\partial X} \right] &= -\frac{1}{3} p'(X) + \frac{\partial E}{\partial Y}. \end{aligned} \right\} (\text{A5.2})$$

Suppose that there is no significant upstream influence and $h(X) = 1$ for $X \leq 0$. Then

$$\left. \begin{aligned} G(0, Y) &= \frac{1}{2}(Y - \frac{1}{3} Y^3), \\ C(0, Y) &= \frac{1}{2}(1 - Y^2), \\ E(0, Y) &= -Y, \\ p(0) &= 0. \end{aligned} \right\} (\text{A5.3})$$

The boundary conditions are

$$\left. \begin{aligned} G(X, \pm 1) &= \pm \frac{1}{3}, \\ C(X, \pm 1) &= 0, \end{aligned} \right\} \quad (\text{A5.4})$$

from conservation of mass and no slip at the walls respectively. If it is assumed that the flow is symmetric, then (A5.4) can be replaced by

$$\left. \begin{aligned} G(X,0) &= C(X,1) = E(X,0) = 0, \\ G(X,1) &= \frac{1}{3}. \end{aligned} \right\} \quad (\text{A5.5})$$

We adopt the rectangular network $X_i = i\delta X$, $Y_j = j\delta Y$, where $N\delta Y = 1$, $i \geq 0$, $-N \leq j \leq N$ and i, j and N are integers. The values of G , C and E at (X_i, Y_j) will be denoted by G_j^i , C_j^i and E_j^i respectively, and that of $p(X_i)$ by p^i . In the manner of Smith (1974), the three first order equations in (A5.2) can be approximated by three first order difference equations which have second order accuracy. These difference equations are centred on the midpoints $(X_{i-1/2}, Y_{j-1/2})$. Suppose that for a particular i the G_j^{i-1} , etc. are known. For convenience we will write G_j for G_j^i , etc. If $G_j^{(n)}$ is the n -th approximation to G_j , we write the $(n+1)$ th approximation as

$$G_j^{(n+1)} = G_j^{(n)} + \delta G_j^{(n)}, \quad (\text{A5.6})$$

with similar expressions for the other dependent variables. The boundary conditions (A5.4) become

$$\delta G_N^{(n)} = \delta G_{-N}^{(n)} = \delta C_N^{(n)} = \delta C_{-N}^{(n)} = 0, \quad (\text{A5.7})$$

and those of (A5.5) become

$$\delta G_0^{(n)} = \delta G_N^{(n)} = \delta C_N^{(n)} = \delta E_0^{(n)} = 0. \quad (\text{A5.8})$$

The finite difference analogue to equations (A5.2) can be linearised by neglecting all terms involving δ^2 . The linear system so obtained

and the boundary conditions (A5.7) or (A5.8), can be assembled into a single matrix equation

$$\underline{Ax} = \underline{b}. \quad (\text{A5.9})$$

If the flow is assumed symmetric and (A5.8) is used, then \underline{A} is a $(3N+4)$ by $(3N+4)$ matrix, and \underline{x} and \underline{b} are $(3N+4)$ element vectors. For any particular n , \underline{A} and \underline{b} are known, and \underline{x} is the vector formed by the unknowns; that is, by $\delta p^{(n)}$ and the $\delta G_j^{(n)}$, $\delta C_j^{(n)}$ and $\delta E_j^{(n)}$. The difference equations, the construction of \underline{A} , \underline{b} and \underline{x} , and the method of solution of (A5.9) can all be found in Smith (1974). We omit the details here.

An iterative scheme can now be defined. Let

$$\left. \begin{aligned} p^{(0)} &= p^{i-1} + \delta X \left(\frac{dp}{dX}\right)_{i-3/2} \\ G_j^{(0)} &= G_j^{i-1}, \quad C_j^{(0)} = C_j^{(i-1)}, \quad E_j^{(0)} = E_j^{i-1}, \end{aligned} \right\} \quad (\text{A5.10})$$

where $\left(\frac{dp}{dX}\right)_{i-3/2} = (p^{i-1} - p^{i-2})/\delta X$. Assuming convergence, approximate values for p^i and the G_j^i , etc., can be found to any required tolerance by repeatedly solving (A5.9) and applying (A5.6). Note that the coefficient matrix \underline{A} and the vector \underline{b} must be recalculated for each iteration.

In the above we have assumed that h is known explicitly in terms of X . Suppose that $h = h(p)$ is known as a function of p instead of X . The iterative scheme described above can be used for this problem by applying

$$h_i^{(n+1)} = h(p^{(n+1)}), \quad (\text{A5.11})$$

and

$$\left. \begin{aligned} h_{i-1/2}^{(n+1)} &= \frac{1}{2} [h^{(n+1)} + h^{i-1}], \\ \left(\frac{dh}{dX}\right)_{i-1/2}^{(n+1)} &= \frac{h^{(n+1)} - h^{i-1}}{\delta X} \end{aligned} \right\} \quad (\text{A5.12})$$

after each iteration. However, a more efficient scheme can be obtained by utilising explicitly the pressure dependence of the tube law. Equations (5.12) and

$$h_i^{(n+1)} = h(p^{(n)}) + \delta p^{(n)} \frac{dh}{dp}(p^{(n)}) + O((\delta p^{(n)})^2) \quad (\text{A5.13})$$

can be applied directly to the difference form of the governing equations (A5.2). This modification changes the coefficient of $\delta p^{(n)}$ in the linearised difference equations, and hence alters the matrix \underline{A} . Comparisons indicated that with the usual tolerance of 10^{-7} , the scheme implied by (A5.13) required four to eight fewer iterations for convergence than the scheme implied by (A5.11), a significant reduction.

The scheme derived from (A5.12) and (A5.13) was used in calculating all the relevant numerical solutions presented in this study. Usually, the flow was assumed to be symmetric, and (A5.8) was used for the boundary conditions. The grid size was varied to suit the particular problem. With the pressure response μ small, $\delta X = .1$ and $N = 50$ were adequate. For $\mu = 0(1)$, $\delta X = .01$ and $N = 100$ were commonly used. With $\mu \gg 1$, the collapse is driven by the boundary layer flow (see Sections 2.1, 3.4), and to increase the accuracy near the walls, while keeping the number of equations to a manageable size, the coordinate transformation $Y = 2z - z^2$ was adopted. With this transformation the grid used was $X_j = i\delta X$ and $z_j = j\delta z$, where $N\delta z = 1$. For large μ , 50 or 100 say, δX was taken as 10^{-4} or 10^{-5} , and N as 200 or 400, depending on the problem. In general, 12 or less iterations were required at each step for convergence to a tolerance of 10^{-7} . Usually, if more than about 40 iterations were required, then convergence would not be achieved.

Smith (1974) applies the above method of solving the boundary layer equations to the problem of flow near a discontinuity in wall conditions, and concludes that it is reasonably fast, stable and accurate. In as far as solutions were found, our experience supports this conclusion. In particular, we note the excellent agreement between the numerical and analytical solutions for a range of problems (see Figures 3.4 - 3.6 and 3.10).

Consider now the nonlinear boundary layer problem posed by equations (3.57) and (3.58). This problem arose in the study of a channel obeying (3.3) with $\varepsilon = 1$, $q = O(1)$ and $\mu \gg 1$. With appropriate changes of variable, the governing equations (3.57) reduce to (A5.2) with h set to one. The boundary conditions (3.58) become

$$\left. \begin{aligned} C = G = 0 \text{ at } Y = 0, \\ C \sim Y + \frac{1}{2} q p^2 \text{ as } Y \rightarrow \infty, \\ E \rightarrow 1 \text{ as } Y \rightarrow \infty, \end{aligned} \right\} \quad (\text{A5.14})$$

and the initial conditions are

$$G \rightarrow \frac{1}{2} Y^2, \quad C \rightarrow Y, \quad E \rightarrow 1 \quad \text{and} \quad p \rightarrow 0 \quad \text{as} \quad X \rightarrow -\infty. \quad (\text{A5.15})$$

The grid used for this problem is $X_i = X_0 + i\delta X$, $Y_j = j\delta Y$, where $-X_0$ and $N\delta Y = Y_\infty$ are large. With notation as above, the linearised discrete form of the boundary conditions (A5.14) is

$$\left. \begin{aligned} \delta G_0^{(n)} = \delta C_0^{(n)} = 0, \\ C_N^{(n)} + \delta C_N^{(n)} = Y_\infty + \frac{1}{2} q (p^{(n)})^2 + q p^{(n)} \delta p^{(n)}, \\ \delta E_N^{(n)} = 0. \end{aligned} \right\} \quad (\text{A5.16})$$

The initial conditions (A5.15) can be approximated by

$$\left. \begin{aligned} G_j^0 &= \frac{1}{2} (1 + \beta Y_\infty) Y_j^2 - \frac{1}{6} \beta Y_j^3, \\ C_j^0 &= (1 + \beta Y_\infty) Y_j - \frac{1}{2} \beta Y_j^2, \\ E_j^0 &= 1 + \beta Y_\infty - \beta Y_j, \\ p^0 &= p_0, \end{aligned} \right\} \quad (\text{A5.17})$$

where $\beta = q (p_0/Y_\infty)^2$ and p_0 is small and negative. This form was chosen because it is consistent with the definitions of G , C and E , with the boundary conditions (A5.14), and to leading order with the initial conditions (A5.15).

Clearly, an iterative scheme similar to that described above can be defined using (A5.16), (A5.17), and the linearised discrete form of (A5.12). The numerical solution obtained from this scheme with $\delta X = .1$, $N = 200$, $Y_\infty = 20$ and a tolerance of 10^{-7} showed the expected behaviour for $-p \ll 1$, that is $p \propto (X + X_S)^{-1/3}$ for some constant X_S such that $X + X_S \gg 1$ (see Section 3.4). However, this iterative procedure failed to converge when $\frac{1}{2} qp^2$ became $O(1)$. Examination of successive iterations revealed that, at some point as $\frac{1}{2} qp^2$ approached $O(1)$, the numerical process became divergent in an oscillatory manner. The point at which this occurred was basically insensitive to changes in any combination of δX , δY , and Y_∞ . However, changing q tended to change the value of p at which the process diverged such that $\frac{1}{2} qp^2$ remained roughly constant. Using the coordinate transformation $Y = Z^2$ to increase the accuracy near the wall made no significant difference to the results. To conclude, the iterative scheme described here did not provide a full numerical solution to the problem posed by equations (3.57) and (3.58). We do not know whether a solution exists.

A similar iterative can be defined for the problem with the non-linear boundary layer equations and (3.46) as boundary conditions.

Other numerical methods

Consider the integro-differential equation

$$S(\lambda P) = K \left\{ \int_0^X (X - t)^{-1/3} \frac{dP}{dt} dt + \frac{3}{2} X^{2/3} \right\}, \quad (\text{A5.18})$$

where K and λ are constants and $X > 0$. Equations (3.45), (4.26) and (4.41) are of the form (A5.18), as are (2.20) and (3.48) with suitable transformations. Let $X_j = j\Delta X$, where $\Delta X \ll 1$ and $j > 0$ is integer. Then

$$\left(\frac{dP}{dX} \right)_{j+1/2} = \frac{P_{j+1} - P_j}{\Delta X} + O(\Delta X^2). \quad (\text{A5.19})$$

Therefore

$$\begin{aligned}
& \int_{X_j}^{X_{j+1}} (X_i - t)^{-1/3} \frac{dP}{dt} dt = \\
& = \frac{P_{j+1} - P_j}{\Delta X} \frac{3}{2} \{ (X_i - X_j)^{2/3} - (X_i - X_{j+1})^{2/3} \} + \\
& + O((\Delta X)^3), \tag{A5.20}
\end{aligned}$$

where $i > j$. Applying (A5.20) to (A5.18) produces

$$P_1 = \Delta X \left\{ \frac{2}{3} \frac{S(P_1)}{(\Delta X)^{2/3}} - 1 \right\} \tag{A5.21}$$

and for $i > 1$

$$\begin{aligned}
P_i = & \frac{2}{3} \frac{(\Delta X)^{1/3}}{K} S(\lambda P_i) + P_{i-1} + i^{2/3} \Delta X - \\
& - \sum_{j=1}^{i-1} (P_j - P_{j-1}) [(i-j+1)^{2/3} - (i-j)^{2/3}], \tag{A5.22}
\end{aligned}$$

assuming that $P_0 = 0$. The direct iteration scheme defined by (A5.21) and (A5.22) was used to solve (2.20), and could be used for (4.26). With (3.45) and (4.41), $S(\lambda P) \propto (\lambda P)^2$ and the resulting quadratic equations for P_1 and P_i can be solved directly. A step length of $\Delta X = 10^{-3}$ was found to be adequate for all the $S(\lambda P)$ considered in the present study.

Consider now the integral

$$I(g) = \int_0^g \frac{dt}{\{(g_0 - t)(a - t)(t - b)\}^{1/2}} \tag{A5.23}$$

where $a = \frac{1}{2} [-g_0 + (12 - 3g_0^2)^{1/2}]$, $b = -\frac{1}{2} [g_0 + (12 - 3g_0^2)^{1/2}]$, $0 < g_0 < 1$, and $0 < g \leq g_0$. This integral arose in the analysis for a channel with a complete collapse and a moderate pressure response (equations 3.23 and 3.24, Section 3.2). The integrand has a singularity at g_0 , which can be removed by the transformation $t = g_0 - y^2$. However, $a \rightarrow g_0$ as $g_0 \rightarrow 1$, and to increase the accuracy of the numerical evaluation of (A5.23) for $1 - g_0$ small, we use the transformation

$$t = g_0 - \eta^n \quad (\text{A5.24})$$

with $n \geq 2$. Applying (A5.24) to (A5.23) produces

$$I(g) = n \int_{\alpha(g)}^{\beta} \frac{\eta^{(n-2)/2} d\eta}{\{(\eta^n + a - g_0)(g_0 - \eta^n - b)\}^{1/2}} \quad (\text{A.25})$$

where $\alpha(g) = (g_0 - g)^{1/n}$ and $\beta = g_0^{1/n}$. Simpson's rule was used to evaluate $I(g)$ numerically from (A5.25). For $1 - g_0$ of $0(1)$, $n = 2$ and 201 points were used. For $1 - g_0 \ll 1$, $n = 6$ and 501 points were found to be adequate for values of $1 - g_0$ as small as 10^{-7} .

In a similar manner, the integral in equation (3.25) was evaluated using the transformation (A5.24) and Simpson's rule.

Appendix 6. The Flow and Phase Velocity of an Inviscid Fluid in a Collapsible Tube

a) A tube with a constant steady stream

In dimensionless form, the equations of motion of an inviscid, incompressible fluid in a collapsible tube are

$$\left. \begin{aligned} \frac{\partial u}{\partial t} + u \frac{\partial u}{\partial x} &= - \frac{\partial p}{\partial x}, \\ \frac{\partial A}{\partial t} + \frac{\partial}{\partial x} (Au) &= 0, \end{aligned} \right\} \quad (\text{A6.1})$$

where the fluid motion is assumed uniform across the tube, x and t are the axial and time coordinates, $u(x,t)$ is the velocity, $p(x,t)$ the pressure, and $A(p)$ the cross-sectional area. A steady solution of (A6.1) is $u = u_i$, $p = p_i$, where u_i and p_i are constants. We will now investigate the propagation of small pressure waves superposed on this steady stream. Consider

$$\left. \begin{aligned} u &= u_i + \delta u e^{in(x-ct)}, \\ p &= p_i + \delta p e^{in(x-ct)}, \end{aligned} \right\} \quad (\text{A6.2})$$

where δp and δu are constants such that $|\delta p| = O(\delta u) \ll |u_i|$, c is the pulse velocity, and $\omega = n \operatorname{Re}(c)$ is the constant angular frequency of the disturbance. Substituting (A6.2) into (A6.1) produces

$$\left. \begin{aligned} \delta p &= \delta u(c - u_i), \\ \delta p(u_i - c) \frac{dA}{dp}(p_i) + \delta u A(p_i) &= 0, \end{aligned} \right\} \quad (\text{A6.3})$$

which yields

$$c = u_i + c_o(p_i) \quad (\text{A6.4})$$

where $c_o(p) = [A(p) dp/dA(p)]^{1/2}$ is the inviscid phase velocity for a system at rest. Thus, for a system with constant fluid velocity, there is simply a superposition of the phase velocity for a system at rest on the fluid velocity of the steady stream, a result which

applies also to an elastic tube (see Morgan and Ferrante 1955).

We see from (A6.4) that if $0 \leq u_i < c_0$ then we have a "forward travelling" wave which propagates downstream and a "backward travelling" wave which propagates upstream, while if $c_0 < u_i$ we have two forward travelling waves. If $u_i = c_0$ then (A6.4) gives $c = 2c_0$ and $c = 0$. It is worth remembering that (A6.4) does not give exact values for the pulse velocity, merely values correct to $O(\delta u)$. Inspection of the governing equations indicates that if $u_i - c_0 = O(\delta u)$ then the solutions for c are $c = 2c_0 + O(\delta u)$ and $c = O(\delta u)$. Thus in all cases the phase velocity is given to leading order by $c_0(p_i)$. We note that if $u_i \geq c_0$ or $u_i - c_0 = O(\delta u)$ then the ability of the system to disperse the energy of the disturbances is considerably restricted.

b) A tube with a non-constant steady stream

For a steady system (A6.1) reduces to

$$\frac{du}{dx} \left(A - u^2 \frac{dA}{dp} \right) = 0.$$

Thus the possible solutions for u are $u = \text{constant}$ and $u = \pm c_0(p)$. We now assume that p is not constant. Therefore, $u = \pm c_0$. Mass conservation requires $Au = Q$, where Q is a constant. Hence

$$\frac{dA}{dp} = A^3/Q^2,$$

the solution of which is

$$A(p) = (B - 2p/Q^2)^{-1/2}, \quad (\text{A6.5})$$

where $B = 1/A^2(p = 0)$ is a constant. Thus we see that a non-constant one-dimensional steady flow of an inviscid, incompressible fluid can exist in a collapsible tube only if the tube law has the form of (A6.5), and that in such a system the fluid velocity must necessarily match the inviscid phase velocity of a system at rest.

Consider a steady system with $u = c_0(p)$ and $p(x)$ non-constant. The phase and pulse velocities of this system cannot be assumed constant. If a small pressure disturbance travelling with velocity $c(x)$ is at position $x = x_0$ at time $t = t_0$, then it will be at position x at time t where

$$t - t_0 = \int_{x_0}^x \frac{d\eta}{c(\eta)} .$$

Accordingly, we study travelling waves of the form

$$\left. \begin{aligned} u &= c_0(x) + \hat{u}(x) e^{i\omega f(x,t)} \\ p &= p_i(x) + \hat{p}(x) e^{i\omega f(x,t)}, \end{aligned} \right\} \quad (\text{A6.6})$$

where $f(x,t) = \int_{x_0}^x \frac{d\eta}{c(\eta)} - t$, $c_0(x) = c_0(p_i)$, $\hat{u} = 0(c_0)$,

$\hat{p} = 0(p_i)$, and ω and $\Delta \ll 1$ are constants. We make the further assumptions that $Q = 0(1)$ and that the flow develops slowly in x , i.e. that $x = 0(\alpha)$, where $\alpha \gg 1$. Then if ω satisfies

$$\left. \begin{aligned} c &\ll \omega\alpha \ll c/\Delta \\ \text{and} \\ c_0 &\ll \omega\alpha \ll c_0/\Delta, \end{aligned} \right\} \quad (\text{A6.7})$$

substitution of (A6.6) into (A6.1) produces

$$\left. \begin{aligned} \hat{u} [c - c_0(x)] &= \hat{p}, \\ -\hat{p} [c - c_0(x)] \frac{dA}{dp}(p_i) + \hat{u}A(p_i) &= 0, \end{aligned} \right\} \quad (\text{A6.8})$$

which have solutions

$$c = 0 \text{ and } c = 2c_0(x). \quad (\text{A6.9})$$

Clearly $c = 0$ violates (A6.7). Equation (A6.7) and the results from (a) above suggest that the next step would be to study the

problem with $c = O(\Delta c_0)$. However, we will not investigate further, but note that the phase velocity is given to leading order by $c_0(p_i)$ even if a nontrivial solution for c of $O(\Delta c_0)$ exists.

R E F E R E N C E S

- ABRAMOWITZ, M. and STEGUN, I.A. (Ed) (1963), Handbook of Mathematical Functions, Dover Publications, New York.
- ATABEK , H.B. (1968), Wave propagation through a viscous fluid contained in a tethered, initially stressed, orthotropic elastic tube, *Biophys. J.* 8 626-649.
- ATABEK , H.B. and LEW, H.S. (1966), Wave propagation through a viscous incompressible fluid contained in an initially stressed elastic tube, *Biophys. J.* 6 481-503.
- BERGEL, D.H. (Ed.) (1972), Cardiovascular Fluid Dynamics, Vols. 1 and 2, Academic Press, London.
- BRAMWELL, J.C. and HILL, A.V. (1922), The velocity of the pulse wave in man, *Proc. R. Soc. B* 93 298-306.
- BROWER, R.W. and SCHOLTEN, C. (1975), Experimental evidence on the mechanism for the instability of flow in collapsible vessels, *Med. & Biol. Engng* 13 839-844.
- BURKILL, J.C. (1975), The Theory of Ordinary Differential Equations, 3rd Edition, Longman.
- CARO, C.G., FITZ-GERALD, J.M. and SCHROTER, R.C. (1969), Arterial wall shear and distribution of early atheroma in man, *Nature* 223 1159-1161.
- CARO, C.G., FITZ-GERALD, J.M. and SCHROTER, R.C. (1971), Atheroma and arterial wall shear. Observations, correlation and proposal of a shear dependent mass transfer mechanism for atherogenesis, *Proc. R. Soc. B* 177 109-159.
- CARO, C.G., PEDLEY, T.J., SCHROTER, R.C. and SEED, W.A. (1978), The Mechanics of the Circulation, Oxford University Press, Oxford.
- CHARM, S.E. and KURLAND, G.S. (1974), Blood Flow and Microcirculation, John Wiley and Sons, New York.
- COLE, J.D. and AROESTY, J. (1968), The blowhard problem - Inviscid flows with surface injection, *Int. J. Heat and Mass Transfer* 11 1167-1183.
- CONRAD, W.A. (1969), Pressure flow relationships in collapsible tubes, *IEEE trans., BME-16* 4 284-295.
- COX, R.H. (1968), Wave propagation through a Newtonian fluid contained within a thickwalled viscoelastic vessel, *Biophys. J.* 8 691-709.

- COX R.H. (1970), Wave propagation through a Newtonian fluid contained within a thick-walled viscoelastic tube: the effect of wall compressibility, *J. Biomech.* 3 317-335.
- DESHPANDE, M.D., GIDDENS, D.P. and MABON, F.R. (1976), Steady laminar flow through modelled vascular stenoses, *J. Biomech.* 9 165.
- EAGLES, P.M. and SMITH, F.T. (1980), The influence of nonparallelism in channel flow stability, *J. Eng. Math.* 14 219-237.
- FLAHERTY, J.E., KELLER, J.B. and RUBINOW, S.I. (1972), Post buckling behaviour of elastic tubes and rings with opposite sides in contact, *SIAM J. Appl. Math.* 23 446-455.
- FRAENKEL, L.E. (1962), Laminar flow in symmetrical channels with slightly curved walls I. On the Jeffery-Hamel solutions for flow between plane walls, *Proc. R. Soc. A* 267 119-138.
- FUNG, Y.C., PERRONE, N. and ANLIKER, Y. (Eds.) (1972), *Biomechanics. Its Foundations and Objectives*, Prentice-Hall, New Jersey.
- FUNG, Y.C. and SOBIN, S.S. (1972), Pulmonary alveolar blood flow, *Circulation Res.* 30 470-490.
- GRADSHTEYN, I.S. and RYZHIK, I.M. (1965), *Table of Integrals, Series and Products*, 4th edition, Academic Press, New York.
- GRIFFITHS, D.J. (1969), Urethral elasticity and micturition hydrodynamics in females, *Med. & Biol. Engng* 7 201-215.
- GRIFFITHS, D.J. (1971a), Hydrodynamics of male micturition, I: theory of steady flow through elastic-walled tubes, *Med. & Biol. Engng* 9 581-588.
- GRIFFITHS, D.J. (1971b), Steady flow through veins and collapsible tubes, *Med. & Biol. Engng* 9 597-602.
- GRIFFITHS, D.J. (1975a), Negative resistance effects in flow through collapsible tubes, 2: Two dimensional theory of flow near an elastic constriction, *Med. & Biol. Engng* 13 791-796.
- GRIFFITHS, D.J. (1975b), Negative resistance effects in flow through collapsible tubes, 3: Two dimensional treatment of the elastic properties in an elastic constriction, *Med. & Biol. Engng* 13 797-801.
- HAMEL, G. (1917), Sparilförmige Bewegungen zäher Flüssigkeiten, *Jber. dtsch. MatVer.* 25 34-60.
- HOLT, J.P. (1944), The collapse factor in the measurement of venous pressure; the flow of fluid through collapsible tubes, *J. Physiol.* (London) 44 206-216.

- HOLT, J.P. (1953), Flow of liquids through collapsible tubes, Am. Heart J. 46 715-725.
- HOLT, J.P. (1959), Flow of liquids through collapsible tubes, Circulation Res. 7 342-353.
- HWANG, N.H.C. and NORMAN, N.A. (Eds.) (1972), Cardiovascular Flow Dynamics and Measurements, University Park Press, Baltimore.
- JAFFRIN, M.Y. and SHAPIRO, A.H. (1971), Peristaltic pumping, Annu. Rev. Fluid Mech. 3 13-36.
- JEFFERY, G.B. (1915), The two dimensional steady motion of a viscous fluid, Phil. Mag. Series 6, 29 455-465.
- JONES, C.W. and WATSON, E.J. (1963), Two-dimensional boundary layers, pp. 198-257 in 'Laminar Boundary Layers'. Ed. L. Rosenhead, Oxford University Press, Oxford.
- KAMM, R.D. and SHAPIRO, A.H. (1979), Unsteady flow in a collapsible tube subjected to external pressure or body forces, J. Fluid Mech. 95 1-78.
- KATZ, A.I., CHEN, Y. and MORENO, A.H. (1969), Flow through a collapsible tube; Experimental analysis and mathematical model, Biophys. J. 9 1261-1279.
- KIRCHHOFF, G. (1869), Zur Theorie freier Flüssigkeitsstrahlen, J. reine angew. Math. 70 289.
- KNOPP, K. (1956), Infinite Sequences and Series, Dover Publications, New York.
- KRESH, E. and NOORDERGRAAF, A. (1969), A mathematical model for the pressure-flow relationship in a segment of pure vein, IEEE trans., BME-16 4 296-307.
- LAMB, H. (1898), On the velocity of sound in a tube as affected by the elasticity of the walls, Mem. Manchester Lit. and Phil. Soc. 42 No. 9.
- LIGHTHILL, M.J. (1972), Physiological fluid dynamics: a survey, J. Fluid Mech. 52 475-497.
- LING, S.C. and ATABEK, H.B. (1972), A nonlinear analysis of pulsatile flow in arteries, J. Fluid Mech. 55 493-511.
- MCDONALD, D.A. (1974), Blood Flow in Arteries, 2nd Edition, Edward Arnold, London.

- MILLSAPS, K. and POHLHAUSEN, K. (1953), Thermal distributions in Jeffery-Hamel flows between non-parallel plane walls, *J. aero. Sci.* 20 187-196.
- MORENO, A.H., KATZ, A.I., GOLD, L.D. and REDDY, R.V. (1970), Mechanics of distension of dog veins and other very thin-walled tubular structures, *Circulation Res.* 27 1069-1080.
- MORGAN, G.W. and FERRANTE, W.R. (1955), Wave propagation in elastic tubes fluid with streaming liquid, *J. acoust. Soc. Am.* 27 715-725.
- MORGAN, G.W. and KIELY, J.P. (1954), Wave propagation in a viscous fluid contained in a flexible tube, *J. acoust. Soc. Am.* 26 323-328.
- OATES, G.C. (1975), Fluid flow in a soft walled tube I: Steady flow, *Med. & Biol. Engng* 13 773-779.
- PATEL, D.J. and FRY, D.F. (1966), Longitudinal tethering of arteries in dogs, *Circulation Res.* 19 1011.
- PATEL, D.J. and VAISHNAV, R.N. (1972), The rheology of large blood vessels, Chapter 11 in 'Cardiovascular Fluid Dynamics, Vol 2', Ed. D.H. Bergel, Academic Press, London.
- POHLHAUSEN, K. (1921), Zur näherungsweise Integration der Differentialgleichung der laminar Grenzschicht, *Z. angew. Math. Mech.* 1 252-268.
- ROSENHEAD, L. (1940); The steady two dimensional flow of viscous fluid between two inclined plane walls, *Proc. R. Soc. A* 175 436-467.
- ROSENHEAD, L. (Ed.) (1963), *Laminar Boundary Layers*, Oxford University Press, Oxford.
- RUBINOW, S.I. and KELLER, J.B. (1971), Wave propagation in a fluid filled tube. *J. acoust. Soc. Am.* 50 198-223.
- RUBINOW, S.I. and KELLER, J.B. (1972), Flow of a viscous fluid through an elastic tube with applications to blood flow, *J. Theor. Biol.* 35 299-313.
- RUBINOW, S.I. and KELLER, J.B. (1978), Wave propagation in a visco-elastic tube containing a viscous fluid, *J. Fluid Mech.* 88 181-203.

- SCHWERDT, H. and CONSTANTINESCO, A. (1976), Periodic flow of a viscous fluid superimposed on steady flow in an orthotropic initially stressed elastic tube, *Biorheology* 13 7-20.
- SECOMB, T.W. (1978), Flow in a channel with pulsating walls, *J. Fluid Mech.* 86 273-288.
- SHAPIRO, A.H. (1977), Steady flow in collapsible tubes, *J. Biomech. Engng* 99 126-147.
- SMITH, F.T. (1974), Boundary layer flow near a discontinuity in wall conditions, *J. Inst. Math. Applics.* 13 127-145.
- SMITH, F.T. (1976a), Flow through constricted or dilated pipes and channels: Part 1, *Quart. J. Mech. appl. Math.* 29 343-364.
- SMITH, F.T. (1976b), Flow through constricted or dilated pipes and channels: Part 2, *Quart. J. Mech. appl. Math.* 29 365-376.
- SMITH, F.T. (1976c), Fluid flow in a curved pipe, *Proc. R. Soc. A* 351 71-87.
- SMITH, F.T. (1976d), Pipe flows distorted by nonsymmetric indentation or branching, *Mathematika* 23 62-83.
- SMITH, F.T. (1976e), On entry flow effects in bifurcating, blocked or constricted tubes, *J. Fluid Mech.* 78 709-736.
- SMITH, F.T. (1977a), The laminar separation of an incompressible fluid streaming past a smooth surface, *Proc. R. Soc. A* 356 443-463.
- SMITH, F.T. (1977b), Upstream interactions in channel flows, *J. Fluid Mech.* 79 631-655.
- SMITH, F.T. (1978), Flow through symmetrically constricted tubes, *J. Inst. Math. Applics.* 21 145-156.
- SMITH, F.T. (1979), The separating flow through a severely constricted symmetric tube, *J. Fluid Mech.* 90 725-754.
- STEWARTSON, K. (1970a), On supersonic laminar boundary layers near convex corners, *Proc. R. Soc. A* 319 289-305.
- STEWARTSON, K. (1970b), On laminar boundary layers near corners, *Quart. J. Mech. appl. Math.* 23 137-152. See also 24 387-389.
- STEWARTSON, K. (1974), Multistructured boundary layers on flat plates and related bodies, *Adv. appl. Mech.* 14 145.
- SYCHEV, V.Ya. (1972), Concerning Laminar Separation, *Izv. Akad. Nauk SSSR, Mekh, Zhidk. Gaza* 3 47.

- TAYLOR, L.A. and GERRARD, J.H. (1977), Pressure-radius relationships for elastic tubes and their applications to arteries, Med. & Biol. Eng. & Comput. 15 11-21.
- UCHIDA, S. and AOKI, H. (1977), Unsteady flows in a semi-infinite contracting or expanding pipe, J. Fluid Mech. 82 371-387.
- WHITHAM, G.B. (1963), The Navier-Stokes equations of motion. Part II Some exact solutions, pp. 134-162 in 'Laminar Boundary Layers', Ed. L. Rosenhead, Oxford University Press, Oxford.
- WHITMORE, R.L. (1968), Rheology of the Circulation, Pergamon.
- WILD, Rosemary, PEDLEY, T.J. and RILEY, D.S. (1977), Viscous flow in collapsible tubes of slowly varying cross section, J. Fluid Mech. 81 273-294.
- WILSON, S. (1969), The development of Poiseuille flow, J. Fluid Mech. 38 793-806.
- WOMERSLEY, J.R. (1955), Oscillatory motion of a viscous liquid in a thin-walled elastic tube I: The linear approximation for long waves, Phil. Mag. Series 7, 46 199-221.
- WOMERSLEY, J.R. (1957), An elastic tube theory of pulse transmission and oscillatory flow in mammalian arteries, Wright Air Development Centre, Tech. Rep. No. 56-614.